

**LOW ENRICHMENT URANIUM (LEU)-FUELED SLOWPOKE-2 NUCLEAR  
REACTOR SIMULATION WITH THE MONTE-CARLO BASED MCNP 4A CODE**

By

J.R.M. Pierre, Beng (Royal Military College of Canada - Collège Militaire Royal du Canada)

Lieutenant Navy

A thesis submitted to the Department of Chemistry

and Chemical Engineering

in partial fulfilment of the requirements of

the Degree of Master of Engineering

in Nuclear Engineering

Royal Military College of Canada - Collège Militaire Royal du Canada

Kingston, Ontario

May, 1996

©Copyright by J.R.M. Pierre 1996

This thesis may be used within the Department of National Defence but copyright for open publication remains the property of the author.

National Library  
of Canada

Acquisitions and  
Bibliographic Services

395 Wellington Street  
Ottawa ON K1A 0N4  
Canada

Bibliothèque nationale  
du Canada

Acquisitions et  
services bibliographiques

395, rue Wellington  
Ottawa ON K1A 0N4  
Canada

*Your file* *Votre référence*

ISBN: 0-612-82848-4

*Our file* *Notre référence*

ISBN: 0-612-82848-4

The author has granted a non-exclusive licence allowing the National Library of Canada to reproduce, loan, distribute or sell copies of this thesis in microform, paper or electronic formats.

The author retains ownership of the copyright in this thesis. Neither the thesis nor substantial extracts from it may be printed or otherwise reproduced without the author's permission.

L'auteur a accordé une licence non exclusive permettant à la Bibliothèque nationale du Canada de reproduire, prêter, distribuer ou vendre des copies de cette thèse sous la forme de microfiche/film, de reproduction sur papier ou sur format électronique.

L'auteur conserve la propriété du droit d'auteur qui protège cette thèse. Ni la thèse ni des extraits substantiels de celle-ci ne doivent être imprimés ou autrement reproduits sans son autorisation.

# Canada

## ABSTRACT

Following the commissioning of the Low Enrichment Uranium (LEU) Fuelled SLOWPOKE-2 research reactor at the Royal Military College-Collège Militaire Royal (RMC-CMR), excess reactivity measurements were conducted over a range of temperature and power. The results showed a maximum excess reactivity of 3.37 mk at 33°C. Several deterministic models using computer codes like WIMS-CRNL, CITATION, TRIVAC and DRAGON have been used to try to reproduce the excess reactivity and temperature trend of both the LEU and HEU SLOWPOKE-2 reactors. The best simulations had been obtained at École Polytechnique de Montréal. They were able to reproduce the temperature trend of their HEU-fuelled reactor using TRIVAC calculations, but this model over-estimated the absolute value of the excess reactivity by 119 mk. Although calculations using DRAGON did not reproduce the temperature trend as well as TRIVAC, these calculations represented a significant improvement on the absolute value at 20°C reducing the discrepancy to 13 mk.

Given the advance in computer technology, a probabilistic approach was tried in this work, using **the** Monte-Carlo N-Particle Transport Code System MCNP 4A, to model the RMC-CMR SLOWPOKE-2 reactor. The main advantages of MCNP 4A were the ability to model the entire reactor in three dimensions and to use an accurate transport approach instead of diffusion calculations. These advantages lead to a significant improvement in reproducing the experimental excess reactivity of the RMC-CMR SLOWPOKE-2 reactor, reducing the discrepancy between the calculated value and the experimental value to the standard deviation of the calculated value (0.2 mk). Although the error on the calculated value due to modelling uncertainties could not be

accurately determined, the analysis suggests that the error should be between 1 and 2 mk. MCNP 4A also allowed the modelling of the single control rod in different positions. From these simulations, it was possible to calculate the reactivity worth of the control rod. Although the simulation overestimated the control rod reactivity worth, the discrepancy with the experimental data was only 2.4 mk.

Within the limitation of the computing facilities and the code, the temperature trend was simulated for three different control rod positions. These curves clearly show that the reactivity of the RMC-CMR SLOWPOKE-2 reactor decreases as the temperature increases. This is very useful as it verifies the inherent safety of the reactor, and demonstrates that the model has the potential to investigate safety issues when modifications are proposed. The experimentally determined reactivity peak of the RMC-CMR SLOWPOKE-2 reactor could not be reproduced accurately in the present work. There are however some indications that this may be due to temperature effects on the cross sections.

## ACKNOWLEDGEMENTS

I particularly want to extend my appreciation to Dr. H.W. Bonin for his guidance and his excellent advice. His genuine interest and support in this project have been invaluable.

I would also like to extent my appreciation to Dr. M. Milgram from Atomic Energy Canada Limited, who taught me how to use MCNP 4A and for answering many questions regarding various aspect of the code. I also thank W. Grant from Atomic Energy Control Board for running the simulations presented in Chapter 4.

Finally to the love of my life, Deborah my wife, I want to express my gratitude for her patience, her help and encouragement during this period.

## TABLE OF CONTENTS

ABSTRACT	i
ACKNOWLEDGMENTS	iii
TABLE OF CONTENTS	iv
LIST OF FIGURES	vi
LIST OF TABLES	vii
<b>1.0 INTRODUCTION</b>	
1.1 THE LEU-FUELED SLOWPOKE-2 REACTOR	1
1.2 HISTORY OF THE PROBLEM	2
1.3 AIM	2
<b>2.0 COMPUTER CODE</b>	
2.1 THE MONTE CARLO METHOD	4
2.2 GENERAL DESCRIPTION OF MCNP 4A	4
2.3 CRITICALITY CALCULATIONS	5
2.4 EVALUATION OF THE PRECISION IN MCNP 4A	14
2.5 THE ACCURACY IN MCNP 4A	16
2.6 VARIANCE REDUCTION TECHNIQUES	18
<b>3.0 THREE DIMENSIONAL REACTOR MODEL</b>	
3.1 GENERAL DESCRIPTION OF RMC SLOWPOKE-2 REACTOR	20
3.2 THE INPUT DECK	22
3.3 THE FUEL	22
3.4 THE CONTROL ROD	25
3.5 IRRADIATION SITES	30
3.6 REFLECTOR	35
3.7 THERMAL COLUMN	35
3.8 REACTOR CONTAINER AND POOL	39
3.9 GENERAL	39
<b>4.0 SIMPLIFIED MODEL</b>	
4.1 DESCRIPTION OF THE SIMPLIFIED MODEL	43
4.2 TEMPERATURE SIMULATION BY UO <sub>2</sub> AND H <sub>2</sub> O DENSITY	44
4.3 FREE GAS TREATMENT	46
4.4 S(A,B) TREATMENT	47
4.5 LATTICE STEP	48
<b>5.0 RESULTS</b>	
5.1 EXPERIMENTAL DATA	50
5.2 EXCESS REACTIVITY CALCULATIONS	51
5.3 CONTROL ROD WORTH CALCULATIONS	53

5.4	EXCESS REACTIVITY VS AVERAGE CORE TEMPERATURE	54
5.5	DOUBLED LINEAR COEFFICIENT OF EXPANSION	59
5.6	TEMPERATURE EFFECT ON CROSS SECTION	62
<b>6.0</b>	<b>DISCUSSION</b>	
6.1	EXCESS REACTIVITY	63
6.2	CONTROL ROD WORTH	64
6.3	TEMPERATURE EFFECTS	65
<b>CONCLUSION</b>		70
<b>RECOMMENDATIONS</b>		72
<b>REFERENCES</b>		74
APPENDIX A	MCNP 4 A SAMPLE INPUT DECK	
APPENDIX B	BERYLLIUM IMPURITIES	
APPENDIX C	THERMAL COLUMN VOLUME CALCULATION	
APPENDIX D	KEFF TRENDS	
APPENDIX E	OUTPUT DECK	
APPENDIX F	DEVELOPMENT OF THE THREE $k_{\text{eff}}$ ESTIMATORS	

## LIST OF FIGURES

2.1	Flow chart of MCNP 4A	7
3.1a	Photograph of the bottom of the reactor vessel showing the thermal column in place against the vessel wall	21
3.1b	SLOWPOKE-2 reactor core	21
3.2	Cross section of fuel element	23
3.3	Horizontal cut showing fuel element distribution	26
3.4	Horizontal cut showing top fuel cage grid	27
3.5	Horizontal cut showing bottom fuel cage grid	28
3.6	Cross section of control rod	29
3.7	General layout of irradiation sites	31
3.8	External irradiation sites	32
3.9	Reactor reflectors	36
3.10	Thermal Column	37
3.11	Horizontal cut of reactor pool	40
3.12	Vertical cut of reactor pool	41
4.1	Infinite lattice in Y and Z direction of simplified model	43
5.1	RMC-CMR SLOWPOKE-2 excess reactivity measurements by control rod balance at 10 W thermal	50
5.2	RMC-CMR SLOWPOKE-2 excess reactivity measurements by control rod balance at 2 kW thermal	50
5.3	RMC-CMR SLOWPOKE-2 excess reactivity measurements by period at 2 kW thermal	50
5.4	RMC-CMR SLOWPOKE-2 excess reactivity measurements by control rod balance at 10 kW thermal	50
5.5	RMC-CMR SLOWPOKE-2 excess reactivity measurements by period at 10 kW thermal	51
5.6	RMC-CMR SLOWPOKE-2 excess reactivity measurements by control rod balance at 100 W thermal (while cooling)	51
5.7	$k_{\text{eff}}$ combined estimator vs cycle control rod fully out	52
5.8	$k_{\text{eff}}$ combined estimator vs cycle control rod fully out	52
5.9	$k_{\text{eff}}$ combined estimator vs cycle control rod fully out	52
5.10	$k_{\text{eff}}$ combined estimator vs cycle control rod fully out	52
5.11	Excess reactivity vs temperature control rod fully inserted	56
5.12	Excess reactivity vs temperature control rod centred	58
5.13	Excess reactivity vs temperature control rod fully out	59
5.14	Excess reactivity vs temperature control rod fully inserted linear expansion coef. doubled	60
5.15	Excess reactivity vs temperature control rod centred linear expansion coef. doubled	61

## LIST OF TABLES

2.1	Perturbation of i, j, and k for the Combining of the Three $k_{\text{eff}}$ Estimators	14
3.1	Calculation of $\Sigma_a$ Thermal for Zircalloy-4	24
3.2	Comparison of Cadmium-Lining of Irradiation Site	34
3.3	Calculation of $\Sigma_a$ Thermal for Al 6061 T6	38
4.3	Calculation of $k_{\text{eff}}$ at 32°C	46
4.2	Calculation of $k_{\text{eff}}$ at 32°C with “tmp” Command	47
4.3	Variation in Macroscopic Cross Sections Relative to the Use of the 300K Cross Section Library	48
4.4	Calculation of $k_{\text{eff}}$ at 32°C Including Lattice Expansion	49
5.1	Excess Reactivity	53
5.2	Control Rod Reactivity Worth	54
5.3	Excess Reactivity vs Temperature Control Rod Fully Inserted	55
5.4	Excess Reactivity vs Temperature Control Rod Centred	57
5.5	Excess Reactivity vs Temperature Control Rod Fully Out	58
5.6	Excess Reactivity vs Temperature Control Rod Fully Inserted (doubled $\alpha_{\text{linear}}$ )	60
5.7	Excess Reactivity vs Temperature Control Rod Centred (doubled $\alpha_{\text{linear}}$ )	61
5.8	Excess Reactivity vs Temperature Control Rod Fully Out (doubled $\alpha_{\text{linear}}$ )	62
5.9	Cross Section Library Comparison	62

## CHAPTER 1 - INTRODUCTION

### 1.1 THE LEU-FUELED SLOWPOKE-2 REACTOR

The manufacturer of the second generation Safe Low Powered Critical Experiment (SLOWPOKE-2) nuclear reactor, Atomic Energy of Canada (AECL), conforming to the world trend to restrict the use of Highly Enriched Uranium (HEU) fuel, developed the Low Enriched Uranium (LEU) fuel core. Safety analysis for the SLOWPOKE-2 revealed that the LEU core benefits from the same inherent negative reactivity feedback with temperature increases as the HEU core. The first LEU SLOWPOKE-2 nuclear reactor was installed at the Royal Military College of Canada/Collège Militaire Royal Du Canada and achieved criticality on September 6, 1985. Previously, six HEU SLOWPOKE-2 reactors had been commissioned in Canada and one in Jamaica.

To facilitate refuelling of the existing reactor with the LEU core, the overall geometry of the SLOWPOKE-2 nuclear reactor was retained. Only the fuel elements and the fuel cage were modified. The fuel elements are based on the Zircalloy-4 clad uranium dioxide ( $\text{UO}_2$ ) fuel of the CANDU design. Although the LEU fueled reactor requires more uranium 235 to counteract the additional neutron absorptions in the uranium 238, it contains fewer fuel elements since the uranium density is higher. From a set of WIMS calculation it was decided that the 342 site layout was to be retained, and a compromise between reactivity and an acceptable sample site flux to power ratio resulted in an initial 180 element fuel layout. The final fuel loading included 198 fuel elements and achieved an excess reactivity of 3.15 mk when corrected to  $19.6^\circ\text{C}$ .<sup>(1)</sup>

## **1.2 HISTORY OF THE PROBLEM**

During the first months of operation, the RMC reactor exhibited higher than theoretically predicted excess reactivity for temperatures above 20°C. Therefore, in May 1986 a set of reactivity measurements were performed on the LEU-fueled SLOWPOKE-2 at RMC over a range of temperatures and at several power levels. The maximum excess reactivity 3.37mk was observed at 33°C and 10W (low power). Maxima for other power levels, although lower than 3.37 mk, appeared from 29°C to 37°C.<sup>(2)</sup> An initial model of the RMC SLOWPOKE-2 showed a similar temperature trend but a maximum excess reactivity located at 12°C.<sup>(1)</sup> The absolute values of the excess reactivity presented a significantly larger discrepancy, calculating it at 80 mk by WIMS-CRNL and 45 mk by CITATION coupled with WINS-CRNL. Another attempt at modelling the RMC SLOWPOKE-2 was performed later at RMC .<sup>(3)</sup> Although an error in the ENDF/B-V library reduced the improvement initially made with the temperature trend, a code developed at RMC resolved the discrepancies between WIMS-CRNL and WIMS-CITATION.<sup>(3)</sup> Furthermore, the discrepancies between CITATION and experiment was reduced to 16 mk at 20°C .<sup>(3)</sup> École Polytechnique de Montréal also attempted to simulate their HEU SLOWPOKE-2 core. They were able to reproduce the temperature trend of their reactor using TRIVAC calculations, but this model over-estimated the absolute value of the excess reactivity by 119 mk. Although calculations using DRAGON did not reproduce the temperature trend as well as TRIVAC, these calculations made a significant improvement to the absolute value at 20°C reducing the discrepancy to 13 mk.<sup>(4)</sup>

## **1.3 AIM**

Given recent advances in computer technology, simulation requiring significantly more computation power, such as Monte-Carlo methods, can now be performed at a reasonable cost. The

aim of this work is therefore to develop a model of the RMC SLOWPOKE-2 using a Monte-Carlo method that will:

- a. Improve on the accuracy of the absolute value of the excess reactivity;
- b. Be able to simulate various positions of the control rod; and
- c. Reproduce accurately the temperature trend.

At this time the existing HEU SLOWPOKE-2 are entering a phase of their life that will require refuelling. École Polytechnique de Montréal has already started the process of replacing their HEU core with a LEU core similar to that of the RMC-CMR SLOWPOKE-2. Therefore, it is important that the modelling include enough versatility to be applied to other facilities.

## CHAPTER 2 - COMPUTER CODE

### 2.1 THE MONTE CARLO METHOD

The Monte Carlo Method uses random sampling to solve mathematical problems.

This method can be traced as far back as 1772 with the Comte de Buffon.<sup>(5)</sup> But it was very tedious to use due to the large number of hand calculations that had to be performed. It was really during the Second World War that the method emerged as a mathematical tool. Stan Ulam at Los Alamos realized that statistical sampling techniques could be made practical by the use of electronic computing machines.<sup>(5)</sup> When he discussed the idea with co-workers, everyone was reminded of a game of chance, and the name Monte-Carlo was adopted after the world renowned Casino in the principality of Monaco.

The method is generally applied to two types of problems:

- a. Simulation: refers to methods of providing arithmetical imitation of some real phenomena. The classical example is the simulation of the neutrons' motion;
- b. Sampling: refers to the methods of deducing the properties of a system by studying a random subset of that system. Thus, the average value of  $f(x)$  over an interval may be estimated from its average over a finite, random number of points in the interval.

This amounts to evaluating an integral.

### 2.2 GENERAL DESCRIPTION OF MCNP 4A

Monte-Carlo N-Particle Transport Code version 4A (MCNP 4A) is a general purpose, continuous energy, generalized geometry, time dependent, coupled neutron, photon and electron transport code with the ability to calculate  $k_{\text{eff}}$  for fissile systems.<sup>(5)</sup> Its approach is to solve a transport problem by simulating particle histories. As a result, one could extract the integral

transport equation from the probability density of particles. This is quite different than the deterministic methods used in previous models, which attempted to solve the transport equations or used diffusion equations.

MCNP 4A was developed at Los Alamos and is written in the style of Dr. Thomas N.K. Godfrey who was the principal programmer from 1975 to 1989; it represents the effort of 400 person-years of work. The information about the problem, including the geometry, the materials, the cross sections, the location of the particles and the output desired is supplied by the user in an input file. MCNP 4A treats the three dimensional configuration of the geometry defined by the user as cells bounded by first and second degree surfaces, or fourth degree elliptical tori (the simulation of the geometry of the SLOWPOKE-2 was principally described by planes, cylinders and spheres). The user defines the surfaces by entering the coefficients of formulas from plane analytical geometry, or in certain cases, by entering known points on the surfaces. Then the user defines cells as intersections, unions and complements of regions bounded by the predefined surfaces. Finally, the user assigns a material, which is made up of one or more radioisotopes, to each cell.

### 2.3 CRITICALITY CALCULATIONS

In order to sustain a nuclear chain reaction in a given system, the number of fissions in one generation must be equal to the number of fissions in the previous generation. Qualitatively this can be measured by the multiplication factor  $k_{eff}$  where

$$k_{eff} = \frac{\text{number fissions in one generation}}{\text{number fissions in the previous generation}} \quad (1)$$

If  $k_{eff}$  is greater than one, the number of fissions increases with time and the system is said to be supercritical. If  $k_{eff}$  is equal to one, the number of fissions is stable and the system is said to

be critical. If it is smaller than one, the number of fissions decreases and the system is said to be subcritical.

The aim of this section is to introduce the important principles involved in the evaluation of the multiplication factor. It is not a complete description of MCNP 4A, therefore the reader is directed to Reference 5 for more detailed information. First, some of the terminology and characteristics of the code need to be introduced. MCNP 4A uses the term “cycle” when calculating the  $k_{eff}$ , this term basically has the same meaning as the fission generation. Cycles are divided in two categories; the active and inactive cycles. Active cycles refer to the cycles used in the calculation of the average  $k_{eff}$ . Inactive cycles refer to the cycles used to build the source term, and are not included in the calculation of the average  $k_{eff}$ . The code terminates the fission neutrons in the present cycle and uses them as the source for the next cycle. Furthermore, the fission process in the present cycle is treated as capture. Since the average total number of neutrons produced per fission  $\bar{v}$  is used, the effect of the delayed neutrons are treated in the same cycle as the prompt neutrons. The source for the first cycle is supplied by the user by guessing or using results from a previous run of MCNP 4A. The statistical weight of each source is set to keep the number of starting particles constant through all cycles. Here, the weight of a particle can be defined as the number of neutrons which make up that particle, this weight is adjusted after every collision to simulate neutron capture. Figure 2.1 illustrates the progression of these particles in a cycle, and the evaluation of  $k_{eff}$ .

As seen in Figure 2.1 the particles are first transported through the user-defined geometry by standard random walk, defined as follows:<sup>(5)</sup>

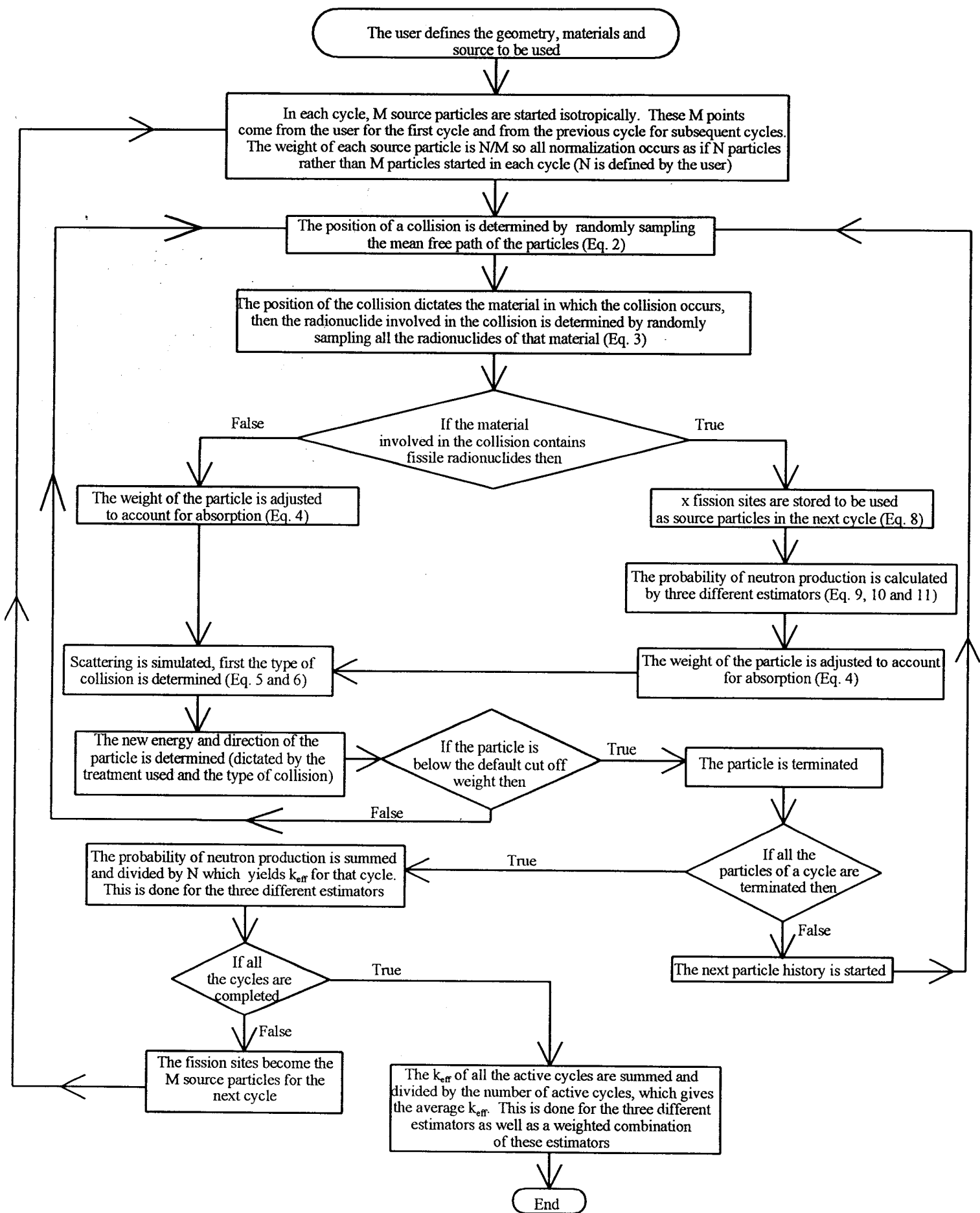


Figure 2.1 Flow chart of MCNP 4A

$$l = \frac{1}{\Sigma_t} \ln(\xi) \quad (2)$$

where  $l$  = Distance to collision

$\xi$  =  $0 < \text{random number} \leq 1$

$\Sigma_t$  = total macroscopic cross section of the material

Once the location of the collision has been calculated, the  $k^{\text{th}}$  nuclide of the material in which the collision occurred is chosen as the collision nuclide by random sampling, weighed on the macroscopic cross sections, using:

$$\sum_{i=1}^{k-1} \Sigma_{ti} < \xi \sum_{i=1}^{nu} \Sigma_{ti} \leq \sum_{i=1}^k \Sigma_{ti} \quad (3)$$

where:  $k$  = sequentially takes values from 1 to  $nu$

$\Sigma_{ti}$  = macroscopic total cross section of nuclide  $i$

$nu$  = number of different nuclides forming the material in which the collision takes place

The total cross section is taken from the cross-section tables, and is adjusted for thermal effect using a free gas thermal treatment. The MCNP 4A free gas treatment simply consists of adjusting the elastic cross section, taking into account the velocity of the nucleus involved in the collision. This treatment applies only to the elastic scattering. Another treatment is also available for certain materials when the incident neutron energy is below about 4 eV, the “S( $\alpha, \beta$ ) treatment”.

If this treatment is selected, the total cross section is calculated as the sum of the capture cross section from the regular cross-section table and the elastic and inelastic scattering cross sections from the  $S(\alpha,\beta)$  table. This treatment is a complete representation of thermal neutron scattering by molecules and crystalline solids.

The weight of the particles is adjusted at every collision, thus simulating neutron capture using:<sup>(5)</sup>

$$W_n^* = \left( 1 - \frac{\sigma_a}{\sigma_T} \right) W_n \quad (4)$$

where  $W_n^*$  = weight of particle  $n$  after collision

$W_n$  = weight of particle  $n$  before collision

$\sigma_a$  = microscopic absorption cross section

$\sigma_T$  = microscopic total cross section

Then the neutrons can either undergo an elastic or inelastic collision, the selection is done by:<sup>(5)</sup>

$$P(el) = \frac{\sigma_{el}}{\sigma_{el} + \sigma_{in}} = \frac{\sigma_{el}}{\sigma_T - \sigma_a} \quad (5)$$

where  $P(el)$  = probability of elastic collision

$\sigma_{el}$  = microscopic elastic cross section

$\sigma_{in}$  = microscopic inelastic cross section

and

$$P(\text{in}) = 1 - P(\text{el}) \quad (6)$$

where  $P(\text{in})$  = probability of inelastic collision

In most cases, for the free gas treatment the direction of the emitted particle is sampled the same way for both elastic and inelastic collision. The angle between the incident and scattered particle is sampled from angular distribution tables in the collision nuclide cross sections library. For elastic collisions, the associated exiting energy is given by a two-body kinematics expression:<sup>(5)</sup>

$$\begin{aligned} E_{\text{out}} &= \frac{1}{2} E_{\text{in}} [(1 - \alpha) \mu_{\text{cm}} + 1 + \alpha] \\ \alpha &= \left( \frac{A - 1}{A + 1} \right) \\ E_{\text{out}} &= E_{\text{in}} \left[ \frac{1 + A^2 + 2 A \mu_{\text{cm}}}{(1 + A)^2} \right] \end{aligned} \quad (7)$$

where  $E_{\text{out}}$  = exiting neutron energy

$E_{\text{in}}$  = incident neutron energy

$\mu_{\text{cm}}$  = centre of mass cosine of the angle between incident and exciting particle directions

$A$  = mass of collision nuclide in units of the mass of a neutron

For inelastic collisions, the treatment depends on the particulars inelastic reaction chosen i.e., (n,n'), (n,2n) etc. The total weight of the exiting particle or particles is the same as the incident particle minus the fraction lost to capture. The energy of the exiting particles are determined by various laws sampled independently for each exiting particle.<sup>(5)</sup>

For the S( $\alpha, \beta$ ) treatment, both the energy and angle of the exiting particles are sampled from a set of tabulated energies and associated angles, which are dependent on the incident energy. This treatment applies to both the elastic and the inelastic scattering.

At each collision site the prompt neutron lifetimes by absorption and collision estimates are accumulated and, if fission is possible, a number  $x$  of fission sites are stored for use as source particles in the next generation, where:<sup>(5)</sup>

$$x = W_n \bar{v} \left( \frac{\sigma_f}{\sigma_t} \right) \left( \frac{1}{k_{eff}} \right) + \text{random number between 0 and 1} \quad (8)$$

where  $\bar{v}$  = total average number of neutrons produced by fission at the incident energy of this collision  
 $\sigma_f$  = microscopic material fission cross section  
 $\sigma_t$  = microscopic material total cross section  
 $k_{eff}$  = estimated collision  $k_{eff}$  from previous cycle or as entered by user for the first cycle.

Again, if fission is possible,  $k_{eff}$  is estimated by collision, absorption and track length (see Appendix F for development). The collision estimator sums the probability of neutron production when a particle collides in a fissile material over the source size:<sup>(5)</sup>

$$k_{eff}^C = \frac{1}{N} \sum_i \omega_i \left[ \frac{\sum_k f_k \bar{v}_k \sigma_{f_k}}{\sum_k f_k \sigma_{t_k}} \right]_i \quad (9)$$

$i$  = summed over all collisions in a cycle in fissile material

$k$	=	summed over all isotopes of the material involved in the collision
$\sigma_f$	=	microscopic fission cross section
$\sigma_t$	=	total microscopic cross section
$\bar{v}_k$	=	total average number of neutrons produced by fission at the incident energy of this collision
$f_k$	=	atomic fraction for nuclide $k$
$N$	=	nominal source size for cycle
$\omega_i$	=	weight of particle entering collision

The absorption estimator sums the probability of neutron production when a particle collides with a fissile nuclide over the source size<sup>(5)</sup>:

$$k_{eff}^A = \frac{1}{N} \sum_i \omega_i^* \left[ \bar{v}_k \frac{\sigma_{f_k}}{\sigma_{f_k} + \sigma_{a_k}} \right]_i \quad (10)$$

and

$$\omega_i^* = \omega_i \frac{\sigma_{f_k} + \sigma_{a_k}}{\sigma_{t_k}} \quad (11)$$

where $i$	=	summed over all collisions with a fissile isotope in a cycle
$k$	=	isotope
$\sigma_{ak}$	=	microscopic absorption cross section

Finally the track length estimator sums the probability of neutron production when a particle

traverses a distance  $d$  in a fissionable material over the source size<sup>(5)</sup>:

$$k_{\text{eff}}^{\text{TL}} = \frac{1}{N} \sum_i \omega_i \rho_i d_i \sum_k f_k \bar{v}_k \sigma_{f_k} \quad (12)$$

where  $i$  = summed over all neutrons trajectories

$\rho$  = atomic density of the material

$d$  = trajectory track length from the last event

Thus  $k_{\text{eff}}^C$ ,  $k_{\text{eff}}^A$  and  $k_{\text{eff}}^{\text{TL}}$  represent the three different estimators of the average number of fission neutrons produced per cycle. These three estimators are based on the same random walk and therefore correlated. The degree of correlation is estimated by their covariance. Then MCNP 4A combines the three individual  $k_{\text{eff}}$  by using a maximum likelihood procedure outlined by Halperin<sup>(6)</sup> and developed in reference 7:

$$k_{\text{eff}}^{\text{combined}} = \frac{\sum_{l=1}^3 f_l \bar{k}^l}{g} \quad (13)$$

where

$$f_l = S_{jj}^2 (S_{kk}^2 - S_{ik}^2) - S_{kk}^2 S_{ij}^2 + S_{jk}^2 (S_{ij}^2 + S_{ik}^2 - S_{jk}^2) \quad (14)$$

$$g = (S_c^2 + S_a^2 - 2S_{ca}^2)(S_c^2 + S_t^2 - S_{ct}^2) - (S_c^2 + S_{at}^2 - 2S_{ca}^2 - S_{ct}^2) \quad (15)$$

$\bar{k}^l$  = individual average  $k_{\text{eff}}$  obtained by averaging the individual cycle  $k_{\text{eff}}$

estimator over the number of active cycles

$S_{ii}^2$  = variance of estimator  $i$

$S_{ij}^2$  = covariance between estimator  $i$  and  $j$

with  $l$  corresponding to the partial permutation of  $i, j$  and  $k$  as listed in table 2.1.

Table 2.1

Perturbation of  $i, j$ , and  $k$  for Combining the Three  $k_{eff}$  Estimators

$l$	estimator	$i$	$j$	$k$
1	collision	1	2	3
2	absorption	2	3	1
3	track length	3	1	2

The three combined  $k_{eff}^{combined}$  is the best final estimate from an MCNP calculation.<sup>(5,6,7)</sup>

## 2.4 EVALUATION OF THE PRECISION IN MCNP4A

In classical methods, the precision of a simulation depends on the number of intervals or steps used. Similarly for Monte-Carlo methods the precision depends on the number of trials and more specifically in MCNP 4A the number of histories. Here the precision can be defined as the difference between the result obtained from a finite number of intervals, trials or histories (whichever is used) and the result obtained if one could run an infinite number of intervals, trials or histories. Since it is not possible to use infinite numbers and therefore calculate the true value of the simulation, one must rely on an estimation of the precision. MCNP 4A uses the variance  $S^2$  to estimate the precision, defining a confidence interval in which the true answer is assumed to be found 68%, 95% and 99% of the time depending on whether one two or three standard deviations

(S) are used. The estimate

of the variance  $S^2$  on the sampled cycle  $k_{eff}$  is given by:<sup>(5)</sup>

$$S^2 = \frac{\sum_{i=1}^N (k_{eff,i}^{estimator} - \bar{k}_{eff}^{estimator})^2}{(N-1)} \quad (16)$$

where  $k_{eff,i}^{estimator}$  = one of the three individual  $k_{eff}$  estimators on cycle  $i$  of the active cycles  
 $\bar{k}_{eff}^{estimator}$  = average of one of the three individual  $k_{eff}$  estimators over the active cycles  
 $N$  = number of active cycles

The estimate of the variance of  $\bar{k}_{eff}^{estimator}$  is given by:  $S^2/N$ . Therefore, in order to increase the precision of the simulation by a factor of two, we need to quadruple the number of histories. This evaluation of the precision is only used for the three individual  $k_{eff}$  estimators. Several of the results listed in this work are based on the three combined  $k_{eff}$  estimators. The evaluation of the standard deviation for the three combined  $k_{eff}$  estimators is given by:<sup>(7)</sup>

$$S = \frac{S_1}{g_s N(N-3)} \left[ 1 + N \left( \frac{S_2 - 2S_3}{g_s} \right) \right] \quad (17)$$

where

$$g_s = (N - 1)^2 g \quad (\text{see eq. 15}) \quad (18)$$

$$S_1 = (N - 1)^3 \sum_{l=1}^3 f_l \sigma_{1l}^2 \quad (\text{see eq. 14}) \quad (19)$$

$$S_2 = (N - 1) \sum_{l=1}^3 (S_{jj}^2 + S_{kk}^2 - 2S_{jk}^2) \bar{k}_{eff_l}^{estimator} \quad (20)$$

$$S_3 = (N - 1) \sum_{l=1}^3 (S_{kk}^2 + S_{ij}^2 - S_{jk}^2 - 2S_{ik}^2) \bar{k}_{eff_i}^{estimator} \bar{k}_{eff_j}^{estimator} \quad (21)$$

With  $l$  corresponding again to the partial permutation of  $i, j$  and  $k$  as listed in Table 2.1

## 2.5 THE ACCURACY IN MCNP 4A

The precision of a simulation is only an internal check and does not give any indication of the accuracy of the simulation. Although one can calculate a highly precise answer by running a large number of histories, if the nature of the problem has not been represented properly the systematic error can be significantly larger than the standard deviation. The following factors affect the systematic error, also referred to as the accuracy, of the simulation:

a. Code:

- i) The theory: in this case transport theory is used and is presently the best tool

- available;
- ii) The uncertainty in the data such as the reaction cross sections. Here the ENDF/B-V library supplied by Los Alamos was used as well as special material commands. Although a more recent library is now available, the ENDF/B-V library was the most complete library available and it has been used successfully in the past by many users;
  - iii) Atomic weight;
  - iv) Avogadro's number;
  - v) Coding error;
  - vi) Compiler error.
- b. Modelling:
- I) The definition of the source;
  - ii) The definition of the geometry;
  - iii) The characteristics of the material;
  - iv) Approximation in modelling; and
- c. User error.

Very little control on the error could be associated with the code, but as mentioned in Reference 5, this is a very mature code which has yielded many successful simulations for many users. To reduce the modelling error associated with the definition of the source, the simulations were first run with a small number of sources and histories, using 20 inactive cycles to allow the model to converge and 40 active cycles to calculate the  $k_{eff}$ . After insuring the model had become stable by plotting the progression of the  $k_{eff}$  with one standard deviation and looking at the figure of

merit, the last source file was used as the starting point for the next simulation which used a larger source and more histories.<sup>(5)</sup> This process was repeated until a satisfactory compromise was reached between the computing time required and the standard deviation. Typical run progresses are shown in figures presented in Chapter 5 and Appendix D.

To address the geometry issue, successively more complex models were developed as described in Chapters 3 and 4. User error being always a possibility, the following precautions were taken. The geometry was plotted at several locations using several viewing angles to ensure that the surfaces and cell represented what they were intended to. A convenient MCNP 4A test was run to ensure that the geometry had no gap (undefined area) and no overlapping of cells. The materials used in the simulation were voided and the entire geometry was flooded with neutrons. Since the geometry contained no material, the track lengths were allowed to transverse the entire geometry and would have therefore been likely to visit all areas of the model. If a neutron had passed through any gap or overlapping area, MCNP 4A would have given an error.

Although several measures were taken to reduce the systematic error, it is impossible to eliminate it completely. Furthermore, the exact determination of the accuracy of the calculated  $k_{\text{eff}}$  is nearly impossible. Accordingly, the standard deviation is used as an indication of the error.

## 2.6 VARIANCE REDUCTION TECHNIQUES

As we have seen, the precision of a Monte-Carlo method is closely related to the amount of histories used. In order to increase the precision one can increase the number of histories. This technique of improving the precision has a high computing cost. Therefore, other techniques are often used; they consist of concentrating the sampling in an important areas of the model and reducing the amount of sampling in the unimportant area of the model.

The most commonly used variance reduction technique is the geometry splitting/Russian roulette technique. Basically, this technique increases the number of particles when particles migrate from an unimportant cell to an important cell, therefore increasing the sampling in the important region. As well, when particles migrate from an important cell to an unimportant cell some particles are killed to avoid wasting time in tracking them. In all cases the weight of the particles are preserved; therefore, when particles split the weight is divided among the daughters, and when particles are killed the weight of the survivors are increased. The importance of each cell is set by the user with command “IMP”. Due to the complexity of the geometry and the nature of the calculation, no variance reduction techniques were used. All the “IMP” commands were set to 1, except in void space where it was set to 0.

## CHAPTER 3 -THREE DIMENSIONAL REACTOR MODEL

### 3.1 GENERAL DESCRIPTION OF RMC SLOWPOKE-2 REACTOR

The main problem encountered, when simulating the SLOWPOKE-2 reactor at RMC-CMR with deterministic methods, has been the lack of symmetry and its small size (Figure 3.1). The core is composed of 198 fuel elements distributed to maximize the neutron flux on the periphery where the irradiation sites are located. It was also designed to have a relatively high flux at the centre where a single control rod is located. The reactor has:

- a. A beryllium reflector composed of an annulus, a lower reflector and a top shim;
- b. Five internal irradiation sites distributed at regular intervals within the beryllium annulus;
- c. One large outside irradiation site in the water of the reactor container, between the beryllium reflector and the container wall;
- d. Two small outside irradiation sites in the water of the reactor container;
- e. One cadmium-lined irradiation site, again, in the water of the reactor container;
- f. A thermal column (Figure 3.1a)(this is a unique feature of the RMC SLOWPOKE). The thermal column is a container of heavy water located between the annulus reflector and the reactor container. The thermal column allows more neutrons to reach the nose piece of a neutron beam tube, located in the pool and used for neutron radiography;
- g. A unique control rod located at the centre of the reactor;
- h. Several structural devices holding these components together (not represented in the

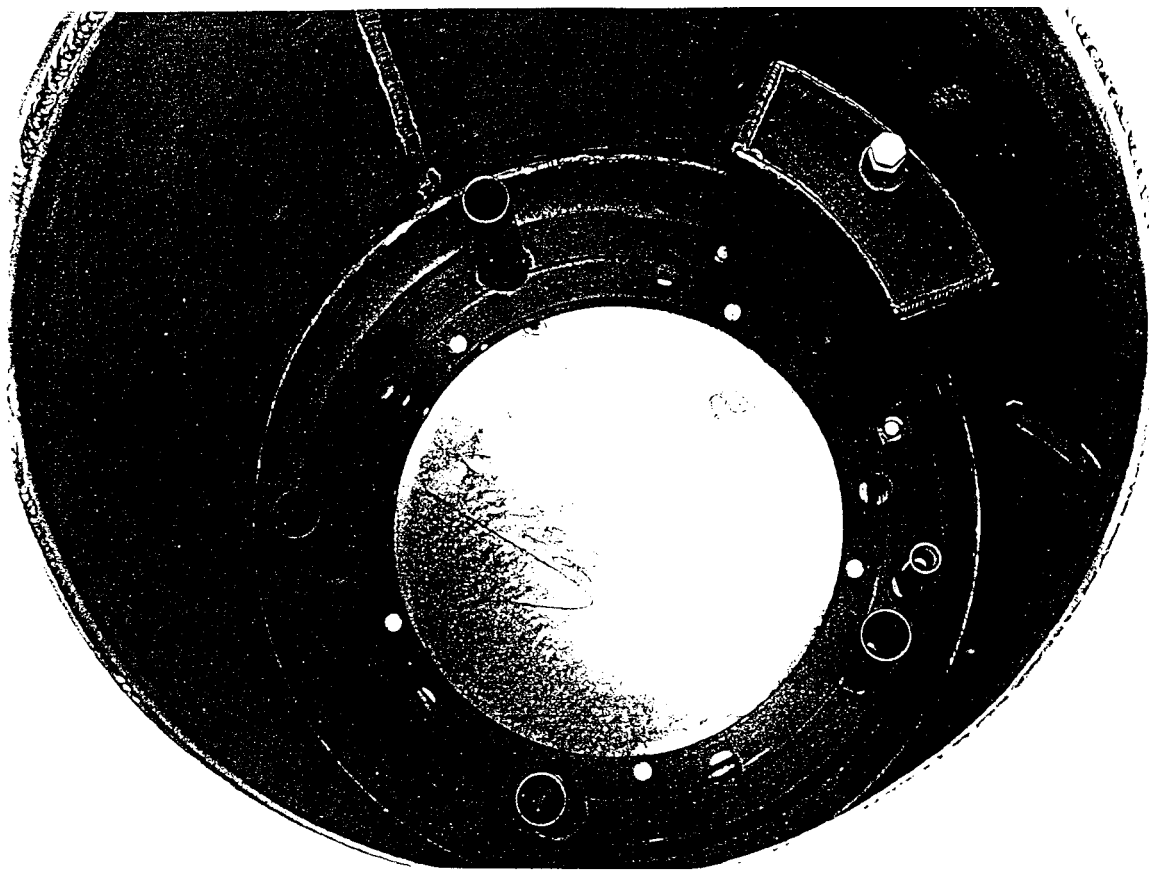


Figure 3.1a Photograph of the bottom of the reactor vessel showing the thermal column in place against the vessel wall

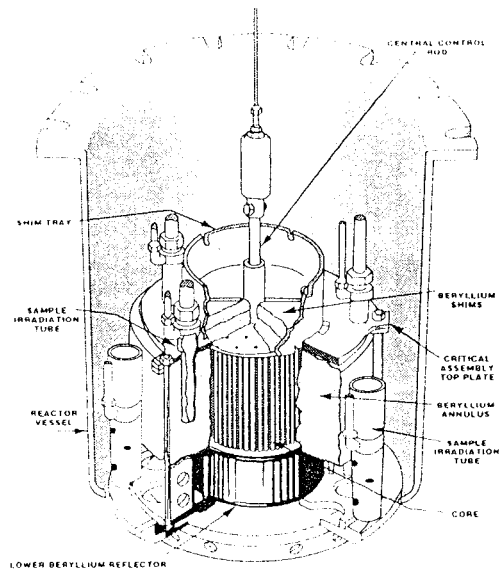


Figure 3.1b SLOWPOKE-2 reactor code

- simulation); and
- i. the reactor container vessel.

### **3.2 THE INPUT FILE**

The model preserved as much as possible the details of the core and facility, in order to maximize the accuracy of the absolute value of the excess reactivity. Furthermore, in order to allow future studies in flux mapping and possibly modelling of the neutron beam tube, the model was extended to the limit of the reactor pool . Therefore, much of the data included in the input deck are proprietary and could not be included in the body of the thesis. Only the generic aspects of the model are described in the following sections, but a more detailed description of the input file included as Appendix A is included in a few copies of this thesis.

### **3.3 THE FUEL**

The fuel elements were defined by three distinct regions, the uranium dioxide, the air gap and the Zircalloy-4 cladding (see Figure 3.2). The uranium dioxide was entered as a mixture of uranium-235 and uranium-238 with an enrichment of 19.89 weight percent of uranium-235, and oxygen 16.<sup>(8,9,10)</sup> The air was entered as a mix of oxygen and nitrogen . The Zircalloy-4 was entered as elemental zirconium since the level of components and impurities were not readily available. Typical composition of Zircalloy-4 cladding is 1.5 percent tin, 0.2 percent iron and 0.1 percent chromium.<sup>(11)</sup> With these numbers the macroscopic cross section of the Zircalloy-4 was calculated in Table 3.1 as  $0.9 \text{ cm}^{-1}$  compared to  $0.8 \text{ cm}^{-1}$  for pure Zr.<sup>(12)</sup> Given the small thickness of the material, the impact on criticality calculation should be minimal.

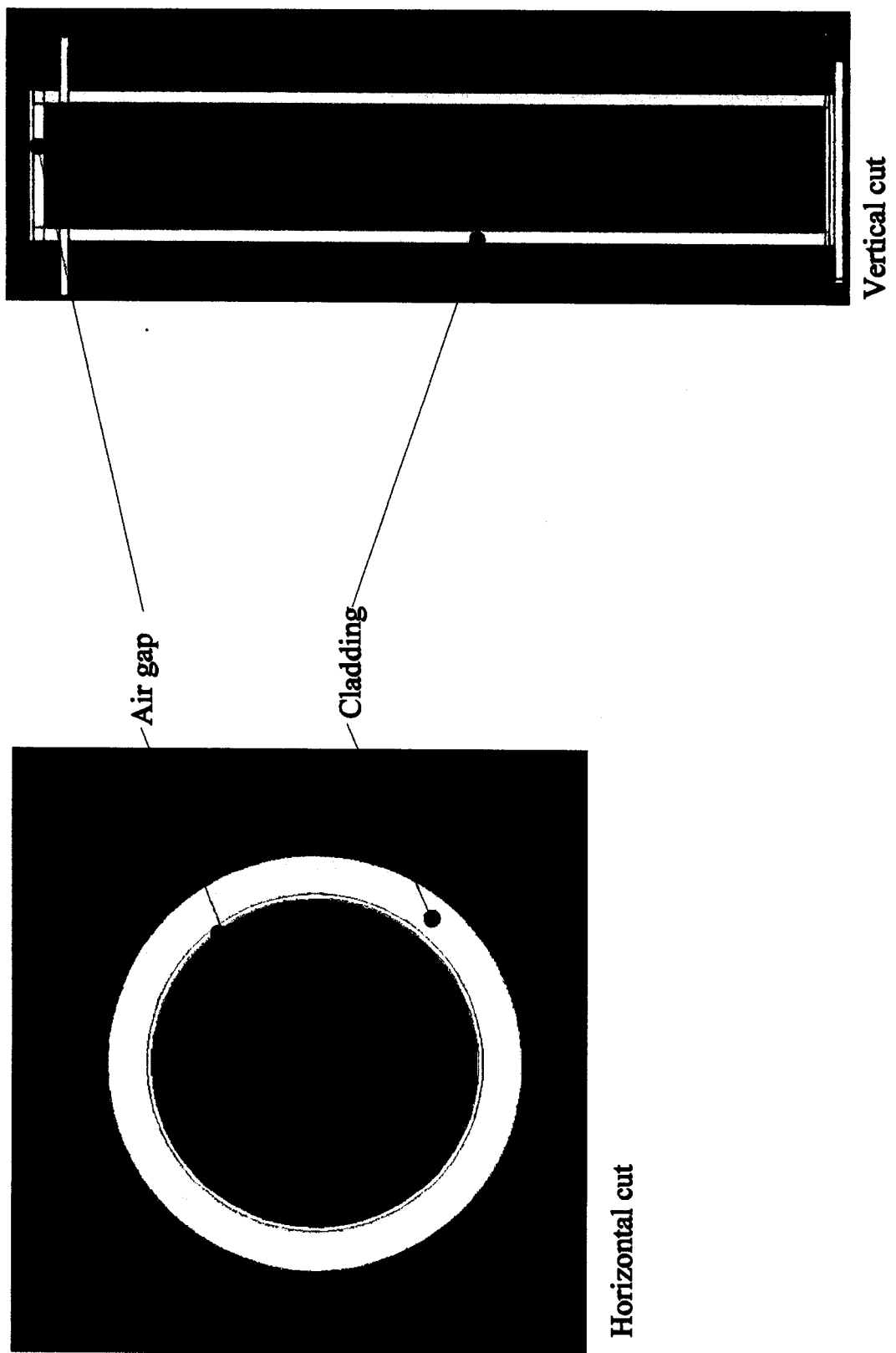


Figure 3.2 Cross section of fuel element

Table 3.1  
Calculation of  $\Sigma_a$  Thermal for Zircalloy-4

Material	Atomic Weight	Fraction by Weight (FW)	Density 6.49g/cm <sup>3</sup> x F W	Atoms x 10 <sup>23</sup> per cm <sup>3</sup>	$\sigma_a$ (barns)	$\Sigma_a$ (cm <sup>-1</sup> ) x 10 <sup>-2</sup>
Zr	91.22	0.982	6.37318	0.42074	0.185	0.78
Sn	118.69	0.015	0.09735	0.00494	.63	0.03
Fe	55.847	0.002	0.01298	0.0014	2.55	0.04
Cr	51.996	0.001	0.00649	0.0008	3.1	0.02
						total $\Sigma_a$ 0.87

The internal radius of the cladding given in Reference 9 was found to be smaller than the radius of the fuel given in Reference 10. The dimensions taken from Reference 10 were similar to the one used in Reference 8. Upon consultation, B. Townes<sup>(13)</sup> and G. Burbidge<sup>(14)</sup> indicated that the data taken from Reference 10 were more accurate than the drawing. Therefore, the average length and radius of the individual dimensions of the fuel as described in Reference 10 were used for the model. An air gap between the fuel and the cladding was included in the model. The radial air gap thickness was entered as the minimum limit stated in Drawing A17997. The representation of the cladding end cap was simplified. The cladding was actually modelled by discs, therefore the axial air gaps were entered as an approximation of the axial clearance given at Reference 9. The internal dimension of the cladding had to be modified to match the dimensions of the air gap, but the thickness of the cladding was preserved. These approximations of the air gap, the zirconium end caps and cladding volumes, should not affect the criticality calculations significantly because the differences in the macroscopic cross sections are relatively small.

Drawing AL82245,<sup>(15)</sup> and Reference 1 were used to derive the position of the fuel elements and their immediate surroundings including the fuel cage grid plate (see Figure 3.3 to 3.5). First the lattice geometry was determined (Appendix A, not all copies) from Drawing AL82245 and then it was defined in the model using the lattice command. Since the fuel elements are not uniformly distributed and several sites do not have fuel elements, the fill command and universe commands were used jointly to define the location of the fuel element as described in Reference 1 (the lattice, fill and universe commands are defined on pages A-5 and A-6). The top and bottom fuel cage grid plate were defined similarly, locating accurately most of the water holes. Some water holes were not modelled. This results in only a small volume of water being displaced by zirconium, and therefore should not influence the criticality calculations. The water in the core and the reactor was defined as a pure substance. A special material command (lwtr.01t) was used in order to account for the effects of chemical binding and crystal structures of the water for incident neutron energies below 4 eV ( $S(\alpha, \beta)$  treatment).

### 3.4 THE CONTROL ROD

The geometry of the control rod was approximated from Drawing A10759 and A15292.<sup>(16,17)</sup> The most important component of the control rod is the cadmium. The dimension and geometry of the cadmium were entered as per Drawing A15292; its location within the control rod sheath had to be approximated from Drawing A10759 and A15292. Although the drawings did not indicate clearly where the control rod insert was located, the uncertainty of this approximation should be less than one centimetre. The control rod's external dimensions were respected but the geometry was simplified. The geometry of the model consists of the cadmium tube inside an aluminum tube with an aluminum cylinder at each end (see Figure 3.6). The modelling of the control rod did not

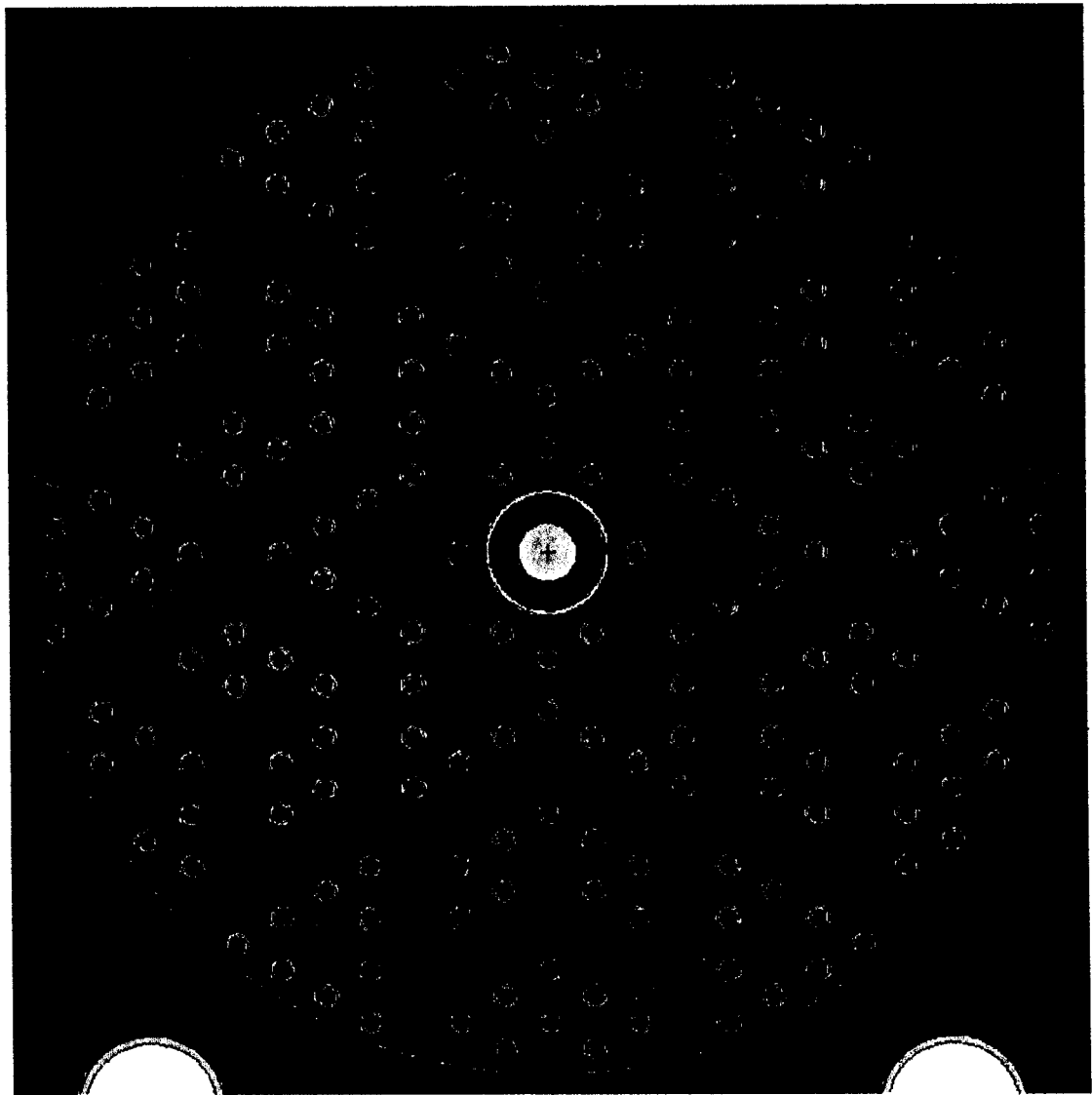
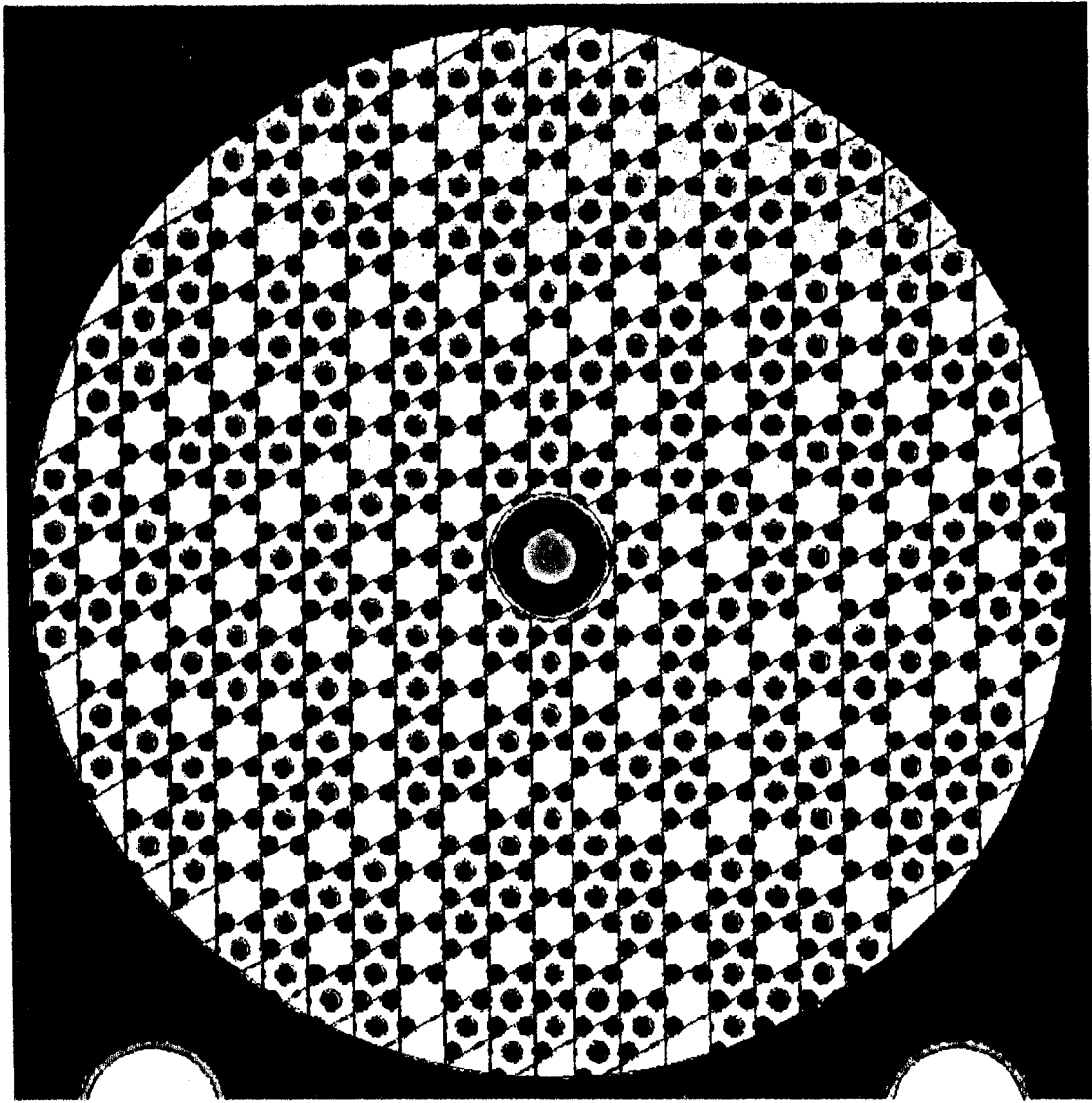


Figure 3.3 Horizontal cut showing fuel element distribution

Green → Fuel  
Blue → Water  
Yellow→ Air in internal  
irradiation sites  
Purple → Annulus reflector  
Light Blue → Aluminum  
cladding of  
control rod



Green -> Fuel  
Pink -> Grid  
Blue -> Water  
Yellow-> Air in internal  
irradiation sites  
Purple -> Annulus reflector  
Light Blue -> Aluminum  
cladding of  
control rod

Figure 3.4 Horizontal cut showing top fuel cage grid

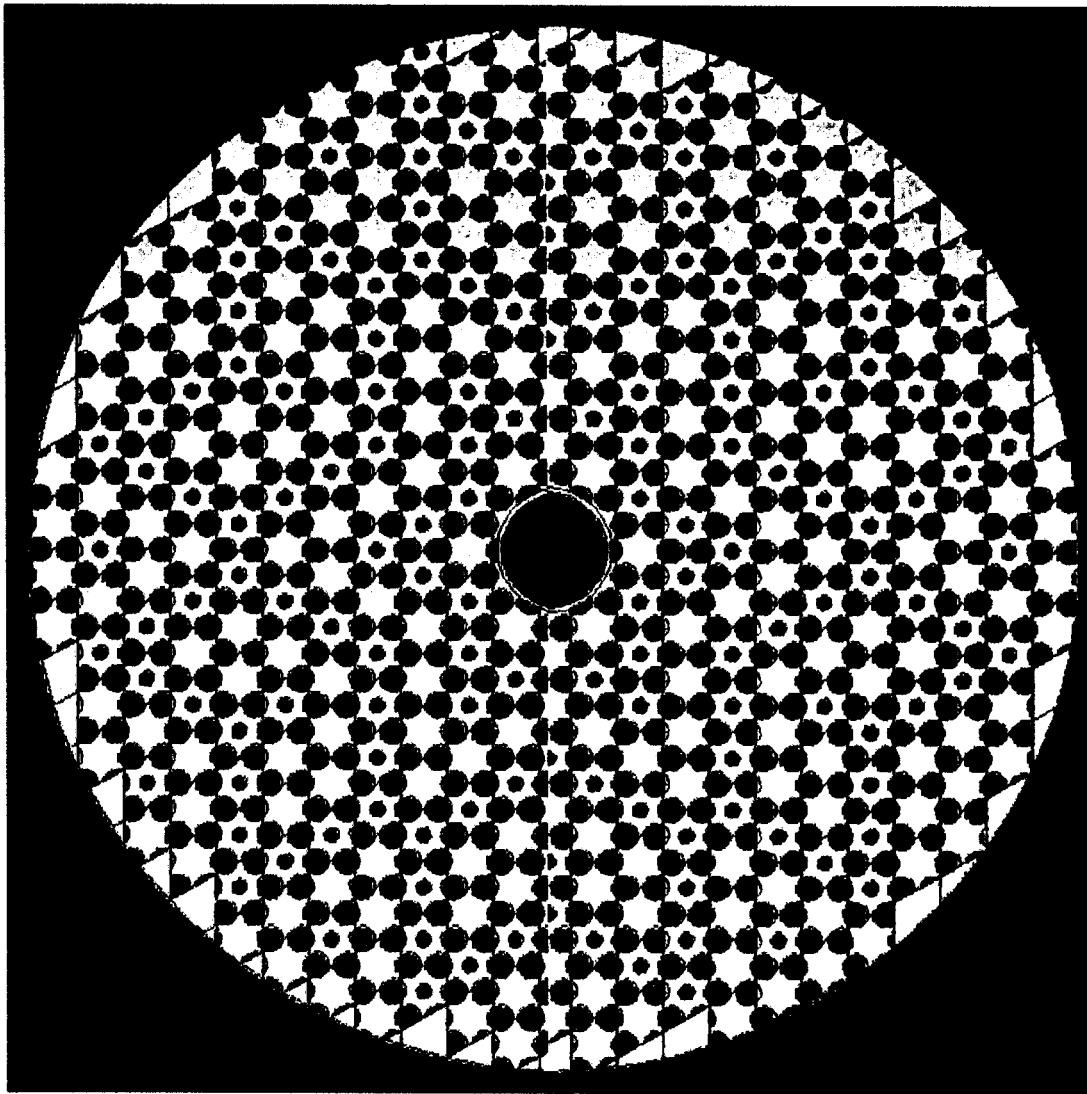
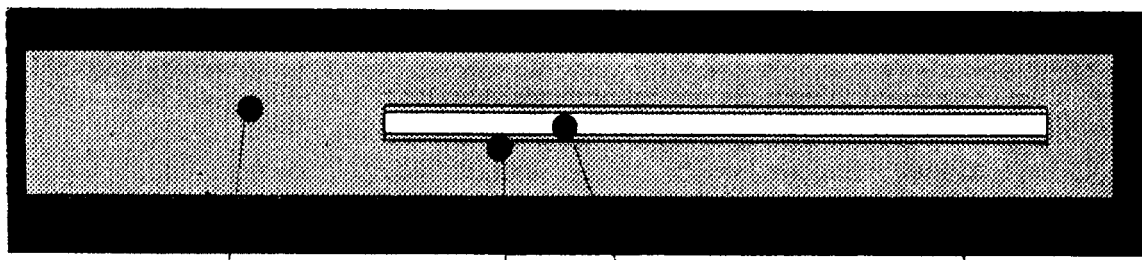
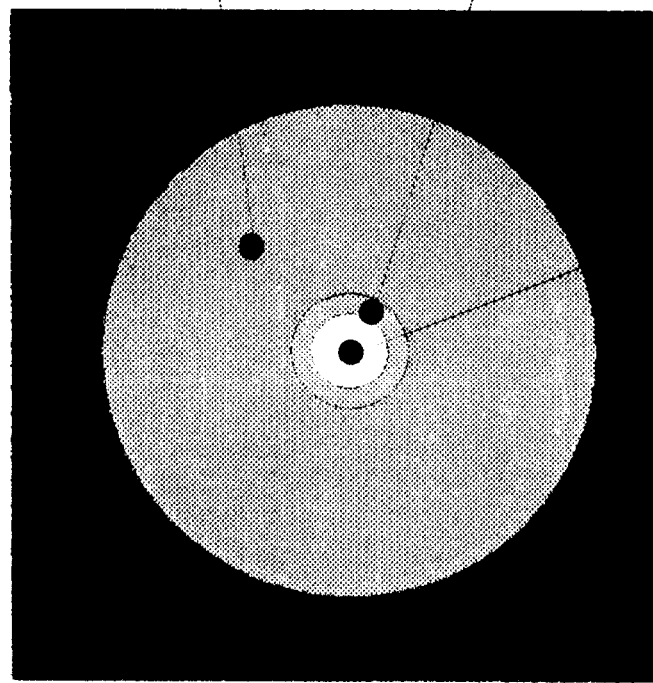


Figure 3.5 Horizontal cut showing bottom fuel cage grid

Pink → Grid  
Blue → Water



Vertical cut



Horizontal cut

Water

Air

Aluminum

Cadmium

Figure 3.6 Cross section of control rod

extend any further than the sheath. The materials used for the control rod were elemental cadmium, aluminium 6061-T6 as defined in Reference 18, and air, as previously described.

### 3.5 IRRADIATION SITES

The five internal irradiation sites are all identical and described in Drawing A10733.<sup>(19)</sup> It would have been very tedious to try to reproduce their geometry in the model, therefore they were represented by straight Aluminium 6061 -T tubes filled with air, which extended all the way to the top of the reactor pool (see Figure 3.7). The bottom location of the internal irradiation site was determined using Drawing A10716.<sup>(20)</sup> Given the size, location and material of the internal irradiation sites, these approximations should have a negligible effect on the criticality calculation.

The four external irradiation sites include one large site, two small sites and a cadmium-lined site (see Figure 3.8). The model was designed to represent the reactor configuration at the time of commissioning, therefore site number 8 which is now flooded was modelled in the same manner as the other sites, with an air-filled centre. One of the sites has been replaced by a thermal column which will be discussed later. The geometry of the external sites were approximated similarly to the internal sites, with the exception that they run all the way down to the bottom of the reflector annulus. Their location was approximated using a sketch taken from Reference 21, as well as measurements taken from the scale model of the SLOWPOKE-2 displayed at RMC-CMR. The larger site reflects the dimension of Drawing A10737.<sup>(22)</sup> The modelling of the small external irradiation sites is exactly the same as the internal one (see Drawing A17979).<sup>(23)</sup> The cadmium site was modelled with the same dimensions as a small irradiation site with the exception of being lined with a cadmium layer on the outside which matches the total length of the reflector annulus. The dimension of this cadmium lining was not initially available. Since the aim of the cadmium lining

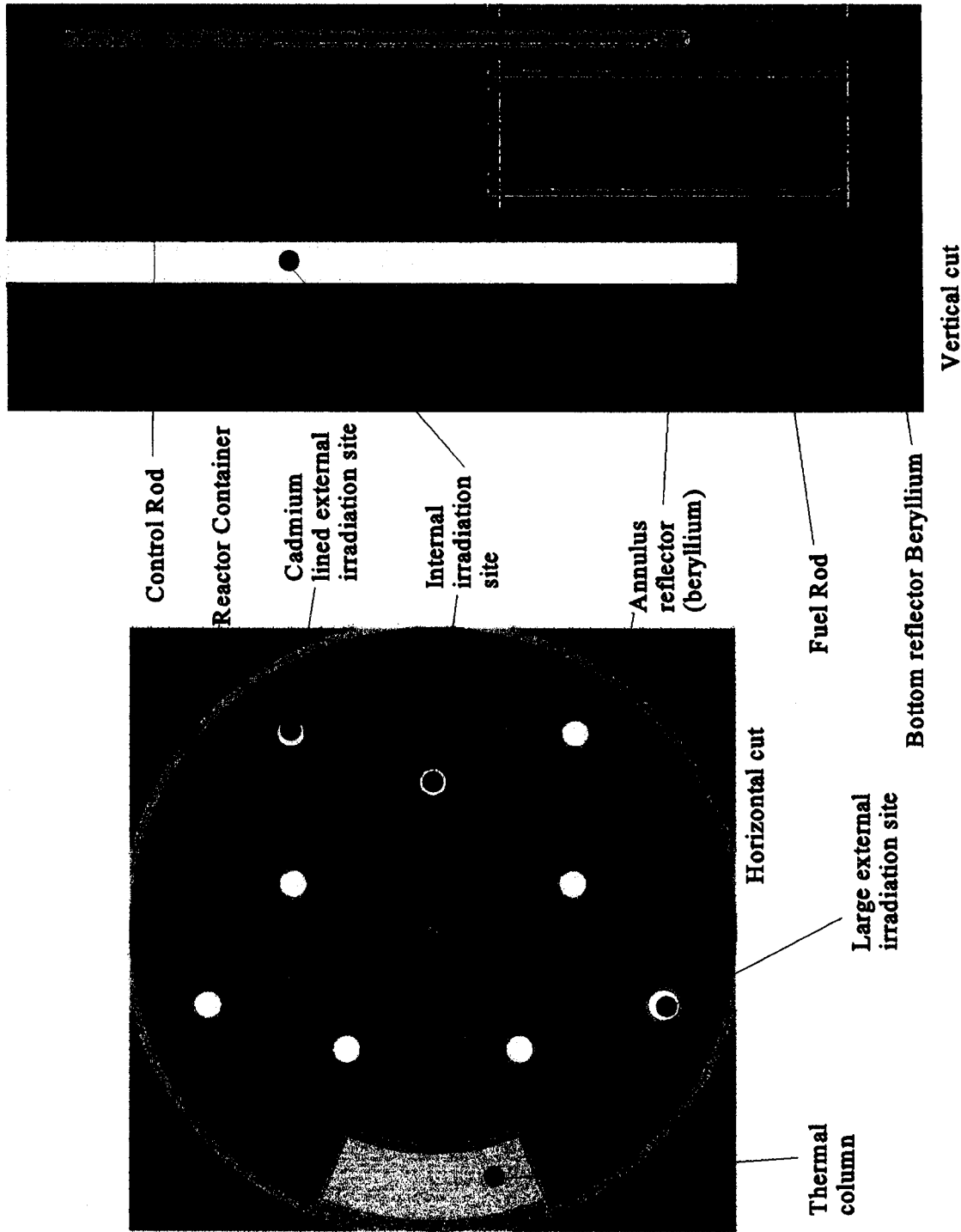


Figure 3.7 General layout of irradiation sites

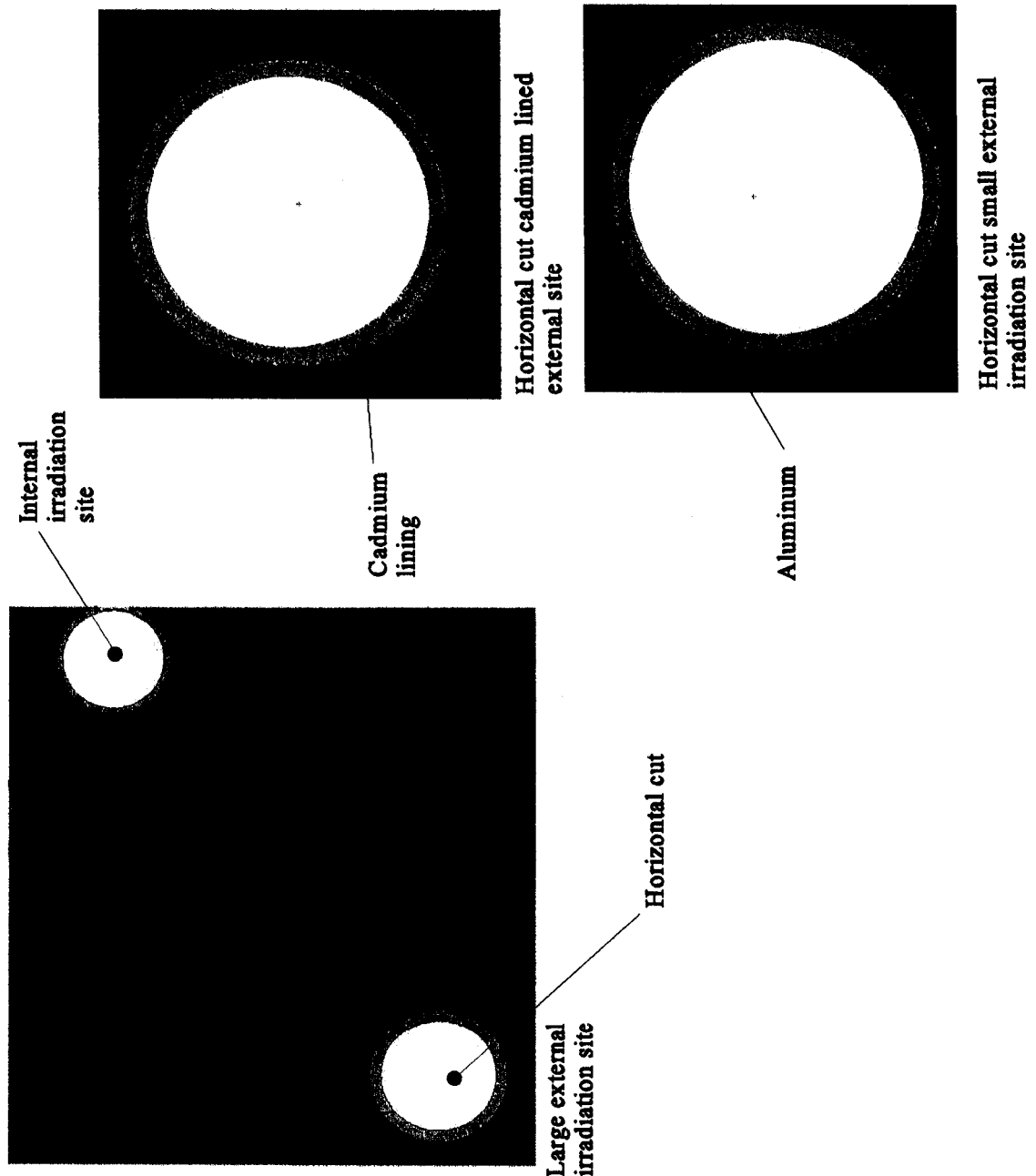


Figure 3.8 External irradiation sites

is to prevent any of the thermal neutrons from reaching the sample, the seven half value layer (HVL) thickness for thermal neutrons was calculated using:<sup>(12)</sup>

$$I(X) = I_0 e^{-\Sigma_a X} \quad (22)$$

such that

$$\frac{I_0}{I(x)} = 2^7 \quad (23)$$

hence, Eqs. (22) and (23) yield

$$X = \frac{\ln(2^7)}{\Sigma_a} \quad (24)$$

Using  $\Sigma_a = 113.56 \text{ cm}^{-1}$  for cadmium,

therefore  $X = 0.0427 \text{ cm}$  (25)

Where  $I_0$  = thermal neutron flux at point 0

$I(X)$  = thermal neutron flux at distance  $X$

$\Sigma_a$  = macroscopic absorption cross section (cadmium)

This calculation provides a minimum thickness for the seven HVL's. However, values of 0.0254 and 0.0508 cm were considered (0.01 and 0.02 inches), as these correspond to cadmium sheaths readily available from the manufacturers. In order to assess the importance of the uncertainty on the

cadmium lining thickness, the  $k_{eff}$  calculation was carried out for these two values of the thickness, with the results reported in Table 3.2. As one would expect, no significant effects were observed on the  $k_{eff}$  calculation. (Although the thickness of the thermal neutron shield has doubled, the effect on the reactivity calculation should be negligible, as the shield is not in a region of the core where the thermal neutrons contribute significantly to fission. Furthermore, the probability of a neutron entering the cadmium shield is similar as the 0.0254 cm thick shield covers 2.11 percent of the solid angle from the reactor centre and the 0.0508 cm thick shield covers 2.16 percent of the solid angle). The .0508 cm cadmium lining was retained as it is similar to the control rod lining.

Table 3.2

Comparison of Cadmium-Lining of Irradiation Site

Number of Neutrons	$k_{eff}$ Calculation performed on IBM RISC 6000 model 350		$k_{eff}$ Calculation performed on HP APOLLO series 700	
	Thickness		Thickness	
	0.0254 cm	0.0508 cm	0.0254 cm	0.0508 cm
100	1.0041±0.0129	0.9950±0.0123	1.0198±0.0152	1.0118±0.0128
1 000	0.9953±0.0048	0.9915±0.0042	0.9982±0.0045	0.9948±0.0039
10 000	0.9932±0.0015	0.9955±0.0011	0.9956±0.0013	0.9953±0.0013
50 000	0.9960±0.0007	0.9970±0.0006	0.9954±0.0006	0.9952±0.0004*

\*was processed with 100 000 neutrons instead of 50 000 neutrons

Modelling these irradiation sites was particularly important as this gives an opportunity to measure the flux and, observe the reactivity changes due to the placement or withdrawal of samples.

### **3.6 REFLECTOR**

The bottom reflector was entered as a disc with the dimensions of Drawing A10712<sup>(24)</sup> (see Figure 3.9). The top reflector was entered as per Drawing A13988<sup>(25)</sup> and Reference 26, to represent the configuration of the reactor at commissioning (see Figure 3.9). The external dimensions of the reflector annulus were entered as per Drawing A10716.<sup>(20)</sup> The internal geometry of the radial reflector was limited to only include the simplified irradiation sites as described previously (see Figure 3.7 and 3.9). Since it was noted<sup>(3)</sup> that the impurities in the Beryllium had a significant effect on the reactivity (approximately 4 mk), the impurities that were available in the cross section library ENDF/B-V were included in the model(Appendix B).<sup>(27)</sup>

### **3.7 THERMAL COLUMN**

Some of the dimensions of the thermal column were not available at the time the model was put together (see Figure 3.10). The circumferential dimension was later found to be in agreement with Drawing A17996,<sup>(28)</sup> but the thickness of the aluminium wall and the height of the column were not found. A quick test performed with 10 000 neutrons, 20 inactive cycles and 40 active cycles was inconclusive as  $k_{eff}$  showed a slight increase on the HP APOLLO series 700 and a slight decrease on the IBM RISC 6000 model 350 when the wall thickness was changed from 1 cm to 0.1 cm (the discrepancy between the two computers may be due to a compiler error). The difference in absorption of thermal neutrons due to a variation in thickness of the circumferential walls ( $\Delta X = 0.9$  cm) was looked at qualitatively. First the  $\Sigma_a$  thermal was calculated for Al 6061 T6 at Table 3.3, using Reference 20. Then, the fractional loss of thermal flux due to  $\Delta X$  was evaluated, using.<sup>(12)</sup>

$$I(X) = I_0 e^{-\Sigma_a \Delta X} \quad (26)$$

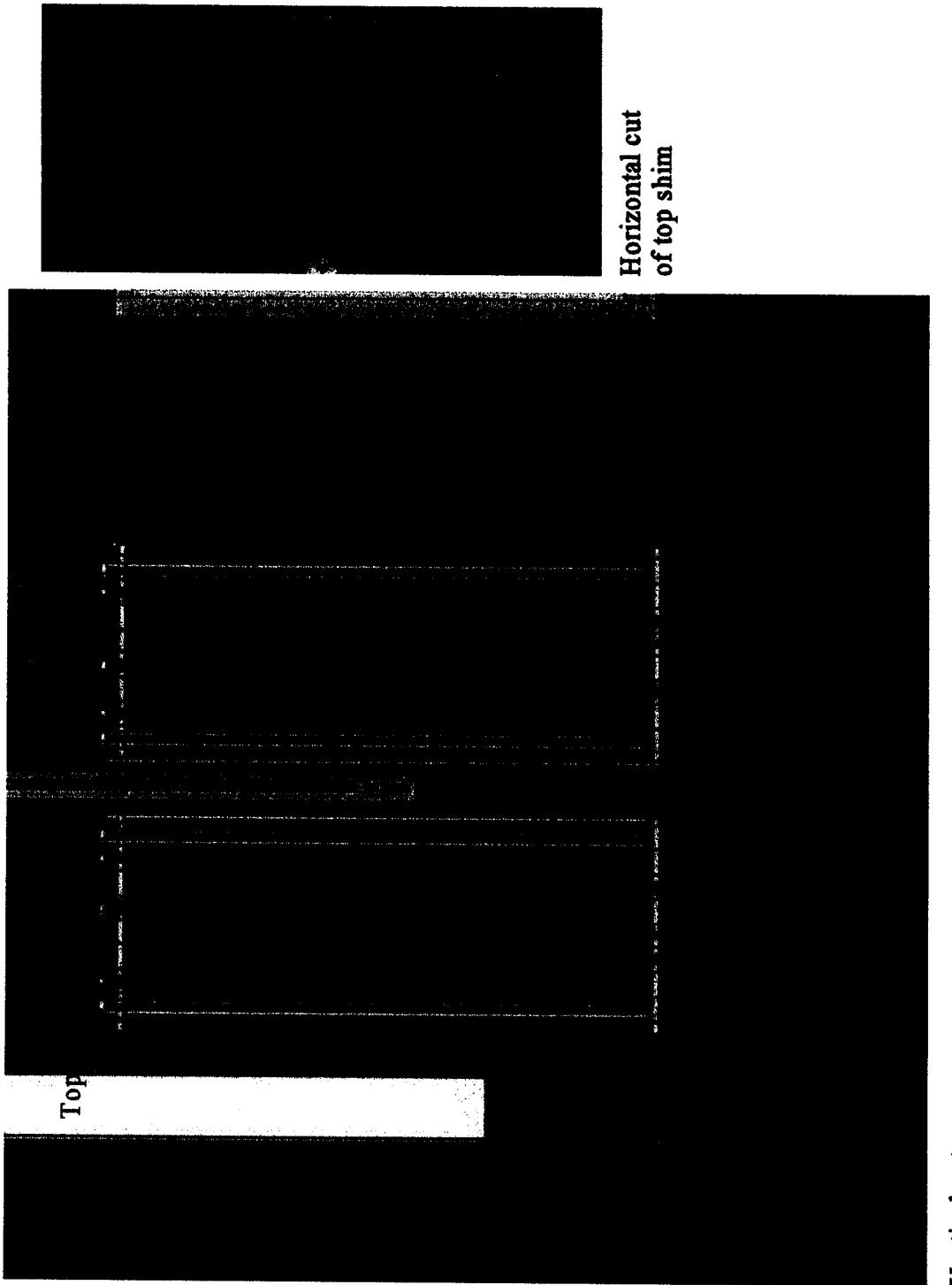


Figure 3.9 Reactor reflectors

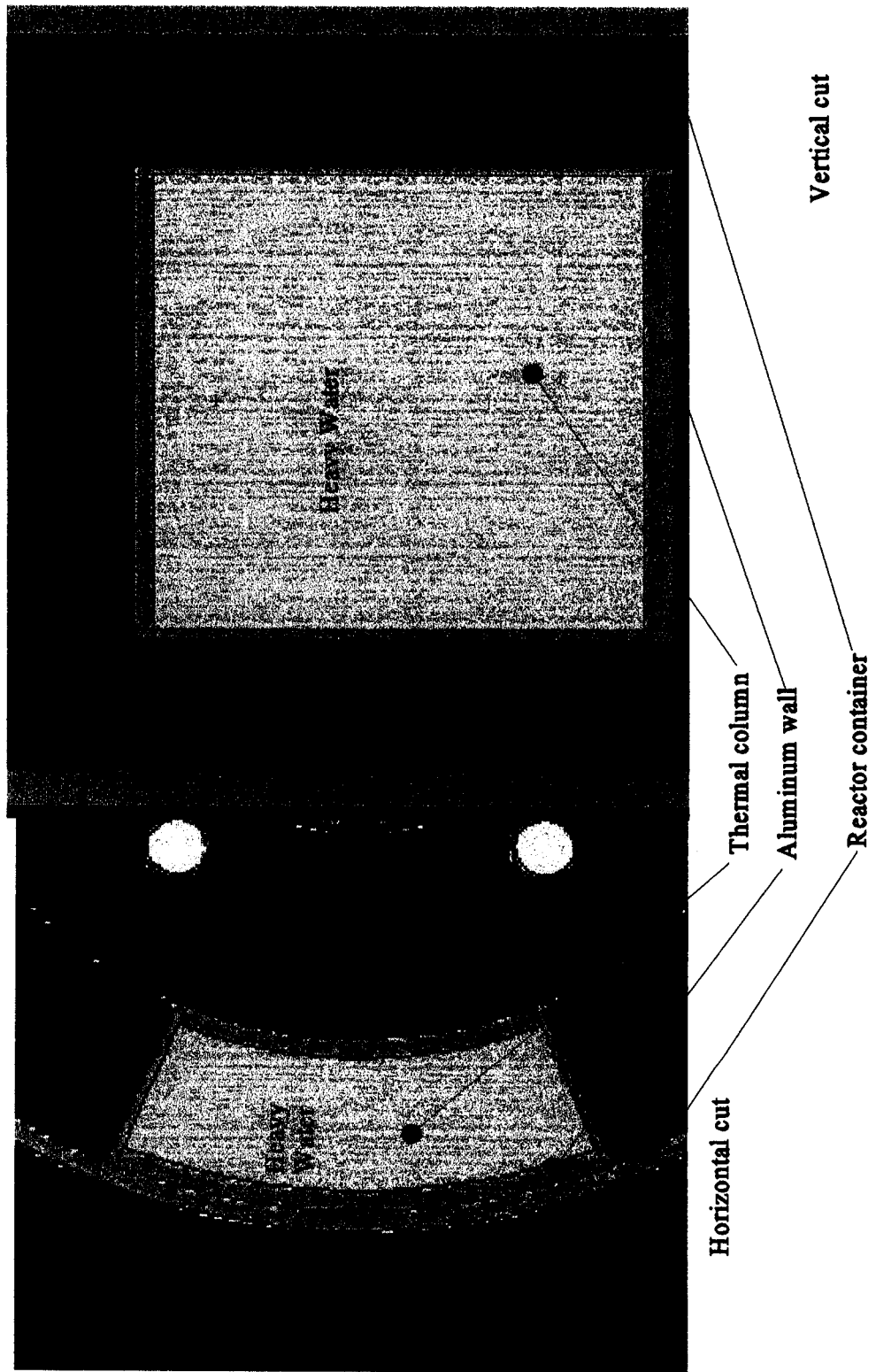


Figure 3.10 Thermal Column

yielding

$$\frac{I(x)}{I_0} = .99 \quad (27)$$

The effect of having an aluminum wall 0.9 cm too thick leads therefore to a reduction of only one percent of the thermal flux outside the reflector over one-eighth of the core, making the effects on the criticality calculation indeed negligible. It is important to realize that this correction should be made to the model before any simulation of the beam tube is considered since the effect on this kind of simulation may be more important.

Table 3.3

Calculation of  $\Sigma_a$  Thermal for Al 6061 T6

Material	Atomic Weight	Fraction by Weight (FW)	Density 2.70g/cm <sup>3</sup> *F W	Atoms x 10 <sup>23</sup> per cm <sup>3</sup>	$\sigma_a$ (barns)	$\Sigma_a$ (cm <sup>-1</sup> ) x 10 <sup>-2</sup>
Al	26.9815	0.9792	2.64384	0.5900952	0.23	1.36
Si	28.086	0.006	0.0162	0.00347	0.16	0.0056
Cu	63.54	0.0028	0.00756	0.0007	3.79	0.027
Mg	24.312	0.01	0.027	0.00669	0.063	0.0042
Cr	51.996	0.002	0.0054	0.0006	3.1	0.019
total $\Sigma_a$						1.41

The thermal column is filled with pure heavy water and uses a special material command hwtr.01t in the same fashion as the light water command. In order to gain some insight on the effects of having a thermal column equal to the entire height of the annulus reflector in the model instead of a partial height as in reality, the heavy water contained in the thermal column was replaced by

light water. The test was performed on the HP APOLLO series 700, with 10 000 neutrons, 20 inactive cycles and 40 active cycles, and showed a  $\Delta k_{\text{eff}}$  of 0.00061 with a standard deviation of 0.002. Therefore, the effect on the modelled  $k_{\text{eff}}$ , given the complete replacement of the thermal column by water, should be within plus or minus 2 mk. The total volume of the thermal column was overestimated by approximately 31% (Appendix C), the error associated with this approximation of the thermal column height should be plus or minus 0.6 mk (or 2 mk x 31%). Since the excess volume of heavy water is located at the top and bottom of the core, hence far from the reactor mid plane, plus or minus 0.6 mk (or 2 mk x 31%) should be the maximum error. Again, this should be corrected before any simulation of the beam tube is considered.

### **3.8 REACTOR CONTAINER AND POOL**

The reactor container was approximated by an aluminum 6061 T6 cylinder with a disk at the bottom (see Figure 3.11 and 3.12). The radius of the cylinder is as per Drawing A10714.<sup>(29)</sup>

The pool was modelled by a cylinder of water with the dimension from Reference 21 with the reactor container located off-centre in the pool. Once the simulations were completed it was noticed that, the emplacement of the reactor container was good, but the orientation relative to the beam tube was incorrect. This should not have any affect on the criticality calculation as the side of the pool is far from the core in all directions, but would have to be corrected before any attempt is made at modelling the neutron beam tube.

### **3.9 GENERAL**

The structural components and everything that is outside of the water pool were not modelled. The relative positioning of the components of the model were based on Drawing A18226<sup>(30)</sup> and measurements taken from the scale model displayed at RMC-CMR. The cross

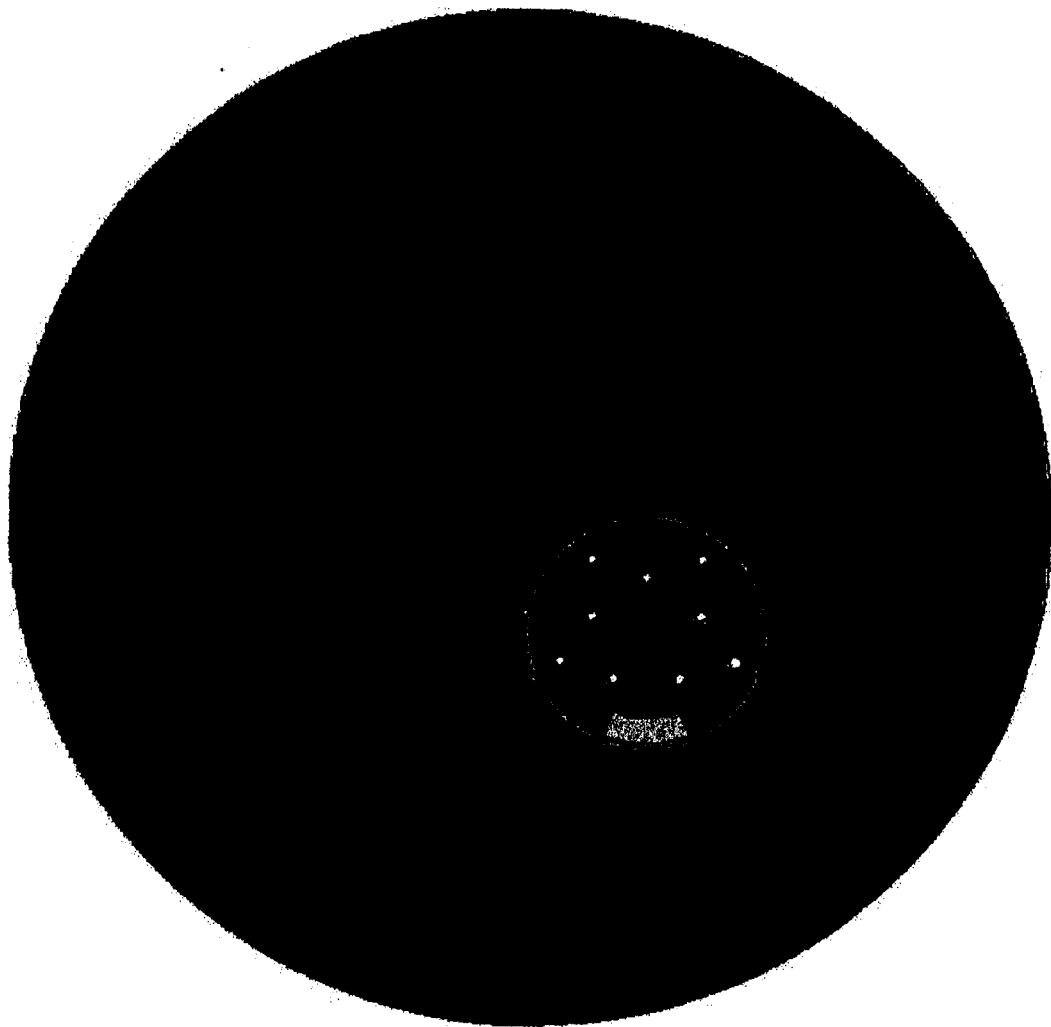


Figure 3.11 Horizontal cut of reactor pool

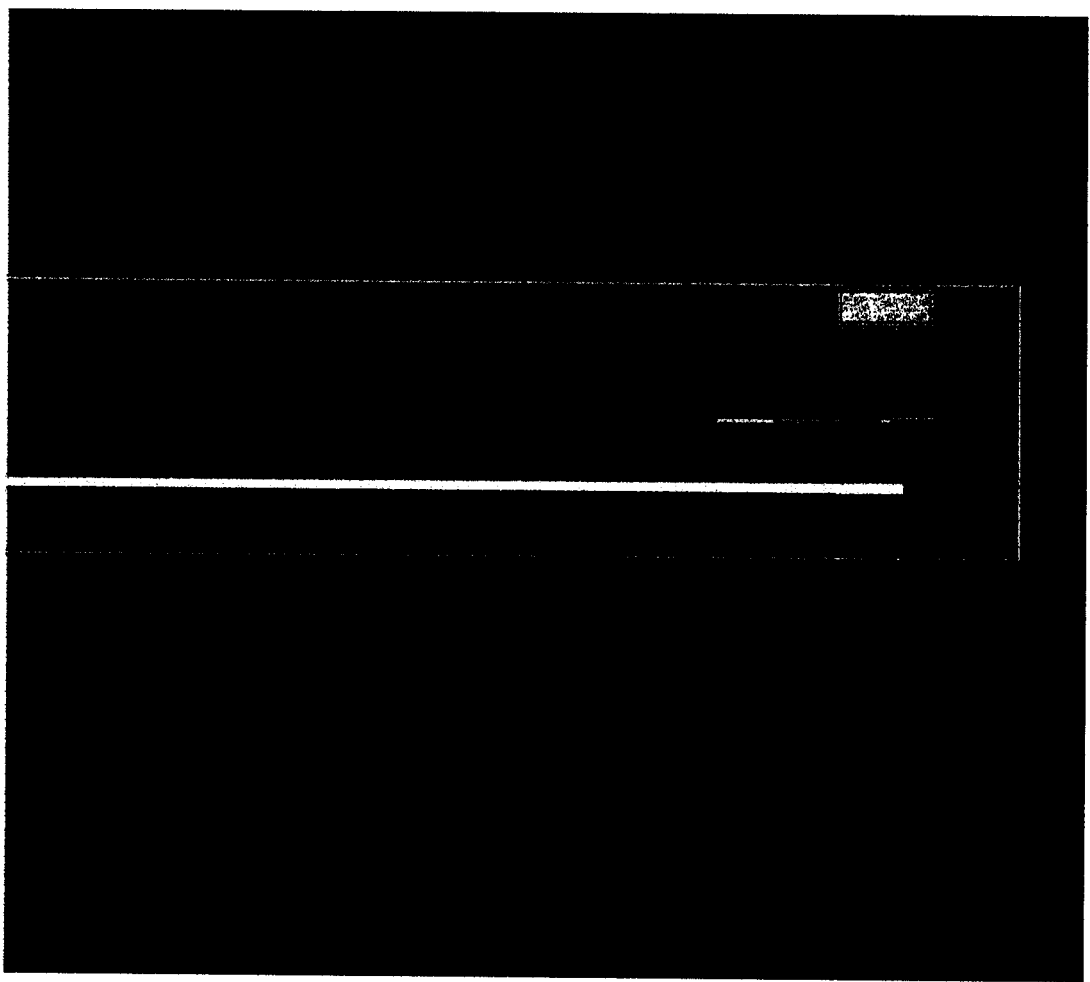


Figure 3.12 Vertical cut of reactor pool

section library used to define the reactor material was ENDF/B-V, which was processed at room temperature (300 K).

In summary the main advantages of this model as provided by the Monte-Carlo approach are:

- a. All the reactor components described above were modelled in three dimensions;
- b. Each of the fuel elements were modelled individually and positioned precisely, reproducing accurately the heterogeneity of the reactor;
- c. Although simplified, the control rod was modelled with the volume of the cadmium conserved;
- d. All the irradiation sites were modelled by cylinders of appropriate material and size;
- e. The reflector was modelled in accordance with the appropriate drawings but the holes containing the irradiation sites were simplified;
- f. The thermal column was included in the model;
- g. Although simplified, the reactor container was modelled in its entirety; and
- h. The pool was modelled up to the stainless steel liner.

## CHAPTER 4 - SIMPLIFIED MODEL

### 4.1 DESCRIPTION OF THE SIMPLIFIED MODEL

The more complex the model is, the more computational power is required for simulation. Therefore in order to gain some insight into various effects without investing large amounts of computing time, the SLOWPOKE-2 reactor was simulated by an infinite lattice having the same pitch as the model described in Chapter 3, as well as the same  $\text{UO}_2$  radius and length (see Figure 4.1). This lattice did not include any correction for the sites where there are no fuel elements. The density of the water was set for 20°C. Therefore, assuming that the nominal density and dimensions as listed in Chapter 3 were given at 20° C, the next  $k_{\text{eff}}$  calculations are for 20°C. The  $k_{\text{eff}}$  calculated on the IBM RISC 6000 model 350, with 150 000 neutrons per cycles, 20 inactive cycles and 180 active cycles, was  $1.27761 \pm 0.00017$ . An IBM RISC 6000 model 370 also made available by the Atomic Energy Control Board and was used to perform the same calculation with 3 000 000 neutrons per cycles, 20 inactive cycles and 180 active cycles, yielding a result of  $k_{\text{eff}} = 1.27764 \pm .00012$ . Assuming that the two simulations are not correlated we can calculate the standard deviation on this sample using:<sup>(31)</sup>

$$\langle M \rangle = \frac{1}{N} \sum_i^N M_i = 1.277625 \quad (28)$$

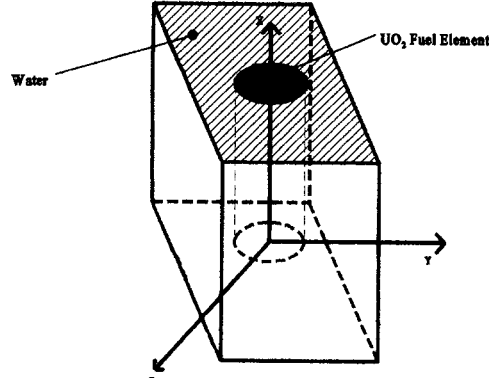


Figure 4.1 Infinite lattice in Y and Z direction, of simplified model

$$\langle M^2 \rangle = \frac{1}{N} \sum_i^N M_i^2 = 1.6323256 \quad (29)$$

$$S^2 = \langle M \rangle^2 - \langle M^2 \rangle = 4 \times 10^{-8} \quad (30)$$

$$S = \sqrt{\langle M \rangle^2 - \langle M^2 \rangle} = 0.0002 \quad (31)$$

where  $M_i$  = final  $k_{eff}^{combined}$  of simulation  $I$

$N$  = number of simulations performed

Given the small size of the sample used to evaluate the standard deviation between  $k_{eff}$  computed on different systems (only two measurements) the results point nevertheless in the right direction. The remaining  $k_{eff}$  calculations in this chapter have all been processed on the IBM RISC 6000 model 370, made available by the Atomic Energy Control Board, with the cooperation of Mr. W. Grant.

#### 4.2 TEMPERATURE SIMULATION BY UO<sub>2</sub> AND H<sub>2</sub>O DENSITY

The macroscopic effect of increasing the temperature of the reactor from 20°C to 32°C is the expansion of materials. The geometry and density change of the UO<sub>2</sub> were calculated using a simple linear expansion model. First, the linear coefficient of expansion for the UO<sub>2</sub> was evaluated with:<sup>(32,33)</sup>

$$\alpha_{linear} = 7.107 \times 10^{-6} + 5.162 \times 10^{-9}T + 3.42 \times 10^{-13}T^2 \quad (32)$$

where  $T$  =  $\text{UO}_2$  temperature in degree Celsius

therefore for  $20^\circ\text{C}$  we have

$$\alpha_{\text{linear}} = 7.16 \times 10^{-6} \text{ cm/cm}/^\circ\text{C} \quad (33)$$

Note that the uncertainty on this evaluation can be as much as a factor of two.<sup>(32)</sup>

This value was compared with the linear expansion coefficient reported in Reference 34,  $9.1 \times 10^{-6} \text{ cm/cm}/^\circ\text{C}$ . Given the large uncertainty on the linear expansion coefficient, these two values are similar and therefore the calculated value was used. The radius for the fuel at  $32^\circ\text{C}$  was calculated using:<sup>(33)</sup>

$$\text{Radius}_{(\text{at } 32^\circ\text{C})} = \text{Radius}_{(\text{at } 20^\circ\text{C})} + \text{Radius}_{(\text{at } 20^\circ\text{C})} T \alpha_{\text{linear}} \quad (34)$$

similarly the length is given by:

$$\text{Length}_{(\text{at } 32^\circ\text{C})} = \text{Length}_{(\text{at } 20^\circ\text{C})} + \text{length}_{(\text{at } 20^\circ\text{C})} T \alpha_{\text{linear}} \quad (35)$$

With these new dimensions the volume of the fuel was calculated for  $32^\circ\text{C}$ , and the density was appropriately corrected. The density of the water was taken from Reference 35. The overall size of the lattice was not modified. The  $k_{\text{eff}}$  was calculated on the IBM RISC 6000 model 370 with 300 000 neutrons per cycles, 20 inactive cycles and 180 active cycles. This calculation was performed four times with different random number sequences (the sequence was changed by skipping some random numbers at the beginning of the sequence). The results are shown in Table 4.1, and indicate a slight drop in reactivity when compared with the results presented in Section 4.1. The standard deviation was calculated in the same manner as in Section 4.1 and again, although not conclusive, indicates an adequate standard deviation as calculated by MCNP 4A.

Table 4.1

Calculation of  $k_{eff}$  at 32°C

Calculations	$k_{eff}$	Standard Deviation
Initial Point Source	1.27643	0.00012
Source From Run At 20°C	1.27655	0.0001
Skipped 61 Random Numbers	1.27626	0.00011
Skipped 353 Random Numbers	1.27634	0.00011
	Average $k_{eff}$ for the 4 calculations	Standard Deviation on the calculations
	1.2764	0.00011

### 4.3 FREE GAS TREATMENT

The free gas treatment as mentioned in Chapter 2 adjusts the elastic cross sections and accounts for the velocity of the nucleus involved in the collision. When the “tmp” command is omitted, the default temperature of the cross section is 300K or  $2.53 \times 10^{-8}$  MeV. Therefore a “tmp=2.56x10<sup>-8</sup>” command was introduced in the simulation at 32° C to observe if there were any effects. The results are compared with the previous run at Table 4.2.

Table 4.2  
Calculation of  $k_{eff}$  at 32°C with “tmp” Command

Evaluation	<i>Individual <math>k_{eff}</math></i>	Individual Standard Deviation
No Random Number Skipped	1.27634	0.00012
Skipped 461 Random Numbers	1.27656	0.00012
	tmp 2.56x10 <sup>-8</sup> Average $k_{eff}$	Standard Deviation on the Evaluations
	1.27645	0.00011
	no tmp Average $k_{eff}$	Standard Deviation on the Evaluations
	1.2764	0.00011

Since no effects were observed, the rest of the simulation was processed with the default setting.

#### 4.4 S( $\alpha,\beta$ ) TREATMENT

There is no other provision in MCNP 4A to change the cross section with the temperature change in the range at which the RMC-CMR SLOWPOKE operates. As a study of possible effects, an out of range cross section library was used for the S( $\alpha,\beta$ ) treatment, the library lwt.02t which was compiled at 400K was used with the same geometry as Section 4.3. A single  $k_{eff}$  calculation gave  $1.27630 \pm 0.00011$  and therefore indicates no apparent effects.

Another attempt was made at observing the effect of the temperature on the cross sections. This time all the cross section libraries were changed to the 600K libraries. The rest of the model was unchanged. This study was conducted on the IBM RISC 6000 model 350 with 10 000 neutrons per cycles, 20 inactive cycles, and 40 active cycles. The relative effects on the macroscopic cross

section as calculated by MCNP 4A are listed in Table 4.3. These results will be further discussed in Section 6.3.

Table 4.3  
Variation in Macroscopic Cross Sections Relative to  
the Use of the 300K Cross Section Library

	600 K cross section library with relative error (no tmp card)	600 K cross section library with relative error (with tmp card)
UO <sub>2</sub> total cross section	2.3 % ± 0.2	2.3 % ± 0.2
UO <sub>2</sub> absorption cross section	3.9 % ± 0.4	3.9 % ± 0.4
UO <sub>2</sub> elastic cross section	3.8 % ± 0.2	4 % ± 0.2
UO <sub>2</sub> fission cross section	-0.4 % ± 0.4	-0.4 % ± 0.4
UO <sub>2</sub> fission neutrons	-0.5 % ± 0.4	-0.7 % ± 0.4
H <sub>2</sub> O total cross section	1.4 % ± 0.2	1.9 % ± 0.2
H <sub>2</sub> O absorption cross section	-8 % ± 0.4	-8 % ± 0.4
H <sub>2</sub> O elastic cross section	1.4 % ± 0.2	1.4 % ± 0.2

#### 4.5 LATTICE STEP

The last study conducted with this simple model was to change the lattice pitch in accordance with the linear expansion coefficient of  $6.0 \times 10^{-6}$  cm/cm/ $^{\circ}$ C for the Zircalloy-4, taken from Reference 18. It was assumed that both the bottom and the top fuel grid plates expand only outwardly and linearly. Again the result shown at Table 4.4 indicates no effects on the  $k_{eff}$  calculations. Therefore no geometrical changes were made to the model when the temperature trend was calculated.

Table 4.4

Calculation of  $k_{eff}$  at 32°C Including Lattice Expansion

Evaluation	<i>Individual</i> $k_{eff}$	Individual Standard Deviation
No Random Number Skipped	1.27655	0.0001
Skipped 461 Random Numbers	1.27648	0.00013
	tmp $2.56 \times 10^{-8}$	Standard Deviation on the Evaluations
	Average $k_{eff}$	
	1.27652	0.00004
	no tmp Average $k_{eff}$	Standard Deviation on the Evaluations
	1.2764	0.00011

## CHAPTER 5 - RESULTS

### 5.1 EXPERIMENTAL DATA

As mentioned in the introduction, measurements of the excess reactivity, over a range of temperature from 15.9°C to 46.8°C at various powers (10 W, 100 W, 2 kW and 10 kW), were performed in May 1986, eight months after commissioning.<sup>(2)</sup> The data is reproduced here for comparison with the simulation.

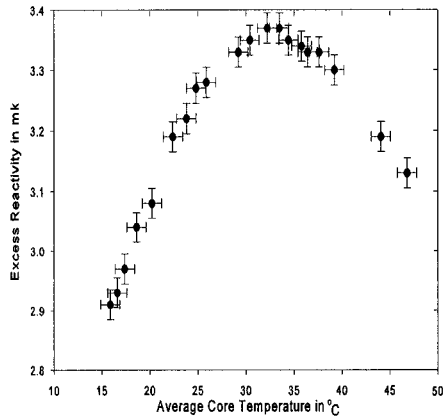


Figure 5.1 RMC-CMR SLOWPOKE-2 excess reactivity measurements by control rod balance at 10 W thermal

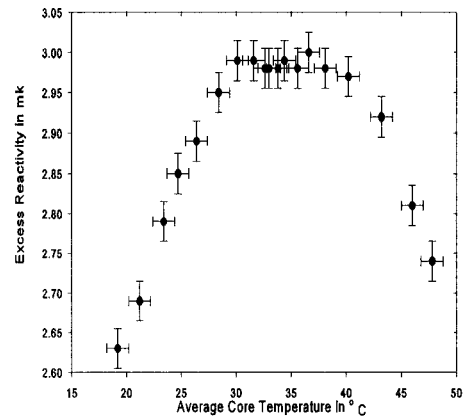


Figure 5.2 RMC-CMR SLOWPOKE-2 excess reactivity measurements by control rod balance at 2 kW thermal

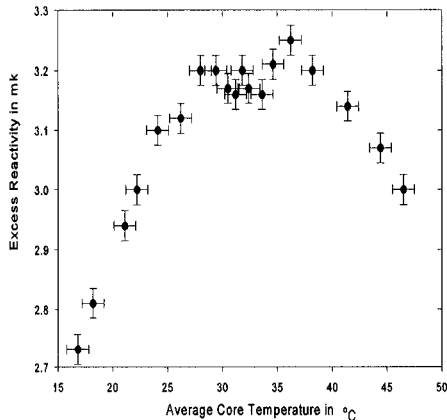


Figure 5.3 RMC-CMR SLOWPOKE-2 excess reactivity measurements by period at 2 kW thermal

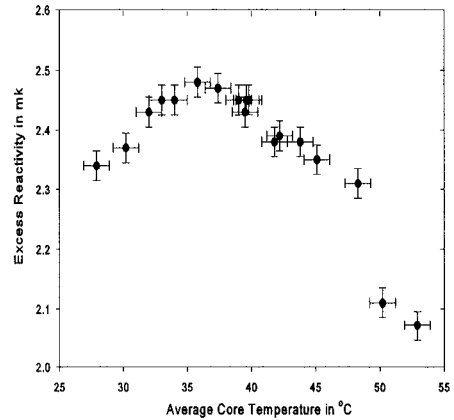


Figure 5.4 RMC-CMR SLOWPOKE-2 excess reactivity measurements by control rod balance at 10 kW thermal

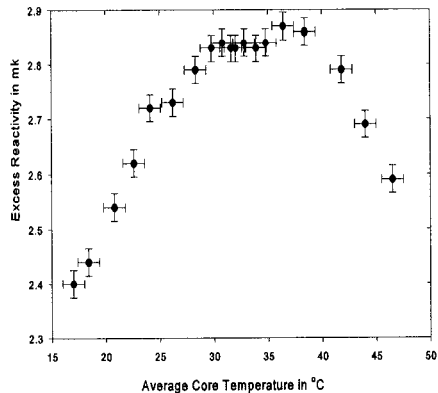


Figure 5.5 RMC-CMR SLOWPOKE-2 excess reactivity measurements by period at 10 kW thermal

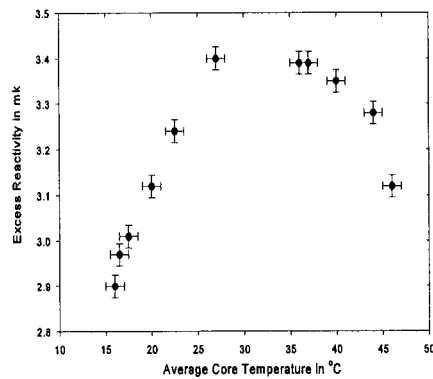


Figure 5.6 RMC-CMR SLOWPOKE-2 excess reactivity measurements by control rod balance at 100 W thermal (while cooling)

## 5.2 EXCESS REACTIVITY CALCULATIONS

The multiplication factor of the reactor was determined at 20°C for the control rod in its fully out position , and for the control rod entirely replaced by water. In accordance with references 5, 6 and 7, which identify the three-combined  $k_{eff}$  estimator as the best final estimate from an MCNP 4A calculation, the results presented here will be based on the final estimated combined collision/absorption/track-length  $k_{eff}$ . This final estimation was obtained from a progression of simulations using more and more histories, which are aimed at building a dependable source. The individual and average three-combined  $k_{eff}$  of each simulations are plotted against the active cycles, to ensure that the model appears stable (Figure 5.7 to 5.10 )(Note: Only the last simulation figures are produced in Appendix D for the other calculations presented in this chapter). The output files (example Appendix E) were also reviewed for any warnings that may have an effect on the computation of the multiplication factor.

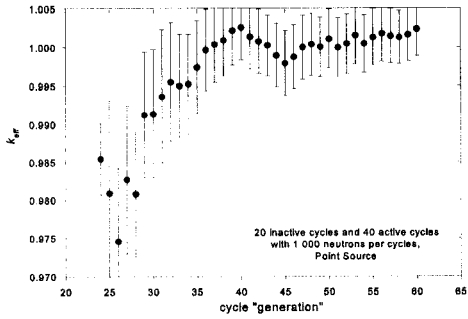


Figure 5.7  $k_{eff}$  Combined estimator vs cycle  
control rod fully out

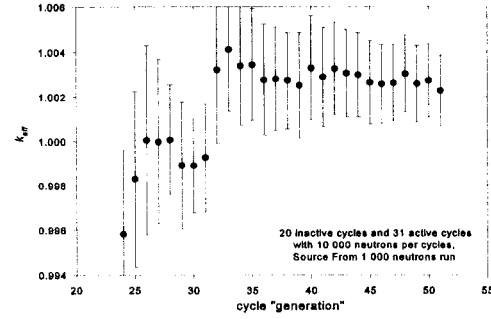


Figure 5.8  $k_{eff}$  Combined Estimator VS Cycle  
Control Rod Fully Out

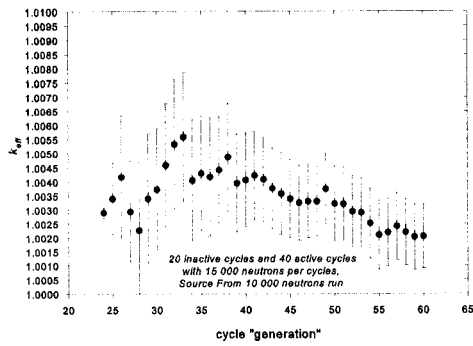


Figure 5.9  $k_{eff}$  Combined estimator vs cycle  
control rod fully out

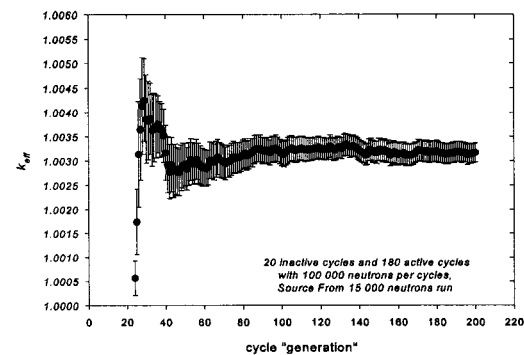


Figure 5.10  $k_{eff}$  Combined estimator vs cycle  
control rod fully out

Then the excess reactivity is calculated with equation:<sup>(12)</sup>

$$\frac{k_{eff} - 1}{k_{eff}}$$

The results are compared with the data taken from the commissioning report<sup>(1)</sup> at Table 5.1,

and discussed in Section 6.1.

Table 5.1

Excess Reactivity in (mk)

	Excess Reactivity	One Standard Deviation	Two Standard Deviation
Control Fully Out	3.17	0.2	0.4
Control Rod Replaced By Water(D-2)	3.84	0.19	0.38
Commissioning Data <sup>(1)</sup>	3.15	Error not available	Error not available

Note: (D-2) refers to Figure D-2 of Appendix D

### 5.3 CONTROL ROD WORTH CALCULATIONS

The reactivity worth of the control rod was determined and compared with the data from Reference 1 at Table 5.2. These results are discussed in Section 6.2.

Table 5.2  
Control Rod Reactivity Worth

	Excess Reactivity (mk)	number active cycle	number neutron /cycle	1 Standard deviation (mk)	2 Standard Deviations (mk)
Control Rod Position (from reflector)	Simulation				
Fully out (20.32 cm)	3.17	180	$1 \times 10^5$	0.2	0.4
Centred (10.16 cm) (D-3)	-0.79	390	$1 \times 10^5$	0.14	0.28
Fully inserted (D-1)	-4.68	100	$1 \times 10^5$	0.26	0.52
Control Rod Worth	7.85			0.33	0.66
Experimental Data					
Estimated Control Rod Worth (Reference 1)(mk)	5.45				
Control Rod Position for 0 excess reactivity and low power from the reflector(Reference 36)	6.86 cm				

#### 5.4 EXCESS REACTIVITY VS AVERAGE CORE TEMPERATURE

The excess reactivity as a function of the average core temperature was calculated for three control rod positions, fully out, centred, and fully in. The temperature effect on this model was simulated as previously described in Chapter 4, by changing the density of the water, and the geometry and density of the UO<sub>2</sub>. The linear coefficient of expansion of the UO<sub>2</sub> calculated at 20°C was used for temperatures from 15°C to 35°C and was recalculated for 40°C and 50°C . The results are discussed in Section 6.3.

Table 5.3  
Excess Reactivity vs Temperature  
Control Rod Fully Inserted

Temperature (°C)	Reactivity (mk)	Number of active cycle	Number of neutron/cycle	One Standard Deviation (mk)	Two Standard Deviations (mk)
15 (D-4)	-3.98	80	1x10 <sup>5</sup>	0.29	0.58
16 (D-5)	-4.07	80	1x10 <sup>5</sup>	0.31	0.62
20 (D-1)	-4.68	100	1x10 <sup>5</sup>	0.26	0.52
25 (D-6)	-5.04	80	1x10 <sup>5</sup>	0.33	0.66
30 (D-7)	-4.82	80	1x10 <sup>5</sup>	0.3	0.6
32 (D-8)	-4.85	80	1x10 <sup>5</sup>	0.31	0.62
35 (D-9)	-5.83	80	1x10 <sup>5</sup>	0.31	0.62

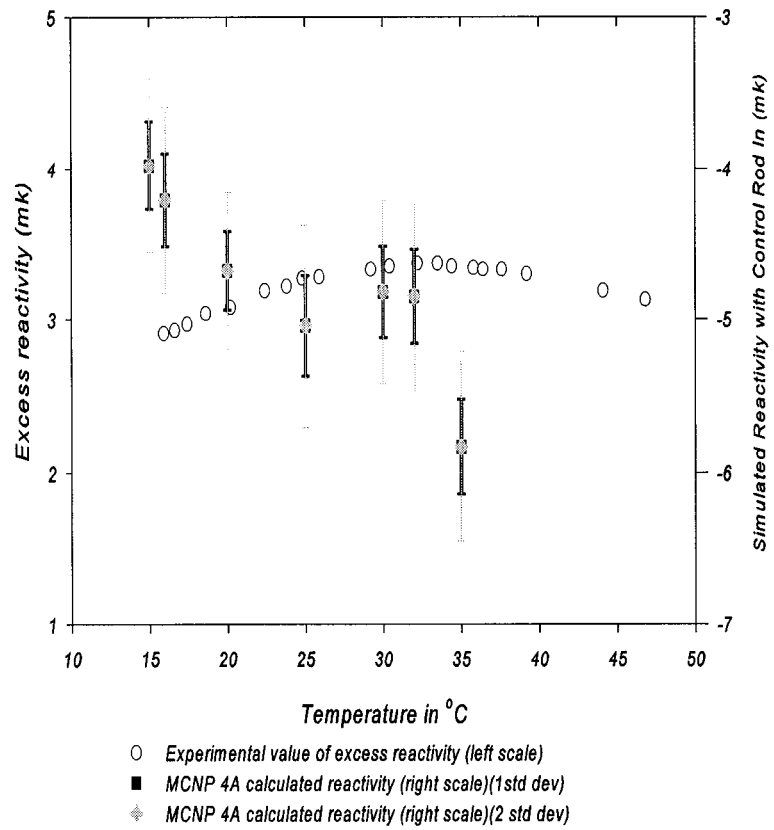
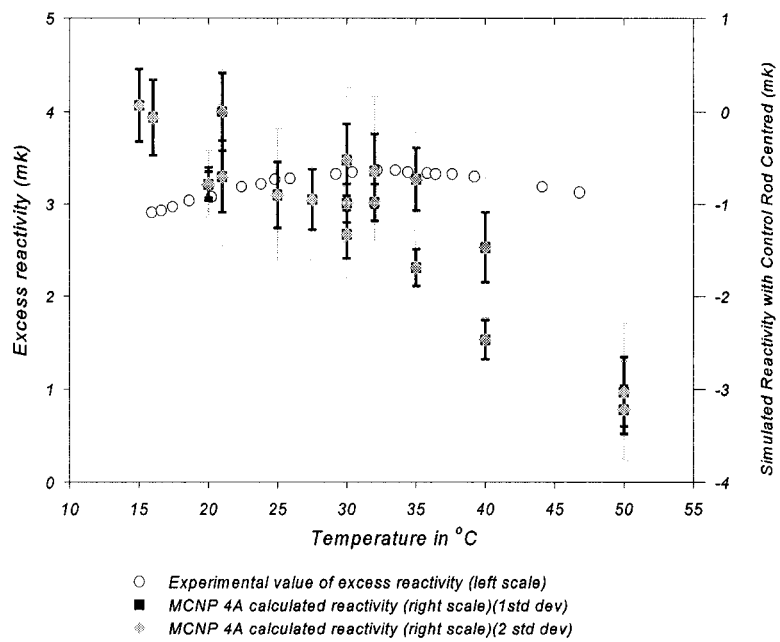


Figure 5.11 Excess reactivity vs temperature  
control rod fully inserted

Table 5.4  
Excess Reactivity vs Temperature  
Control Rod Centred

Temperature (°C)	Reactivity (mk)	Number of active cycles	Number of neutrons/cycle	One Standard Deviation (mk)	Two Standard Deviations (mk)
15 (D-10)	0.07	60	1x10 <sup>5</sup>	0.39	0.78
16 (D-11)	-0.62	60	1x10 <sup>5</sup>	0.41	0.82
20 (D-3)	-0.79	390	1x10 <sup>5</sup>	0.14	0.28
20 (D-12)	-0.78	100	2x10 <sup>5</sup>	0.18	0.36
21 (D-13)	0	60	1x10 <sup>5</sup>	0.42	0.84
21 (D-14)	-0.7	60	1x10 <sup>5</sup>	0.39	0.78
25 (D-15)	-0.9	60	1x10 <sup>5</sup>	0.36	0.72
27.5 (D-16)	-0.95	60	1x10 <sup>5</sup>	0.33	0.66
30 (D-17)	-0.52	60	1x10 <sup>5</sup>	0.39	0.78
30 (D-18)	-0.99	200	1x10 <sup>5</sup>	0.21	0.42
30	-1.33	60	2x10 <sup>5</sup>	0.26	0.52
32 (D-19)	-0.64	60	1x10 <sup>5</sup>	0.4	0.8
32 (D-20)	-0.98	100	2x10 <sup>5</sup>	0.2	0.4
35 (D-21)	-0.73	60	1x10 <sup>5</sup>	0.34	0.68
35 (D-22)	-1.69	60	2x10 <sup>5</sup>	0.2	0.4
40 (D-23)	-1.47	60	1x10 <sup>5</sup>	0.38	0.76
40 (D-24)	-2.47	60	2x10 <sup>5</sup>	0.21	0.42
50 (D-25)	-3.03	60	1x10 <sup>5</sup>	0.37	0.74
50 (D-26)	-3.22	60	2x10 <sup>5</sup>	0.26	0.52



*Figure 5.12 Excess reactivity vs temperature control rod centred*

Table 5.5

Excess Reactivity vs Temperature  
Control Rod Fully Out

Temperature (°C)	Reactivity (mk)	Number of active cycle	Number of neutron/cycle	One Standard Deviation (mk)	Two Standard Deviation (mk)
15 (D-27)	3.47	80	$1 \times 10^5$	0.32	0.64
20 (page 50)	3.25	180	$1 \times 10^5$	0.19	0.38
25 (D-28)	2.74	30	$1 \times 10^5$	0.44	0.88
30 (D-29)	2.23	80	$1 \times 10^5$	0.28	0.56
35 (D-30)	2.54	80	$1 \times 10^5$	0.31	0.62
50 (D-31)	-0.07	60	$1 \times 10^5$	0.31	0.62

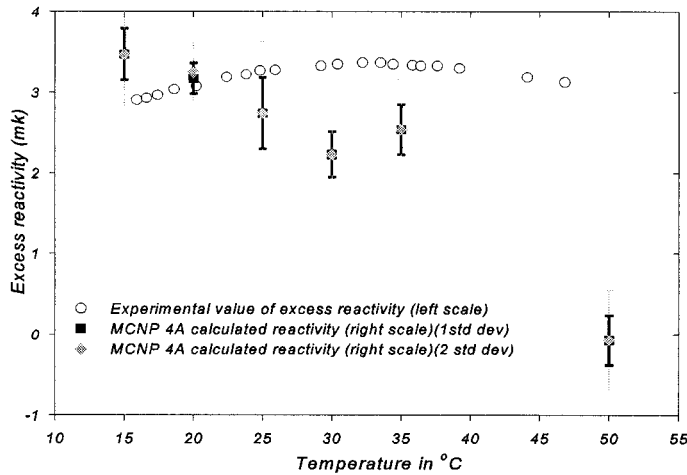


Figure 5.13 Excess reactivity vs temperature  
control rod fully out

## 5.5 DOUBLED LINEAR COEFFICIENT OF EXPANSION

The excess reactivity as a function of the average core temperature was again calculated for three control rod positions, fully out, entered, and fully in. But as mentioned in Chapter 4, since the error in the UO<sub>2</sub> linear coefficient of expansion can be as much as a factor of 2, therefore the temperature effect on the geometry and density of the UO<sub>2</sub> was recalculated with doubled  $\alpha_{\text{linear}}$ .

Table 5.6

Excess Reactivity vs Temperature  
Control Rod Fully Inserted (doubled  $\alpha_{\text{linear}}$ )

Temperature (°C)	Reactivity (mk)	Number of active cycle	Number of neutron/cycle	One Standard Deviation (mk)	Two Standard Deviation(mk)
20 (D-1)	-4.68	100	$1 \times 10^5$	0.26	0.52
27.5 (D-32)	-4.55	80	$1 \times 10^5$	0.33	0.66
32 (D-33)	-5.28	80	$1 \times 10^5$	0.31	0.62

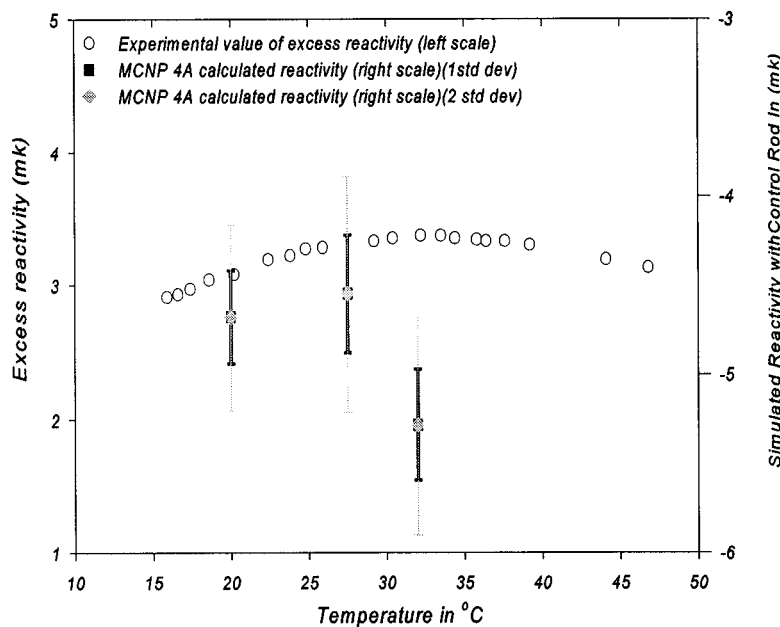


**FIGURE 5.14 Excess reactivity vs temperature  
control rod fully inserted  
linear expansion coef. doubled**

Table 5.7

Excess Reactivity VS Temperature  
Control Rod Centred (doubled  $\alpha_{\text{linear}}$ )

Temperature (°C)	Reactivity (mk)	Number of active cycle	Number of neutron/cycle	One Standard Deviation (mk)	Two Standard Deviation (mk)
16 (D-34)	-0.99	60	$1 \times 10^5$	0.32	0.64
20 (D-3)	-0.79	410	$1 \times 10^5$	0.14	0.28
20 (D-12)	-0.78	100	$2 \times 10^5$	0.18	0.36
27.5 (D-35)	-0.79	430	$1 \times 10^5$	0.12	0.24
32 (D-36)	-1.55	60	$1.5 \times 10^5$	0.37	0.74
32 (D-37)	-0.93	100	$1.5 \times 10^5$	0.23	0.46

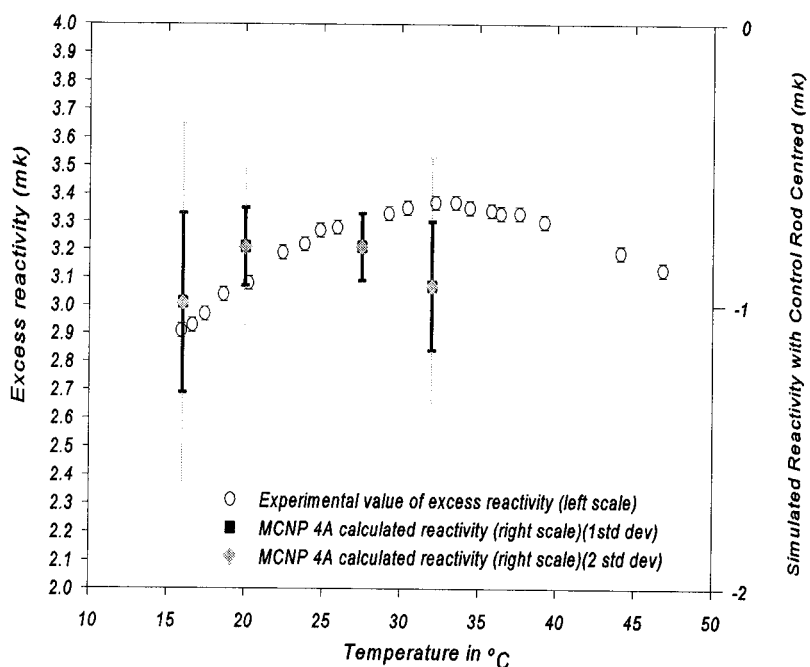


*Figure 5.15 Excess reactivity vs temperature  
control rod centred  
linear expansion coef. doubled*

Table 5.8

Excess Reactivity vs Temperature  
Control Rod Fully Out (doubled  $\alpha_{\text{linear}}$ )

Temperature (°C)	Reactivity (mk)	Number of active cycle	Number of neutron/cycle	One Standard Deviation (mk)	Two Standard Deviation (mk)
16 (D-38)	3.04	115	$1 \times 10^5$	0.25	0.5
20 (page 50)	3.25	180	$1 \times 10^5$	0.2	0.4

## 5.6 TEMPERATURE EFFECT ON CROSS SECTION

As previously mentioned in Chapter 4 there is no provision in MCNP 4A to change the cross section as the temperature changes. Again, as a study of possible effects, cross section libraries at high temperatures were used for both the  $S(\alpha,\beta)$  and free gas treatments. Those libraries were processed at 600 K. The comparison was done with no modification to the model simulating 20°C (Table 5.9). These results will be used in Section 6.3.

Table 5.9

Cross Section Library Comparison

Cross Section Library at	Reactivity (mk)	Number of active cycle	Number of neutron/cycle	One Standard Deviation (mk)	Two Standard Deviation (mk)
300K	-0.79	410	$1 \times 10^5$	0.14	0.28
600K (D-39)	5.71	80	$1 \times 10^5$	0.30	0.60
600K with tmp card (D-40)	4.92	80	$1 \times 10^5$	0.30	0.60

## CHAPTER 6 - DISCUSSION

### 6.1 EXCESS REACTIVITY

The excess reactivity of the RMC-CMR SLOWPOKE-2 reactor as calculated from the MCNP 4A simulation with the control rod in the fully out position, is in close agreement with the experimental data (see Table 5.1). In fact, the difference between the experimental data and the calculated value at 20°C is only 0.02 mk or approximately 1%, which is less than one standard deviation. The standard deviation could be interpreted as the accuracy of the model, if the mathematical and the computer code had been a perfect representation of the reactor and the physical phenomena. Yet as previously mentioned in Chapters 2 and 3, the model and the code are only approximations themselves, involving several assumptions and uncertainty on the data. Therefore, the simulation can only represent the reactor in an approximative way, and the actual accuracy of the simulation cannot be given by the standard deviation alone. The discrepancy between the experimental and the calculated reactivities may be used as an indicator of the actual accuracy of the model, accounting for the uncertainty on the experimental values.

The sensitivity analysis performed on the geometry in Chapter 3, with the hand calculations of various effects of geometrical and material changes, gave us some indication of the actual error. In addition the excess reactivity was calculated without the control rod, as its vertical location had to be approximated (see Chapter 3). Here the difference between the experimental data and the simulation result was approximately 0.8 mk (see Table 5.1). These tests show that the error band is indeed more than the one or even two standard deviations. The error can be assessed in the order of one to two mk. To get a better evaluation of the error several more sensitivity analyses, with a

standard deviation in the order of 0.2 mk, could be performed, but this represents a very large computing investment since one simulation of this magnitude takes approximately 260 hours on an HP Apollo series 700.

## 6.2 CONTROL ROD WORTH

MCNP 4A allowed the modelling of the control rod and also the flexibility to position it at various heights in the core. The simulated control rod exhibits a higher reactivity worth than the experimental data by 2.4 mk that is more than three standard deviations (see Table 5.2). This is also suggested by the fact that the simulated reactor does not become critical even after extracting the control rod by as much as 10 cm. The experimental data show that the reactor is critical with the control rod extracted by less than 7 cm. The modelling error can be attributed to several factors of which the following are probably the most important:

- a. geometry error: as mentioned in Chapter 3, the location of the cadmium lining in the control rod sheath had to be approximated and could well be actually located within  $\pm 1$  cm from the position selected for the model;
- b. material error, no impurities were modelled; and
- c. statistical error, the region of the control rod may not be sampled adequately.

The geometry error and material errors could be investigated by running more simulations with variation in location and composition of the cadmium lining. The statistical error could be investigated by varying the number of neutrons per cycle or by increasing the importance of that region using variance reduction techniques. As previously mentioned such studies represent a very large computing investment. More information concerning the statistical error could also be obtained with MCNP 4A surface current neutron tallies, surface flux neutron tallies and an estimate

of the energy deposition neutron tallies.

### 6.3 TEMPERATURE EFFECTS

As indicated by Figure 5.1 to 5.6, the experimental effect of temperature variation on the reactivity, for temperatures between 20°C and 40°C, is in the order of 0.2 mk. Since the precision of Monte-Carlo simulation increases approximately as one over the square root of the sampling size, performing calculations with a standard deviation of 0.1 mk, giving a 68% confidence interval of 0.2 mk is thus very difficult. In fact to obtain such a precision would require more than a month of computer time with the present technology. Therefore, simulations of approximately 0.2 mk of standard deviation were used for the study of the temperature effect.

The temperature simulations were conducted for three control rod positions, fully in, centred, and fully out, using two linear coefficients of expansion for the UO<sub>2</sub> for a total of six curves. The only experimental data available is the excess reactivity, therefore only the simulations of the temperature with the control rod in the fully out position can be directly compared. The other four simulations were superimposed with the experimental data (using two scales) to facilitate the comparison of the temperature trend of the excess reactivity.

With the control rod in the fully inserted position, (Figure 5.11), the general trend is that the reactivity decreases as the temperature increases. It was also observed that the simulated reactivity variations, for temperatures between 20°C and 32°C are within one or two standard deviations of the experimental data. The discrepancy becoming larger for temperatures outside that range.

A great deal of attention was devoted to the simulation of the control rod in the centred position (Figure 5.12), because it better approximates the power at which the experimental data were collected. Several temperatures were simulated more than once, with only the statistics being varied

by changing the amount of cycles and neutrons per cycle. In most cases the 68% confidence intervals overlapped and in all cases the 95% confidence intervals fully overlapped. This clearly illustrates that the true answer is rather a confidence interval and cannot be used as a single value. Accordingly, only the general reactivity trend should be considered, which here shows a decreasing excess reactivity as the temperature increases. Again in this case it is also observed that for temperatures between 20°C and 32°C, the simulated reactivity variations are within one or two standard deviations from the experimental data. However, for temperature outside that range the reactivity discrepancies between the experimental and the simulated values become quite large.

The simulated temperature trend with the control rod in the fully out position can be directly compared with the experimental data (Figure 5.13). Again, the general trend in reactivity is that it decreases as the temperature increases. But here the decrease in reactivity for temperatures between 20°C and 35°C seems steeper for the calculated values. Here the steep decrease in excess reactivity may be caused by the position of the control rod, which significantly affects the flux distribution.

Far less simulations, using a doubled coefficient of linear expansion for the UO<sub>2</sub>, were performed. From this limited set of results, the following observations can be made:

- a. There was no major change in reactivity at any temperature compared with the previous models; and
- b. It better modelled temperatures below 20°C when comparing with experimental data.

These observations would be confirmed once a more thorough investigation is carried out.

Due to the large standard deviation of each simulation, when compared with the magnitude of the phenomena observed, it is very difficult to comment on the exact shape of the curves besides the fact that the reactivity obviously decreases as the temperature increases. However, this

observation is important as it further supports the inherent safety of the LEU SLOWPOKE-2 reactor. The results also indicate that the model is somewhat deficient when temperatures outside the range of 20°C to 32 C are simulated. Furthermore, the presence of a reactivity peak could not be accurately established. This may be a result of the size of the confidence intervals in comparison to the phenomena that we are trying to simulate, but may also be caused by other factors that were not included in the model, for examples:

- a. Expansion of the reflector;
- b. Change in the relative position of the reactor components due to expansion of structural components; and
- c. Cross sections changes due to temperature.

The cost involved for improving the size of the confidence intervals is indeed too high for the resources presently available. Therefore, the studies presented in Section 4.4 and 5.5 were conducted. The cross section libraries used for those studies are out of the operating range of a SLOWPOKE-2 reactor, so the results cannot be directly linked to the experimental data. The aim here was to see what the reactivity trend would be. Table 5.9 shows a marked increase in reactivity, when the cross section libraries processed at 600K was used. At Table 4.3 we observed a slight increase in the H<sub>2</sub>O elastic cross section (about 1%) and a decrease in absorption cross section (about 8%) when using those libraries, improving the quality of the moderator. The UO<sub>2</sub> absorption and elastic cross section both increased slightly (about 4%). Since the volume of the water in the reactor is much greater than the volume of the fuel, and, more importantly, since the thermal neutron flux in the moderator is considerably larger than in the fuel (hence the neutron importance), this could explain the increased reactivity. The effect was further studied by hand calculation of a

heterogenous cell similar to the model presented in Chapter 4.<sup>(39)</sup> These results show a similar trend and indicate that the initial reactivity increase observed experimentally up to 33°C is due to a dominant positive reactivity temperature coefficient attributed to the thermal neutrons. Obviously, when the reactor temperature exceeds 33°C, other factors (moderator and fuel density, fuel absorption and fission cross sections, Doppler effect, etc) combine to overcome the positive reactivity coefficient and produce a large negative reactivity coefficient, observed both experimentally and with the MCNP 4A model, which provides the desired inherent safety. The positive reactivity coefficient of the moderator cross sections, as observed with MCNP 4A for high temperature (600K), could account for some of the observed discrepancies in the temperature simulation; as it would lower the reactivity of the temperatures below 27°C and increase it for temperatures above 27°C. Several other factors could also be investigated in future studies:

- a. Thermal expansion of the reflector;
- b. Change in density of the D<sub>2</sub>O in the thermal column;
- c. Changes in the fuel cage geometry due to thermal expansion;
- d. Changes in the overall geometry (relative position of the components) due to thermal expansion;
- e. Thermal expansion of the control rod;

In summary, the difference in absolute value of the reactivity at 20°C was reduced to approximately 1 percent. The reactivity of the reactor was calculated for three vertical control rod positions at 20°C , the results differed by about 50 percent when compared with the experimental data. Within the hardware and software limitations, the temperature trend of the reactivity was simulated for three control rod positions. These curves clearly show the inherent safety of the

reactor. Depending on the availability of the resources and the time constraints, the reactivity calculations were performed with a precision of 0.2 mk to 0.4mk. The error on these calculations is however larger and was estimated at one or two mk, based on an assessment of the reactivity worth of the assumptions made in the model.

## CONCLUSION

The simulation of the RMC-CMR SLOWPOKE-2 reactor by Monte-Carlo method was successfully accomplished using MCNP 4A. The main advantages of MCNP 4A were the ability to model the entire reactor in three dimensions and the ability to use transport theory instead of a diffusion calculation. These advantages lead to a significant improvement in reproducing the experimental excess reactivity of the RMC-CMR SLOWPOKE-2 reactor (at 20°C), reducing the discrepancy between the calculated value and the experimental value to less than 1 percent, with a standard deviation of 6 percent (experimental excess reactivity = 3.15 mk, simulated excess reactivity = 3.17 mk). The uncertainty of the model, due to approximations of the geometry and other factors discussed in chapters 2 and 3, was estimated to be between thirty and 60 percent, which is still a large improvement over the previous models.

MCNP 4A also allowed the modelling of the **single** control rod in different positions. From these simulations the reactivity worth of the control rod could be accurately calculated. Although the simulation overestimated the measured reactivity worth, the discrepancy with the experimental data was less than 50 percent (experimental control rod reactivity worth = 5.45 mk, simulated control rod reactivity worth = 7.85 mk).

When attempting to reproduce the temperature trend of the RMC-CMR SLOWPOKE-2 reactor, some of the disadvantages of the Monte-Carlo methods became evident, specifically:

- a. The high computing cost involved in producing the highly precise results, required in the study of the relative effect of the temperature; and
- b. The lack of adequate methodology for modifying cross sections for the temperatures of interest.

Within the limitation of the computing facilities and the code, the temperature trend was simulated for three different control rod positions. Even if the position of the peak of the temperature curves could not be reproduced adequately by the model at this point, these curves nevertheless clearly show that the reactivity of the RMC-CMR SLOWPOKE-2 reactor decreases as the temperature increases. This in itself is very useful as it verifies the inherent safety of the reactor, and demonstrates that the model has the potential to investigate safety-related issues when modifications are proposed.

The problems with the weakness of the model in accurately reproducing the peak of the reactivity-temperature curves have led to investigation of the possible causes, with the most important ones linked to the present incapability of MCNP 4A to accurately represent the detailed cross sections for the temperatures of interest for this study. Any future studies in that domain would first require more precise simulations since the present standard deviation is larger than the peak itself. Continued and rapid development in both computer technology and Monte-Carlo methods may soon allow these studies.

## RECOMMENDATIONS

This initial Monte-Carlo model of the RMC-CMR SLOWPOKE-2 reactor established clearly the adequacy of the methods, but leaves several areas to be improved or further investigated.

- (1) The geometrical and material approximation should be corrected or at least a detailed sensitivity analysis of the unavailable data should be conducted.
- (2) As the neutron flux shape in the reactor is strongly influenced by the position of the control rod, more effort should be invested in improving its modelling through:
  - a. Reducing the uncertainty on the geometrical approximations;
  - b. Better representation of the materials; and
  - c. A detailed study of the statistical error.
- (3) The neutron flux distribution should be investigated with the neutron tally cards in various area of the core for various control rod locations and compared with the experimental data. With this information, the temperature trend simulation should be redone using the control rod position that best simulates the neutron flux of the experimental set up used to determine the temperature trend. This study is essential as accurate flux mapping is needed to assess the neutron doses received at the various irradiation sites in the reactor vessel and the pool.
- (4) The effects of following factors should be studied if further temperature simulations are carried out:
  - a. Thermal expansion of the reflector;
  - b. D<sub>2</sub>O density change in the thermal column;
  - c. Changes in the fuel cage geometry due to thermal expansions;

- d. Changes in the relative position of the reactor components due to thermal expansion;  
and
  - e. Thermal expansion of the control rod.
- (5) Studies of the standard deviation similar to the one performed at reference 7 should be carried out on a few control rod simulations and temperature simulations. These calculations could also be used to reduce the standard deviation in accordance with reference 29.
- (6) The development of a technique which would allow the simulation of the cross section variation with temperature in the range of interest, should be attempted.
- (7) Further testing of the model could be done by modifying it to represent other SLOWPOKE-2 reactors, in particular the new LEU core that will be installed at École Polytechnique de Montréal. It would also be of interest to conduct an excess reactivity measurement over a similar range of temperatures and powers as reference 2 on the new core, to see the effect of eight months of operation on the temperature trend.

Future developments of the model could extent to the simulation of the neutron beam tube installed in the SLOWPOKE-2 reactor pool at RMC-CMR as the major component of the neutron radiography facility presently being commissioned.

## **REFERENCES**

- (1) G.A. Burbidge, R.T. Jones and B.M. Townes, " Commissioning of the SLOWPOKE-2 (RMC) Reactor , "Atomic Energy of Canada Limited Report, RCC/TR-85-004, Rev. 1, 1985.
- (2) P.A Beeley and L.G.I. Bennett, " Reactivity Measurements , " letter to AECB, Royal Militairy College of Canada-Collège Militaire Royale du Canada, 4 June 1986.
- (3) R. T. de Wit, " Reactivity Calculations for the Low Enrichment Uranium Fuelled SLOWPOKE-2 Reactor At the Royal Military College of Canada , "Master Degree Thesis, Royal Militairy College of Canada-Collège Militaire Royale du Canada, April 1989.
- (4) C. Guertin, "Calcul du Coefficient de Temperature du Réacteur SLOWPOKE-2 , " Thèse de Maîtrise, École Polytechnique de Montréal, Octobre 1991.
- (5) RISC Computer Code Collection, MCNP4A, Contributed By Los Alamos National Laboratory, J.Briesmeister (editor), December 1993.
- (6) M. Halperin, "Almost Linearly-Optimum Combination of Unbiased Estimate , "Amer. Stat. Ass. J., 56, 36-43 (1961).
- (7) T. J. Urbatsh, R. A. Forster, R. E. Prael, and R. J. Beckma,. "Estimation and Interpretation of Keff Confidence Intervals in MCNP , " Nucl. Techn., Vol 111, , page 169-182, August 1995 .
- (8) B. J. Lewis, A. C. Harnden-Gillis and L.G.I. Bennett, "Fission Product Release from Uranium-Aluminum Alloy Fuel in SLOWPOKE-2 Reactors , " Nucl. Techn., Vol 109, page 366-380, March 1994.

- (9) Y. Shaw, "LEU Fuel Element Assembly," Drawing no A17997 issue D, Atomic Energy of Canada Limited, 85/01/17.
- (10) Atomic Energy Control Board Nuclear Material Transfer report, From G3, Transfer number 1931, revision 0.
- (11) M.A. Benjamin, "Nuclear Reactor Materials and Applications ,," New York, Van Nostrand Reinhold Company Inc. 1983.
- (12) J. R. Lamarsh, "Introduction To Nuclear Engineering" , Massachusetts, Addison-Wesley, 2nd Edition, November 1982.
- (13) B.M. Townes, Atomic Energy of Canada Limited, Personal Communication, September 1995.
- (14) G.A. Burbidge, Nordion, Personal Communication, September 1995.
- (15) A. Laimite, "Fuel Cage Assembly," Drawing no A18245 issue A, Atomic Energy of Canada Limited, 9 Jan 85.
- (16) Usher, "Control Rod Sheath," Drawing no A10759 issue D, Atomic Energy of Canada Limited, dec 70.
- (17) I. Desrochers, "Control Rod Insert," Drawing no A15292 issue C, Atomic Energy of Canada Limited, 10-8-76
- (18) J.R. Davis, P. Allen, S.R. Lampman, T. B. Zorc, "Metals Handbook", Volume 2, Tenth Edition, ASM International, 1990.
- (19) Usher, "Small Irradiation Tube Assembly," Drawing no A10733 issue B, Atomic Energy of Canada Limited.
- (20) Usher, "Reflector Annulus," Drawing no 10716 issue C, Atomic Energy of Canada

Limited, Aug 11/70.

- (21) Reactor Manual, SLOWPOKE-2 Facility at RMC, Edited by L.G.I. Bennett, September 1994.
- (22) Usher, "Large Irrad. Tube Assembly, Drawing no A10737 issue B, Atomic Energy of Canada Limited, Oct 5/70.
- (23) Y. Shaw, "Small (Outer) Irrad. Tube Assembly," Drawing no A17979, Atomic Energy of Canada Limited.
- (24) Usher, "Lower Beryllium Plate (4")," Drawing no A10712, Atomic Energy of Canada Limited, Aug 12/70.
- (25) H.P., "Beryllium Shim Set (1/8)," Drawing no A13988, issue A, Atomic Energy of Canada Limited, Jan-14-73.
- (26) L.G.I. Bennett, Royal Militairy College of Canada-Collège Militaire Royale du Canada Personal Communication, September 1995.
- (27) R.T. De Wit, Director General Nuclear Safety, Personal Communication, October 1995.
- (28) Y. Shaw, "Thermal Column Assembly," Drawing A17996 issue B, Atomic Energy of Canada Limited, 84/10/05.
- (29) Usher, "Upper Shell Assembly," Drawing A10714 issue K, Atomic Energy of Canada Limited.
- (30) Y. Shaw, "Reactor Lower Section Assembly RMC," Drawing no A18226 issue B, Atomic Energy of Canada Limited, 84-10-09.
- (31) H. Gould and J. Tobochnik, "An Introduction to Computer Simulation Methods Applications to Physical Systems , "Part 2 , Massachusetts, Addison-Wesley, 1988.

- (32) D.R. Olander, "Fundamental Aspect of Nuclear Reactor Fuel Elements", Berkeley, Ca., Technical Information Center, Office of Public Affairs Energy Research and Development Administration, 1976.
- (33) Matpro-Version 11, "A Handbook of Materials Properties for Use in the Analysis of Light Water Reactor Fuel Behavior", NUREG/CR-0497, EG and Idaho, Inc., U.S. Department of Commerce, National Technical Information Service.
- (34) E. Caruso, T. Cominos, A. Leblond, C. Meyer, M. Ross, D. Rozon, L. Vadeboncoeur, "Materiaux Nucleaires", Tome I, École Politehnique de Montréal, Notes de Cours 1969/70.
- (35) R.H. Perry and C.H. Chilton, "Chemical Engineers's Handbook," Fifth Edition, McGraw-Hill Book Company, New York, 1973.
- (36) Daily Operating Log, SLOWPOKE-2 ,Royal Militairy College of Canada-Collège Militaire Royal du Canada, Sept 1985-March 24 1991.

## **APPENDIX A : MCNP 4 A SAMPLE INPUT FILE**

This appendix contains detailed explanations of the input file used to calculate the excess reactivity of the RMC/CMR SLOWPOKE-2 research reactor. The characters of the input file text are bold and the lines are single spaced to clarify the text. This input file contains four sections; the title, the cell definition, the surface definition, and the material source and tally. A single line of less than 80 characters will be referred to as a card, for example a line in the cell section is called a cell card. Similarly to FORTRAN, cards starting with a "c" are comments, and if no entry is made in the first five columns this means that the previous line is continuing.

### **INPUT FILE TITLE**

```
SLOWPOKE simulation control rod out
```

### **CELLS**

The cell definition section comes first and defines the solid regions of the model by the union intersection and complement of other cells or surfaces. The first entry on a cell card is the cell number followed by the number of the material which makes up the cell. Next comes the density of the material, where a negative sign indicates that the units are in g/cm<sup>3</sup>. After the material definition, is the geometrical definition. Finally, some tallies may be directly entered with the cell definition. The "\$" indicates the end of the cell definition and the beginning of the comments.

The first cell card defines the outside word, i.e. that the space outside a sphere that circumscribes all of the reactor geometry. Since the neutron importance was set to zero, there is no neutron flux in that cell (the first "999" is the cell number, 0 is the density of the void and the second "999" refers to the surface number "999" defined later).

```

c
c      cell card definition
c cell# mat density surfaces           comments
c
  999    0    999           imp:n=0      $ outside space

```

The second cell card defines the bottom beryllium reflector. It was assigned the label "1" as the cell number. The next entry is the material number followed by the density of the material in g/cm<sup>3</sup>, followed by the numbers of the surfaces used to define the cell. The negative sign in front of surface 2 indicates that we are using the space located on the negative side of the surfaces (surface 2 is a plane normal to the x axis). The negative sign in front of surface 10 indicates that we are using the space located inside that surface (surface 10 is a cylinder centred on the x axes). Finally, we are also using the space located on the positive side of surface 1. The operator used to define the cell is the intersection (default); therefore, cell 1 is a disc 10.16-cm thick and of 16.113125-cm radius.

```

c cell# mat density surfaces           comments
  1    1   -1.85  -2 -10 1           Imp:n=1      $ Be bottom plate

```

Cell 8 defines the top beryllium reflector. Although slightly more complex, this cell is also defined by the intersection of spaces defined by planes and cylinders (see Figure A-1). Here the half disc with a hole in the centre is defined as the intersection of the space outside surface 20, the space inside surface 19, the spaces on the positive side of surface 7 and 21, and finally the space on the negative side of surface 8.

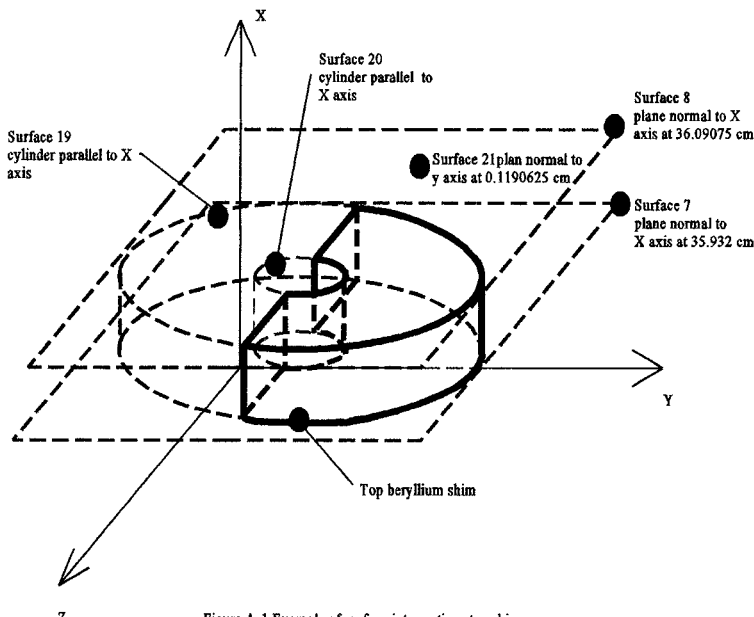


Figure A-1 Example of surface intersections top shim

```

c      Top Beryllium Plate
c
c cell# mat density      surfaces      comments
  8      1    -1.85    21 20 -19 7 -8 Imp:n=1 $ Be top shim

```

Due to its complexity, the beryllium annulus has been divided into two sections:

- the lower section: the top of the cell corresponds with the bottom of the irradiation sites, and therefore is whole; and
- the upper section has been further divided into five equal pie-shaped sections each including an irradiation site.

The upper sections have been selected to centre the irradiation sites.

```

c
c      radial Be reflector including irradiation site
c cell# mat density      surfaces      comments
  2      4 5.0807e-5  9 -113 -131      Imp:n=1 $ inside irradiation site
  3      4 5.0807e-5  9 -113 -141      Imp:n=1 $ inside irradiation site
  4      4 5.0807e-5  9 -113 -151      Imp:n=1 $ inside irradiation site
  5      4 5.0807e-5  9 -113 -161      Imp:n=1 $ inside irradiation site
  6      4 5.0807e-5  9 -113 -171      Imp:n=1 $ inside irradiation site
221     6 -2.70      9 -113 -13 131      Imp:n=1 $ aluminum tubing

```

```

331   6 -2.70      9 -113 -14 141      Imp:n=1 $ aluminum tubing
441   6 -2.70      9 -113 -15 151      Imp:n=1 $ aluminum tubing
551   6 -2.70      9 -113 -16 161      Imp:n=1 $ aluminum tubing
661   6 -2.70      9 -113 -17 171      Imp:n=1 $ aluminum tubing
70    1  -1.85     3 -9  -12 11      Imp:n=1 $ lower sec. of annulus
71    1  -1.85     9 -12 11 -4 71 -70 13 Imp:n=1 $ annulus
72    1  -1.85     9 -12 11 -4 70 74 14 Imp:n=1 $ annulus
73    1  -1.85     9 -12 11 -4 -73 72 16 Imp:n=1 $ annulus
74    1  -1.85     9 -12 11 -4 -72 -71 17 Imp:n=1 $ annulus
75    1  -1.85     9 -12 11 -4 -74 73 15 Imp:n=1 $ annulus

c
c          outside irradiation sites
c cell# mat density      surfaces           comments
  222  4 5.0807e-5  3 -113 -133 Imp:n=1 $ inside of large site
  332  4 5.0807e-5  3 -113 -143 Imp:n=1 $ inside of small site
  442  4 5.0807e-5  3 -113 -154 Imp:n=1 $ inside of cadmium site
  552  4 5.0807e-5  3 -113 -163 imp:n=1 $ flooded site (not at commissioning)

c
c cell# mat  density      surfaces           comments
  223   6  -2.70     3  -113 133 -132  Imp:n=1      $ Al tubing
  333   6  -2.70     3  -113 143 -142  Imp:n=1      $ Al tubing
  443   6  -2.70     3  -113 154 -153  Imp:n=1      $ Al tubing
  553   6  -2.70     3  -113 163 -162  Imp:n=1      $ Al tubing
  444   7 -8.65      3  -4   153 -152  Imp:n=1      $ cadmium lining

```

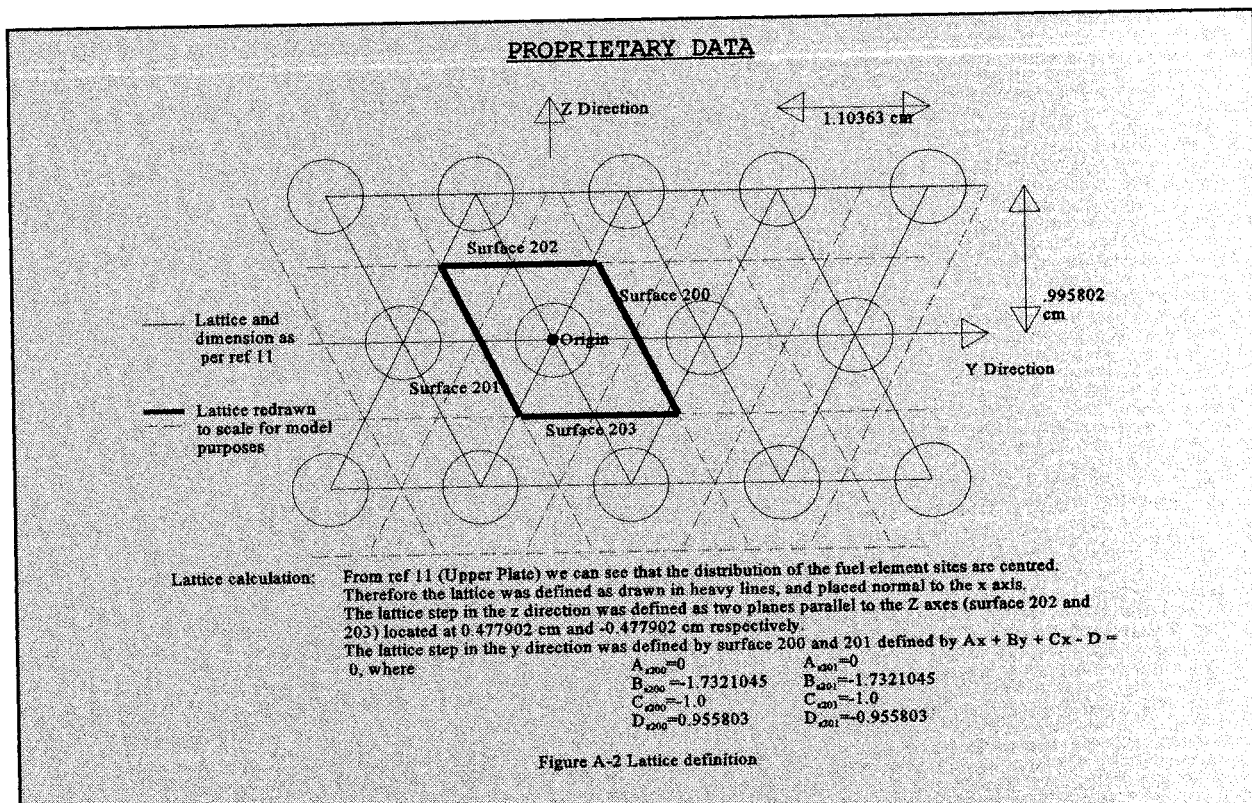
In order to properly define the core of the SLOWPOKE we have sliced it horizontally in 8 section:

- a. The fuel region located below the upper grid plate and above the fuel element lower air gap (cell 10);
- b. The fuel region located above the upper grid plate and below the fuel element upper air gap (note: since the cross section is the same as subparagraph “a” it is defined by the same set of cells) ;
- c. The fuel region within the upper grid plate (cell 52);
- d. The fuel element upper air gap region (cell 30);
- e. The fuel element lower air gap region (note: since the cross section is the same as subparagraph “d” it is defined by the same set of cells);
- f. The fuel element upper end cap region (cell 24);

- g. The fuel element lower end cap region (note: since the cross section is the same as subparagraph “f” it is defined by the same set of cells); and
- h. The lower grid plate region (cell 35).

The definition of these cells requires the introduction of several new concepts which are:

- a. The union operator ":" is used to add spatial areas together;
- b. Parentheses, used to control the order of the operation; the default is complement first, intersection second and union last;
- c. “Fill” indicates that the cell volume is filled with the universe of the corresponding number. When the “fill” card is located in a lattice it can be used to define an array. In cell 11 it is used to define a 2 dimensional symmetrical array; whose coordinates 0,0 are centred on the volumes of cell 10 with respect to the z and y axes. The array has entries from -12 to 12;
- d. Lat, the lattice card used here (lat=1), defines a solid with 6 faces, which forms the basis for the array. The y and z faces are shown in Figure A-2;



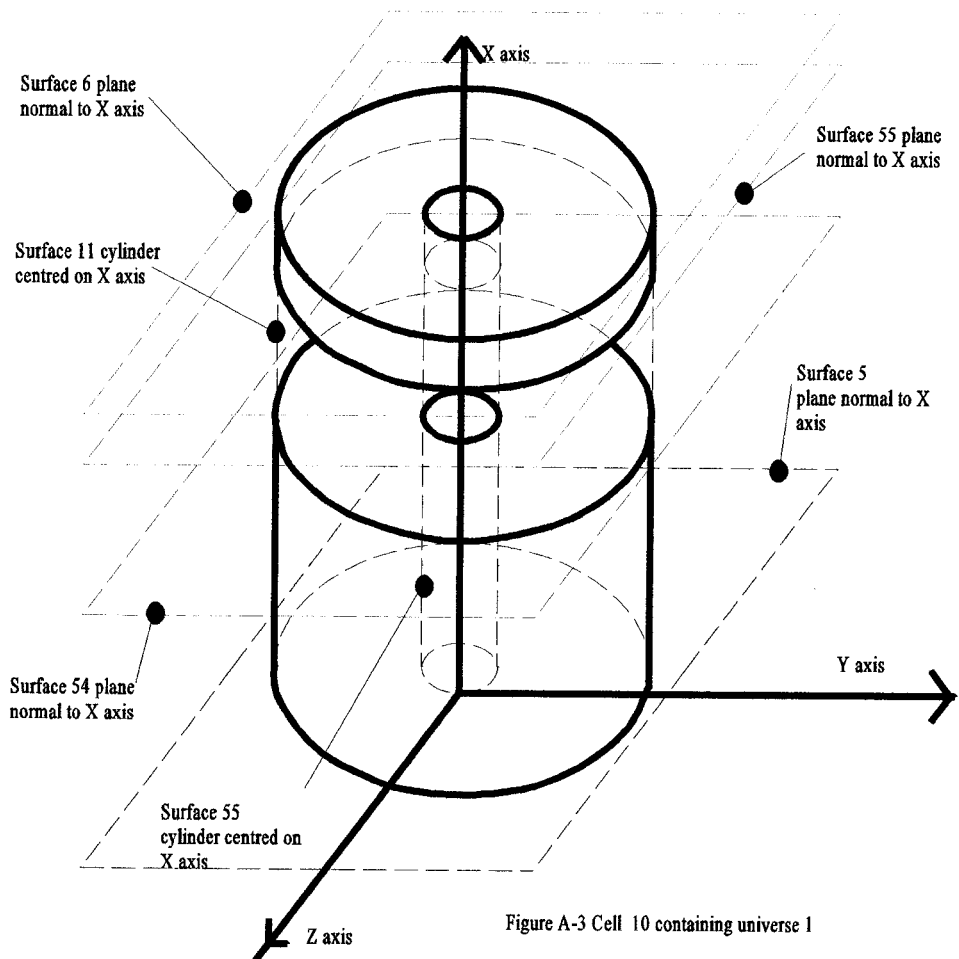
e. U, the universe card can either fill the "fill" card or another universe.

Cell 10 (Figure A-3) is composed of two pieces, the first one is delimited by surface 6 and 55, and the second is defined by surfaces 5 and 55;

- a. Surface 6 represents the plane separating the fuel element air gap and  $\text{UO}_2$  region of the upper fuel cage;
- b. Surface 55 is the plane delimiting the top of the upper grid plate of the fuel cage;
- c. Surface 54 is the plane delimiting the bottom of the upper grid plate of the fuel cage;
- d. Surface 5 represents the plane separating the fuel element air gap and  $\text{UO}_2$  region of the lower fuel cage;

It is filled by universe 1 which is an array 25 by 25 based on the lattice already presented in

Figure A-2 (see also Figure 3.3). Universe 1 is also filled by itself and cells 12 to 16 which define universe 2.



```

c      definition of fuel rod (cladding, radial air gap, uranium oxide)
c
10   2    -0.998  ((5 -54):(55 -6)) 604 -11 fill=1 Imp:n=1 $ fuel bundle
11   2    -0.998  -200 201 -202 203 lat=1 u=1 Imp:n=1 fill=-12:12 -12:12 0:0
     1 1 1 1 1 1 1 1 1 1 1 1 1 1 1 1 1 1 1 1 1 1 1 1 1 1 1 1 1 1 1
     1 1 1 1 1 1 1 1 1 1 1 1 1 1 1 1 1 2 2 2 2 1 1 1 1 1 1
     1 1 1 1 1 1 1 1 1 1 1 1 1 1 1 2 2 1 2 1 2 1 2 2 1 1
     1 1 1 1 1 1 1 1 1 1 1 1 2 1 2 1 1 2 2 1 1 2 2 2 1 1
     1 1 1 1 1 1 1 1 1 1 1 2 2 2 1 2 1 2 1 2 2 2 1 1

```

```

1 1 1 1 1 1 1 1 2 1 1 1 1 2 2 1 1 2 2 1 1 1 1 1 2 1
1 1 1 1 1 1 1 1 2 2 1 2 2 1 2 1 2 1 2 2 1 2 2 1
1 1 1 1 1 1 1 2 1 2 1 2 2 2 1 2 2 1 2 2 2 1 2 1 2 1
1 1 1 1 1 1 2 2 2 2 1 1 1 1 2 1 2 1 1 1 1 2 2 2 2 1
1 1 1 1 1 1 1 1 1 1 1 2 2 2 2 1 1 2 2 2 2 1 1 1 1 1 1
1 1 1 1 1 2 1 2 2 1 2 1 1 1 2 1 2 1 1 1 2 1 2 2 1 2 1
1 1 1 2 2 1 2 2 1 2 1 2 1 1 2 2 1 2 1 1 2 2 1 2 2 1 1
1 1 1 2 2 1 1 2 1 2 2 1 1 1 2 2 1 2 1 1 2 2 1 2 2 1 1
1 1 2 2 1 2 2 1 2 1 2 1 1 2 1 2 1 2 1 2 2 1 2 2 1 1 1
1 1 2 1 2 2 1 2 1 1 1 2 1 1 1 2 1 2 2 1 2 1 2 1 1 1 1 1
1 1 1 1 1 1 2 2 2 2 1 1 2 2 2 2 1 1 2 2 2 2 1 1 1 1 1 1 1
1 2 2 2 2 1 1 1 1 2 1 2 1 1 1 1 2 2 2 2 2 1 1 1 1 1 1 1 1
1 2 1 2 1 2 2 2 1 2 2 1 2 2 2 1 2 1 2 1 2 1 1 1 1 1 1 1 1
1 2 2 1 2 2 1 2 1 2 1 2 1 2 2 2 1 2 1 2 2 1 1 1 1 1 1 1 1
1 2 1 1 1 1 2 2 1 1 2 2 1 1 1 1 2 1 2 2 1 1 1 1 1 1 1 1 1
1 1 2 2 2 1 2 1 2 1 2 1 2 2 2 1 1 1 1 1 1 1 1 1 1 1 1 1 1
1 1 2 2 2 1 1 2 1 2 1 1 2 1 2 1 1 1 1 1 1 1 1 1 1 1 1 1 1
1 1 1 1 1 2 2 2 2 1 1 1 1 1 1 1 1 1 1 1 1 1 1 1 1 1 1 1 1
1 1 1 1 1 1 1 1 1 1 1 1 1 1 1 1 1 1 1 1 1 1 1 1 1 1 1 1 1

```

Universe 2 is shown in Figure A-4

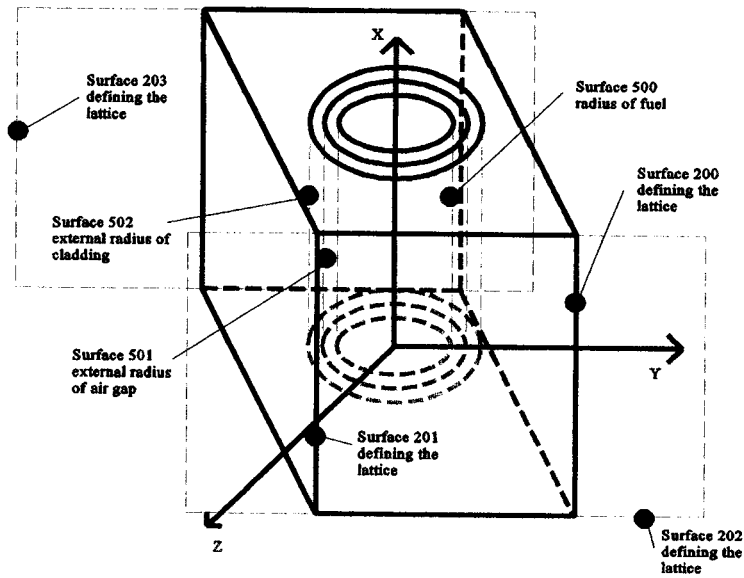


Figure A-4 Universe 2

```

12      3    -10.6   -500 u=2 imp:n=1      $ fuel elements
14      4    5.0807e-5 500   -501 u=2 imp:n=1      $ fuel elements air gap
15      5    -6.49 501   -502 u=2 imp:n=1      $ fuel elements cladding
16      2    -0.998 502 u=2 imp:n=1      $ water between elements

```

The model ends with the water of the pool therefore any neutron that reaches the side of the pool enters a void and therefore disappears.

```

c
c      outside world
c
c cell# mat density      surfaces      comments
  17    0      (113:-112:102) -999  Imp:n=1  $ void cell around core

```

The next cells, 18 to 19, are used to define the control rod and the channel in which it travels in the reactor cage.

```

c
c      definition of control rod
c
c cell# mat density      surfaces      comments
  18    4 5.0807e-5    606 -600 -607      Imp:n=1  $ centre
  19    7 -8.65        600 -601 606 -607      Imp:n=1  $ cadmium
  20    6 -2.70        605 -608 -602 (-606:607:601) Imp:n=1  $ cladding
  21    2 -0.998       50 -58 -603 (-605:608:602) Imp:n=1  $ water
  22    5 -6.49 50     603 -604 -6      Imp:n=1  $ zirconium

```

All the gaps between the reflector, the fuel cage and the irradiation sites were defined as single cells containing water. In order to help with some of the physical representation of these cells, cross sections of the lower core are provided with the cell numbers at Figure A-5 and the surface numbers at Figure A-6. The cross sections of the upper core are also shown at Figure A-7 and A-8.

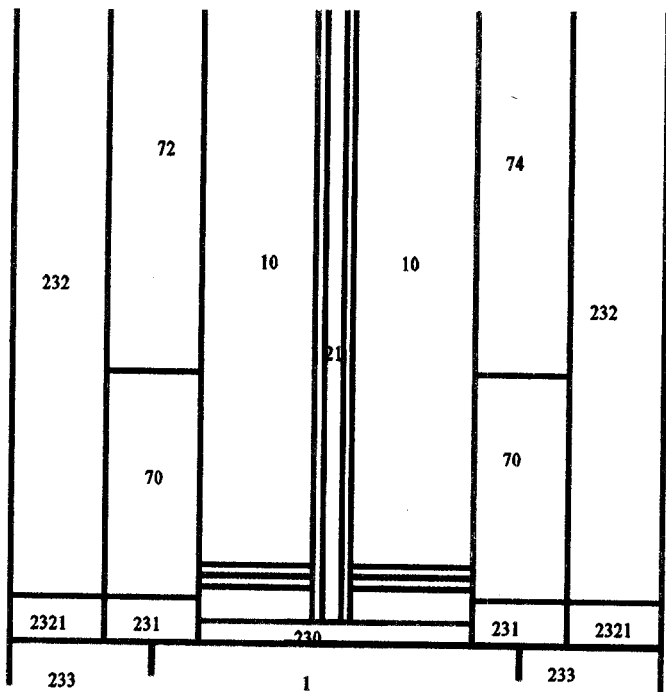


Figure A-5 Cross section with cell number

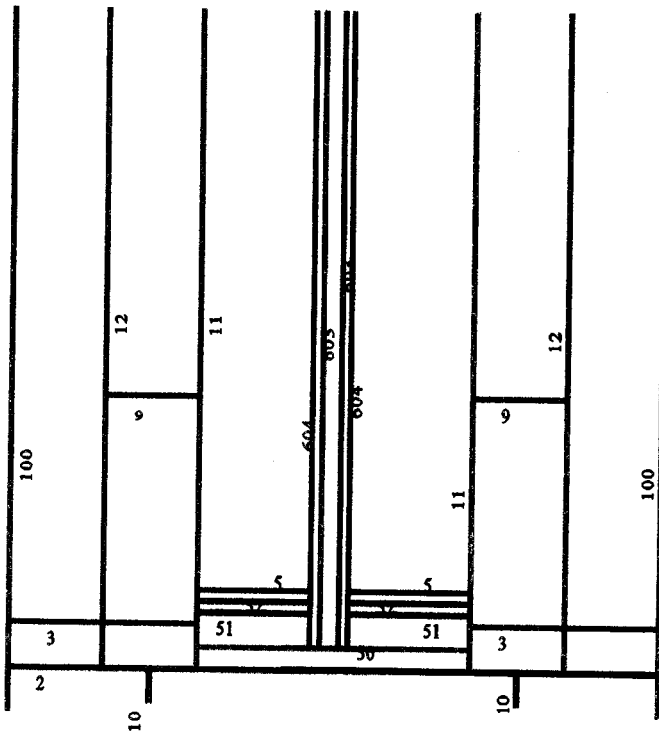


Figure A-6 Cross section with surface number

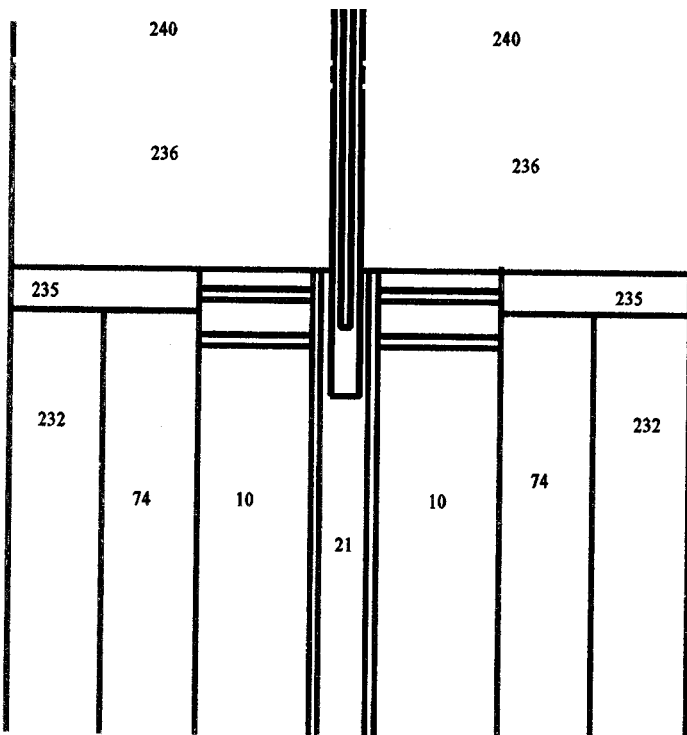


Figure A-7 Cross section with surface number upper part

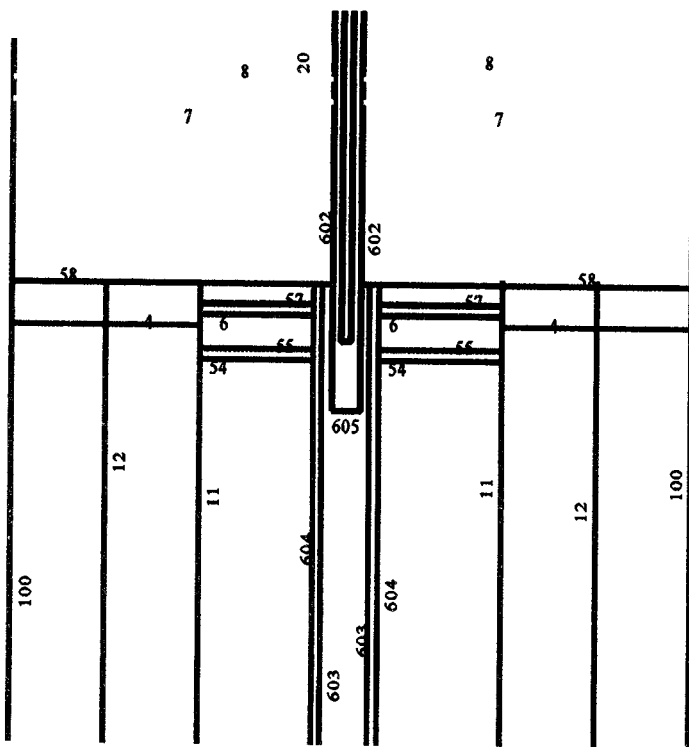


Figure A-8 Cross section with surface number upper part

```

c definition of water surrounding the core
c
c water below UO2 above bottom reflector
230 2 -0.998 2 -50 -11 Imp:n=1
c water below reflector annulus around UO2
231 2 -0.998 11 2 -3 -12 Imp:n=1
c water between annulus and bottom reflector
2321 2 -0.998 12 2 -3 -4 -100 Imp:n=1
c water around reflector annulus
232 2 -0.998 12 3 -4 -100 132 142 152 162 #(-1000 -1003 -1002) Imp:n=1
c water around bottom reflector
233 2 -0.998 10 1 -2 -100 Imp:n=1
c water below bottom reflector
234 2 -0.998 -1 -100 110 Imp:n=1
c water around UO2 above reflector annulus
235 2 -0.998 11 4 -58 -100 132 142 153 162 13 14 15 16 17 Imp:n=1
c water around control rod below top reflector
236 2 -0.998 58 -100 -7 602 132 142 153 162 13 14 15 16 17 Imp:n=1
c water around control rod in top reflector inside radius
237 2 -0.998 -8 7 -20 602 Imp:n=1
c water around top reflector
238 2 -0.998 -8 7 19 21 -100 132 142 153 162 13 14 15 16 17 Imp:n=1
c water on opposite side of top reflector
239 2 -0.998 -8 7 20 -21 -100 132 142 153 162 13 14 15 16 17 Imp:n=1
c water around control rod above top reflector
240 2 -0.998 8 -608 602 -100 132 142 153 162 13 14 15 16 17 Imp:n=1
c water above control rod
241 2 -0.998 608 -100 -113 132 142 153 162 13 14 15 16 17 Imp:n=1
c water outside shell
242 2 -0.998 (-113 -102 101 111):(-102 112 -111) Imp:n=1
c
c aluminium reactor shell
300 6 -2.70 100 -101 -113 110 imp:n=1 $aluminium cylinder
301 6 -2.70 -110 -101 111 imp:n=1 $aluminium plate

```

Cell 24 to 27 use the same notation that was used for the two fuel regions previously.

described, to define the fuel element end cap regions of the core. The other core region will also be defined in the same fashion.

```

c           End caps of fuel rods defined as zirconium
c
c
24   2   -0.998    ((51 -52):(57 -58)) 604 -11 fill=3 Imp:n=1 $ end caps
25   2   -0.998    -200 201 -202 203 lat=1 u=3 Imp:n=1 fill=-12:12 -12:12 0:0
      3 3 3 3 3 3 3 3 3 3 3 3 3 3 3 3 3 3 3 3 3 3 3 3 3 3 3 3 3 3 3
      3 3 3 3 3 3 3 3 3 3 3 3 3 3 3 3 3 3 4 4 4 4 4 3 3 3 3 3 3 3 3
      3 3 3 3 3 3 3 3 3 3 3 3 3 3 3 4 4 3 4 3 4 3 4 4 3 3 3 4 4 4 3 3
      3 3 3 3 3 3 3 3 3 3 3 4 3 4 3 3 4 4 3 3 3 4 4 4 3 3 3 4 4 4 3 3
      3 3 3 3 3 3 3 3 3 3 4 4 4 3 4 3 4 4 4 3 4 4 4 4 3 3 3 4 4 4 3 3

```







```
1002 6 -2.70 -1001 -1004 -1005 12 -4 3 -1002 imp:n=1 $inner arch
1003 6 -2.70 -1001 -1004 1006 -100 -4 3 -1002 imp:n=1 $outer arch
c
1004 6 -2.70 -1001 -1004 1005 -1006 -4 1007 -1002 imp:n=1 $upper
1005 6 -2.70 -1001 -1004 1005 -1006 3 -1008 -1002 imp:n=1 $bottom
c
1006 8 -1.105 -1001 -1004 1005 -1006 -1007 1008 -1002 imp:n=1 $D2O
```

## SURFACES

The surface definition is much simpler than the cell definition. As mentioned in Chapter 2, this model was entirely made of planes, cylinders and spheres. These geometrical figures are simply defined by their mathematical equation using Cartesian coordinates. Although the notation is available in Reference 5, it was reproduced here as Table A-1 in order to assist the reader.

Table A-1  
MCNP 4A Surface Definition

Notation	Type	Description	Equation	Entries
P	Plane	General	$Ax+By+Cz-D=0$	A B C D
PX		Normal to X-axis	$x-D=0$	D
PY		Normal to Y-axis	$y-D=0$	D
PZ		Normal to Z-axis	$z-D=0$	D
SO	Sphere	Centred at origin	$x^2+y^2+z^2-R^2=0$	R
S		General	$(x-\bar{x})^2+(y-\bar{y})^2+(z-\bar{z})^2-R^2=0$	$\bar{x} \bar{y} \bar{z} R$
SX		Centred on X-axis	$(x-\bar{x})^2+y^2+z^2-R^2=0$	$\bar{x} R$
SY		Centred on Y-axis	$x^2+(y-\bar{y})^2+z^2-R^2=0$	$\bar{y} R$
SZ		Centred on Z-axis	$x^2+y^2+(z-\bar{z})^2-R^2=0$	$\bar{z} R$
C/X	Cylinder	Parallel to X-axis	$(y-\bar{y})^2+(z-\bar{z})^2-R^2=0$	$\bar{y} \bar{z} R$
C/Y		Parallel to Y-axis	$(x-\bar{x})^2+(z-\bar{z})^2-R^2=0$	$\bar{x} \bar{z} R$
C/Z		Parallel to Z-axis	$(x-\bar{x})^2+(y-\bar{y})^2-R^2=0$	$\bar{x} \bar{y} R$
CX		On X-axis	$y^2+z^2-R^2=0$	R
CY		On Y-axis	$x^2+z^2-R^2=0$	R
CZ		On Z-axis	$x^2+y^2-R^2=0$	R

Note: The notation is not case sensitive

PROPRIETARY DATA

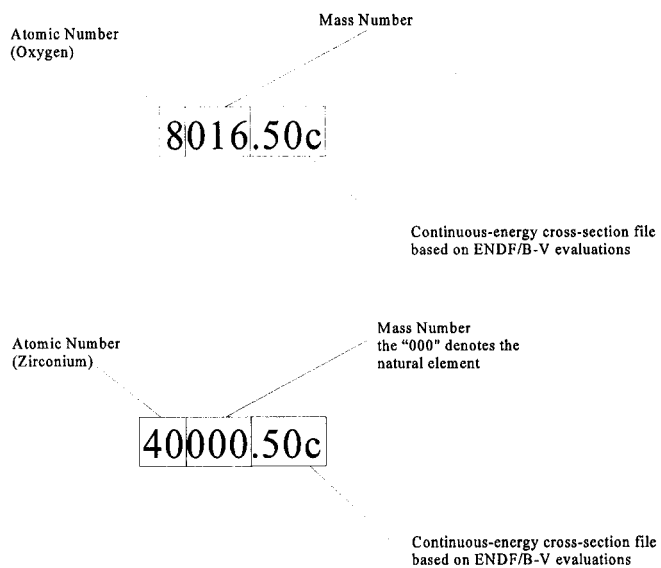
c surface definition  
1 px 0 \$ bottom plate  
2 px 10.16 \$ bottom plate  
c  
3 px 10.668 \$ beryllium annulus  
4 px 33.416 \$ beryllium annulus  
c  
5 px 10.947 \$ fuel bundle  
6 Px 33.6445 \$ fuel bundle  
c  
50 px 10.414 \$ lower grid plate and cap  
51 px 10.693 \$ lower grid plate and cap  
52 px 10.828 \$ lower air gap  
54 px 32.914 \$ upper grid plate  
55 px 33.193 \$ upper grid plate  
57 px 33.9385 \$ upper air gap  
58 px 34.0735 \$ upper cap  
c  
7 px 35.932 \$ top shim  
8 px 36.09075 \$ top shim  
c  
9 px 17.668 \$ annulus holes  
c  
10 cx 16.113125 \$ lower plate  
c  
11 cx 11.049 \$ annulus  
12 cx 21.2344 \$ annulus  
c  
70 p 0.0 -0.7265847 1.0 0.0  
71 p 0.0 0.72658447 1.0 0.0  
72 p 0.0 -3.07768 1.0 0.0  
73 pz 0.0  
74 p 0.0 3.07768 1.0 0.0  
c  
13 c/x 14.56182 0.0 1.56718 \$ annulus hole out D  
14 c/x 4.49985 13.84911 1.56718 \$ annulus hole out D  
15 c/x -11.78076 8.55972 1.56718 \$ annulus hole out D  
16 c/x -11.78076 -8.55972 1.56718 \$ annulus hole out D  
17 c/x 4.49985 -13.84911 1.56718 \$ annulus hole out D  
c  
131 c/x 14.56182 0.0 1.40208 \$ annulus hole ins D  
141 c/x 4.49985 13.84911 1.40208 \$ annulus hole ins D  
151 c/x -11.78076 8.55972 1.40208 \$ annulus hole ins D  
161 c/x -11.78076 -8.55972 1.40208 \$ annulus hole ins D  
171 c/x 4.49985 -13.84911 1.40208 \$ annulus hole ins D  
c  
c outside irradiation sites  
c  
132 c/x -7.416 -22.825 1.905 \$ large site out R  
142 c/x 19.416 -14.107 1.56718 \$ small site out R  
152 c/x 19.416 14.107 1.61798 \$ cadmium lined out R  
162 c/x -7.416 22.285 1.56718 \$ flooded site out R  
c  
153 c/x 19.416 14.107 1.56718 \$ cadmium lined bet R  
c  
133 c/x -7.416 -22.825 1.600 \$ large site ins R  
143 c/x 19.416 -14.107 1.40208 \$ small site ins R  
154 c/x 19.416 14.107 1.40208 \$ cadmium lined ins R  
163 c/x -7.416 22.285 1.40208 \$ flooded site ins R  
c  
19 cx 12.065 \$ top shim  
20 cx 1.3890625 \$ top shim

PROPRIETARY DATA

21 py 0.1190625 \$ top shim  
C  
100 cx 30 \$ water in reactor shell  
101 cx 31 \$ reactor shell  
102 c/x 30 30 133 \$ outside world  
C  
110 px -8 \$ bottom of shell  
111 px -9 \$ bottom of shell  
112 px -31 \$ pool bottom  
113 px 533 \$ pool top  
C  
200 p 0.0 -1.7321045 -1.0 0.955803 \$ lattice  
201 p 0.0 -1.7321045 -1.0 -0.955803 \$ lattice  
202 pz 0.477902 \$ lattice  
203 pz -0.477902 \$ lattice  
C  
500 cx 0.2064 \$ fuel rod  
501 cx 0.212 \$ fuel rod  
502 cx 0.262 \$ fuel rod  
C  
550 c/x 0.551815 0.318516 .262 \$ flange hole  
551 c/x 0.551815 -0.318516 .262 \$ flange hole  
552 c/x -0.551815 0.318516 .262 \$ flange hole  
553 c/x -0.551815 -0.318516 .262 \$ flange hole  
554 c/x 0.0 0.637286 .262 \$ flange hole  
555 c/x 0.0 -0.637286 .262 \$ flange hole  
556 cx 0.15  
C  
560 c/x 0.551815 0.318516 .19 \$ flange hole  
561 c/x 0.551815 -0.318516 .19 \$ flange hole  
562 c/x -0.551815 0.318516 .19 \$ flange hole  
563 c/x -0.551815 -0.318516 .19 \$ flange hole  
564 c/x 0.0 0.637286 .19 \$ flange hole  
565 c/x 0.0 -0.637286 .19 \$ flange hole  
C  
600 cx 0.09652 \$ control rod  
601 cx 0.14732 \$ control rod  
602 cx 0.62357 \$ control rod cladding  
603 cx 1.229 \$ control rod hole  
604 cx 1.331 \$ control rod hole  
605 px 30.82 \$ bottom control rod cladding  
606 px 33.32 \$ bottom control rod  
607 px 58.08 \$ top control rod  
608 px 71.46 \$ top control rod cladding  
C  
999 sx 21 1000  
C  
1000 p 0.0 1.0 2.43 1.082 SD2O side 1  
1001 p 0.0 1.0 2.43 0.0 SD2O side 1  
C  
1002 py 0.0  
C  
1003 p 0.0 1.0 -2.43 1.082 SD2O side 2  
1004 p 0.0 1.0 -2.43 0.0 SD2O side 2  
C  
1005 cx 22.2344 \$ D2O inner arch  
1006 cx 29 \$ D2O outer arch  
C  
1007 px 32.6445 \$ Top  
1008 px 11.947 \$ Bottom

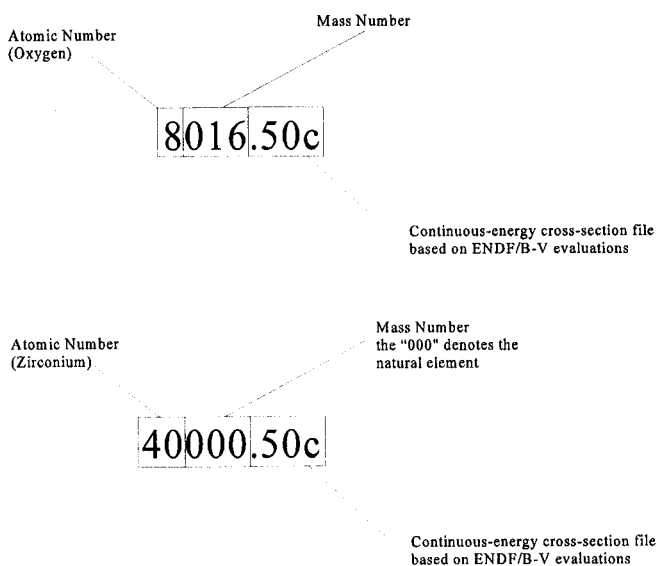
## MATERIAL BLOCK

Each cell, except the void cells, is made of a material, which, up to now, has been referred to by its numeral label . These numbers are defined in this block. As previously mentioned, MCNP 4A uses cross section libraries to calculate the probability of an event. Basically, when the user defines the materials for the model, he selects corresponding cross section libraries. The format of the entry is as follows:



## MATERIAL BLOCK

Each cell, except the void cells, is made of a material, which, up to now, has been referred to by its numeral label . These numbers are defined in this block. As previously mentioned, MCNP 4A uses cross section libraries to calculate the probability of an event. Basically, when the user defines the materials for the model, he selects corresponding cross section libraries. The format of the entry is as follows:



When the material is made of more than one element, the atomic fraction can be entered as an integer, or the weight fraction can be entered as a negative number. The first material defined is the Beryllium. Its definition includes several impurities obtained at reference 27 and listed at Appendix B. Since no cross section files were available for the missing ones, some material were omitted.

<u>PROPRIETARY DATA</u>						
c	material definition					
m1	4009.50c	-.9953863	8016.50c	-9.701130e-6	13027.50c	-1.010534e-3
	6000.50c	-1.515802e-3	26000.50c	-1.31695e-3	14000.50c	
	-6.063207e-4	5011.50c	-1.616855e-6	25055.50c	-1.515802e-4	
	48000.50c	-7.376901e-7	3006.50c	-1.313695e-7	3007.55c	
	-1.92001e-6	62149.50c	-6.497736e-7	64155.50c	-3.53687e-8	
	64157.50c	-3.13265e-8	63151.50c	-2.425283e-7	63153.50c	
	-2.627389e-7	5010.50c	-4.345298e-7	\$ Be plus impurities		

m2	1001.50c	2	8016.50c	1	\$ H2O	
m3	92235.50c	-.1753	92238.50c	-.7059	8016.50c	-.1188 \$ UO2
m4	8016.50c	0.21174	7014.50c	0.78826	\$ Air	
m5	40000.50c	1			\$ Zr	
m6	13027.50c	-.9792	14000.50c	-0.006	29000.50c	-0.0028 12000.50c
	-0.01	24000.50c	-0.002		\$ Al	6061 T6
m7	48000.50c	1			\$ Cd	
m8	1002.50c	2	8016.50c	1	\$ D2O	

The next two lines indicate that the S( $\alpha, \beta$ ) treatment, is to be used for H<sub>2</sub>O and D<sub>2</sub>O

```
mt2 lwtr.01t
mt8 hwtr.01t
```

The entry following kcode are:

- a. Number of neutrons per cycle
- b. Estimated  $k_{\text{eff}}$
- c. Number of inactive cycles to run
- d. Number of active cycles to run

```
kcode 100000 1. 20 200
c single particle source at centre of the core
c coordinates      X          Y          Z
c      ksrc        21           0           0
c      ksrc       32.52      -12.83      2.709
c      ksrc        21          2.25       0.0
```

Note: if no source is specified, MCNP 4A uses the default file SRCTP which is written by a previous run of MCNP 4A.

## APPENDIX B : BERYLLIUM IMPURITIES

This is a list of the impurities for the beryllium reflector as obtained from reference 26.

Element	Atomic Number	Weight fraction	Simulated by
Oxygen	16	$9.4 \times 10^{-4}$	Oxygen 16
Aluminum	Natural	0.1	Aluminum 27
Carbon	Natural	0.15	Natural Carbon
Iron	Natural	0.13	Natural Iron
Silicon	Natural	0.06	Natural Silicon
Boron	10	$4.3 \times 10^{-5}$	Boron 10
Boron	11	$1.6 \times 10^{-4}$	Boron 11
Manganese	Natural	$1.5 \times 10^{-2}$	Manganese 55
Cadmium	112	$4.8 \times 10^{-5}$	Natural Cadmium
Cadmium	113	$2.5 \times 10^{-5}$	Natural Cadmium
Lithium	6	$1.3 \times 10^{-5}$	Lithium 6
Lithium	7	$1.9 \times 10^{-4}$	Lithium 7
Samarium	137	$7.3 \times 10^{-6}$	not available
Samarium	148	$5.5 \times 10^{-6}$	not available
Samarium	149	$6.8 \times 10^{-6}$	Samarium 149
Samarium	150	$3.7 \times 10^{-6}$	not available
Samarium	152	$4.1 \times 10^{-5}$	not available
Gadolinium	155	$3.5 \times 10^{-6}$	Gadolinium 155
Gadolinium	157	$3.1 \times 10^{-6}$	Gadolinium 157
Europium	151	$2.4 \times 10^{-5}$	Europium 151
Europium	153	$2.6 \times 10^{-5}$	Europium 153
Indium	115	$4.8 \times 10^{-4}$	not available
Iridium	191	$1.9 \times 10^{-4}$	not available
Iridium	193	$3.1 \times 10^{-4}$	not available

## **APPENDIX C : THERMAL COLUMN VOLUME CALCULATION**

This Appendix contains the detailed calculations of the difference in volumes between the physical volume of the thermal column and the modelled one.

### **PROPRIETARY DATA**

#### **Physical volume of the thermal column**

$$\text{Inside radius} = 21.4 \text{ cm} = r$$

$$\text{Outside radius} = 29.5 \text{ cm} = R$$

$$\text{Height} = 19.1 \text{ cm} = h$$

$$\text{Core coverage} = 0.125$$

$$\text{Volume of inside cylinder} = \pi r^2 h = 3.1415 * 21.4^2 * 19.1 = 27479.6 \text{ cm}^3$$

$$\text{Volume of outside cylinder} = \pi R^2 h = 3.1415 * 29.5^2 * 19.1 = 52218.8 \text{ cm}^3$$

$$\begin{aligned}\text{Volume of thermal column} &= (\text{Volume of outside cylinder} - \text{Volume of inside cylinder})/8 \\ &= 3092.4 \text{ cm}^3\end{aligned}$$

#### **Model volume of the thermal column**

$$\text{Inside radius} = 21.2 \text{ cm}$$

$$\text{Outside radius} = 30.0 \text{ cm}$$

$$\text{Height} = 23.0 \text{ cm}$$

$$\text{Core coverage} = 0.125$$

$$\text{Volume of inside cylinder} = \pi r^2 h = 3.1415 * 21.2^2 * 23.0 = 32475.0 \text{ cm}^3$$

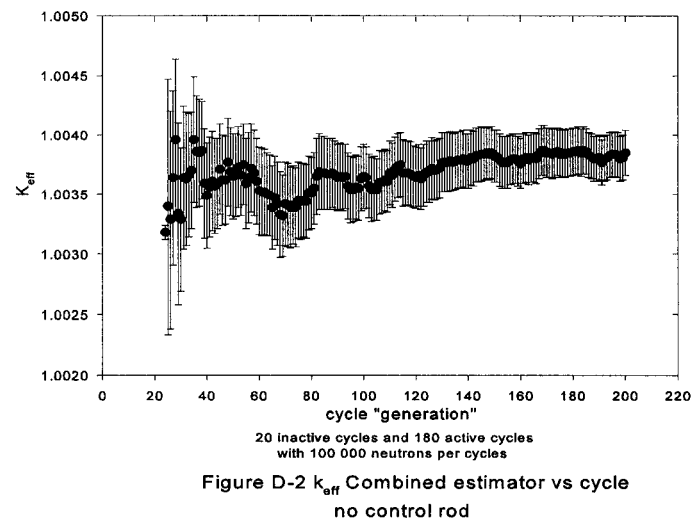
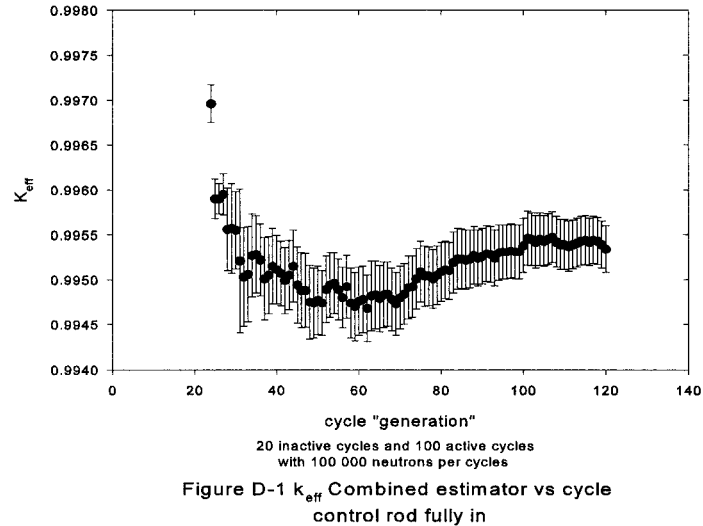
$$\text{Volume of outside cylinder} = \pi R^2 h = 3.1415 * 30.0^2 * 23.0 = 65031.0 \text{ cm}^3$$

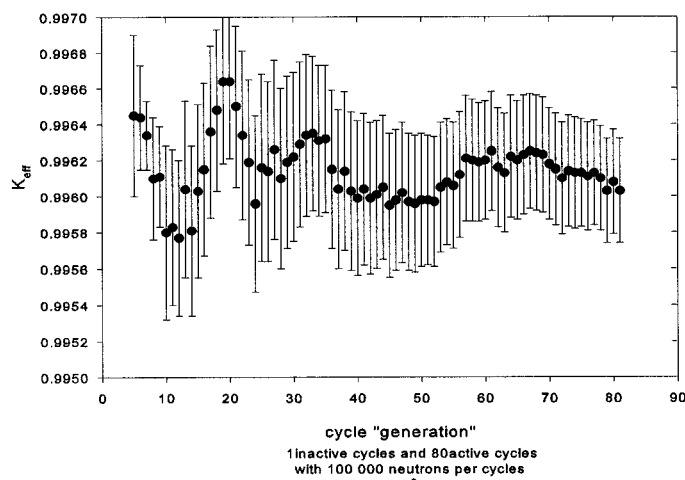
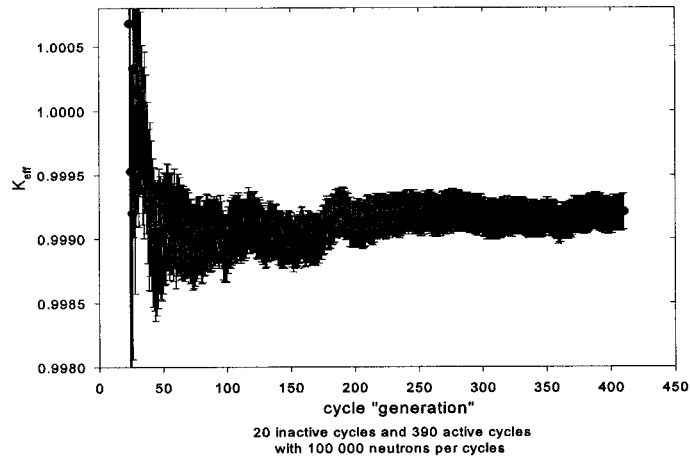
$$\begin{aligned}\text{Volume of thermal column} &= (\text{Volume of outside cylinder} - \text{Volume of inside cylinder})/8 \\ &= 4069.5 \text{ cm}^3\end{aligned}$$

$$\text{Volume difference (percent)} = 31\%$$

## APPENDIX D : $k_{\text{eff}}$ TRENDS

As mentioned in Section 5.2, the average three-combined  $k_{\text{eff}}$  of the final simulation of all the cases studied are presented here to give an indication of the stability of those simulations.





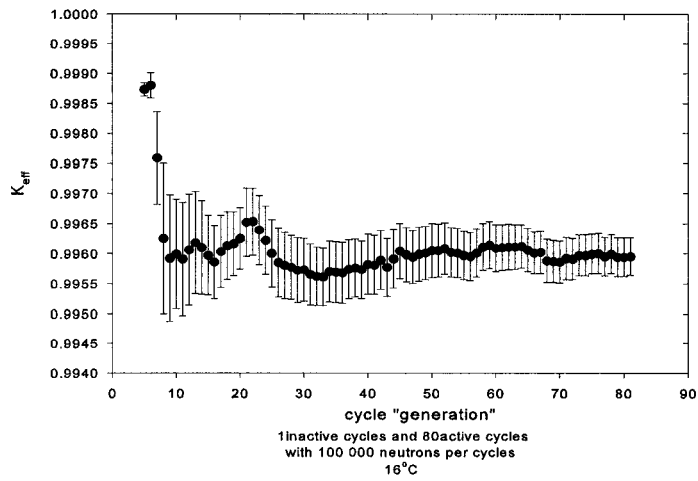


Figure D-5  $k_{\text{eff}}$  Combined estimator vs cycle  
control fully inserted

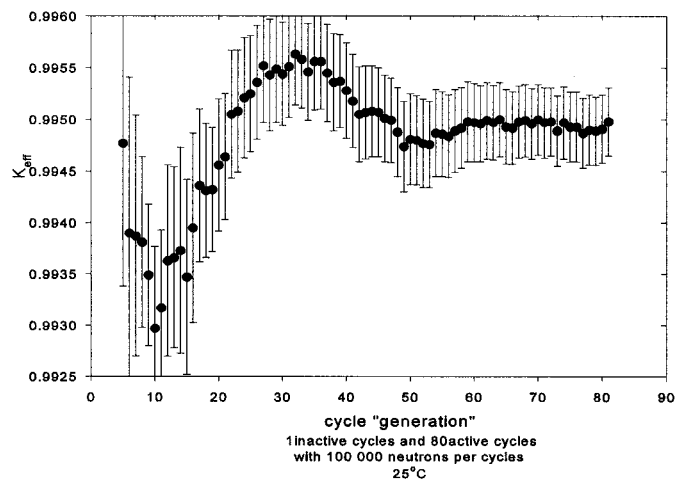
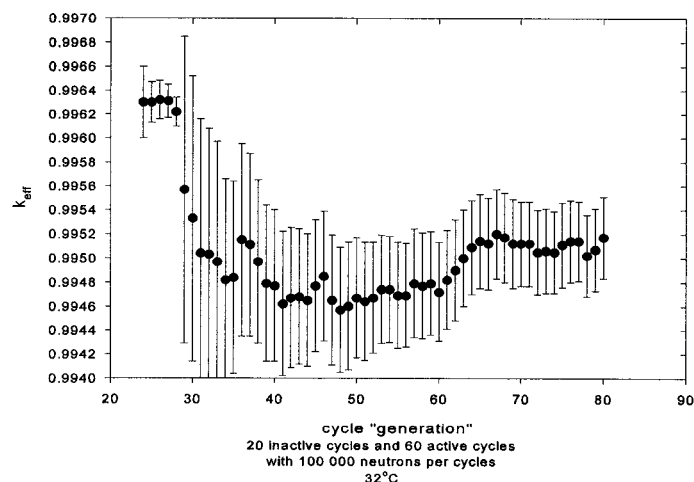
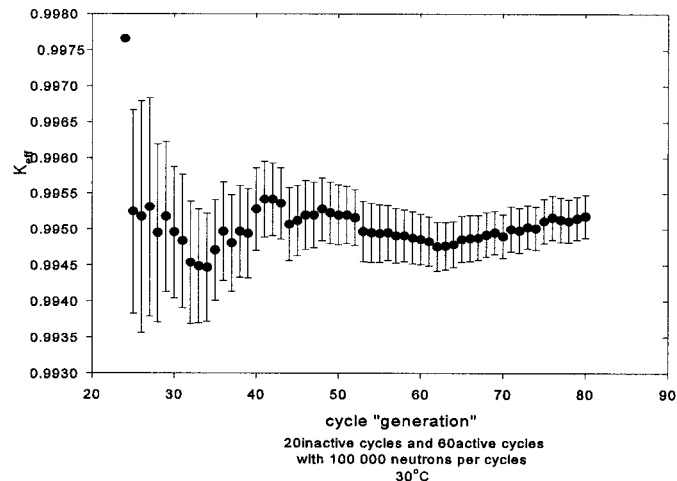


Figure D-6  $k_{\text{eff}}$  Combined estimator vs cycle  
control fully inserted



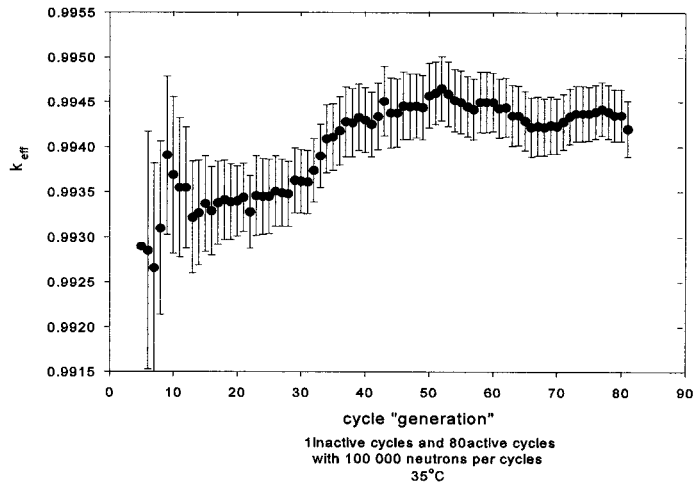


Figure D-9  $k_{\text{eff}}$  Combined Estimator Vs Cycle  
Control Fully Inserted

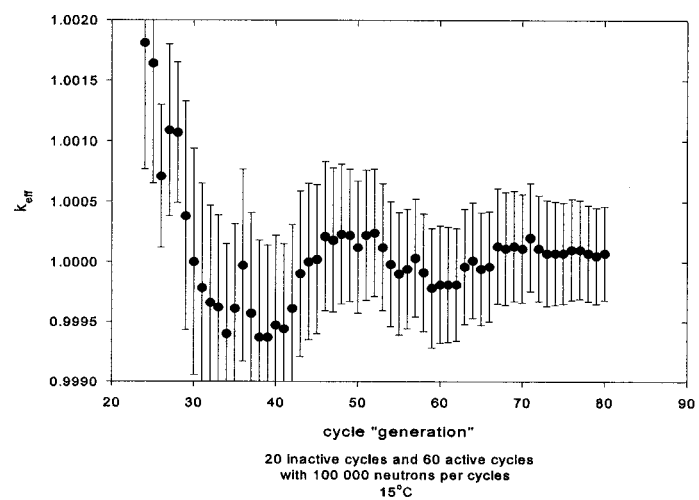
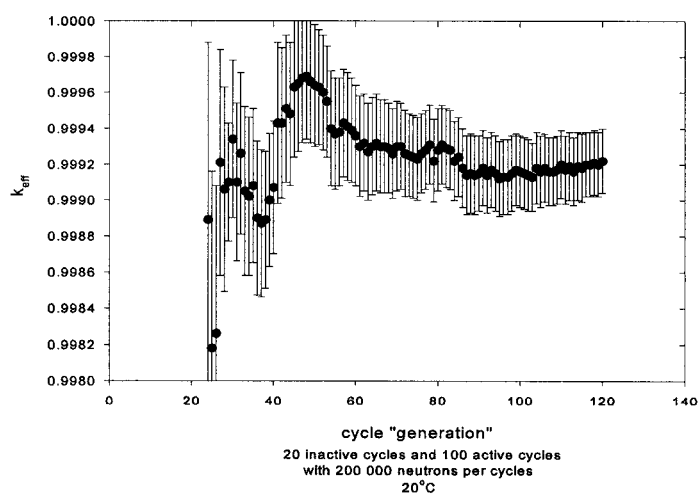
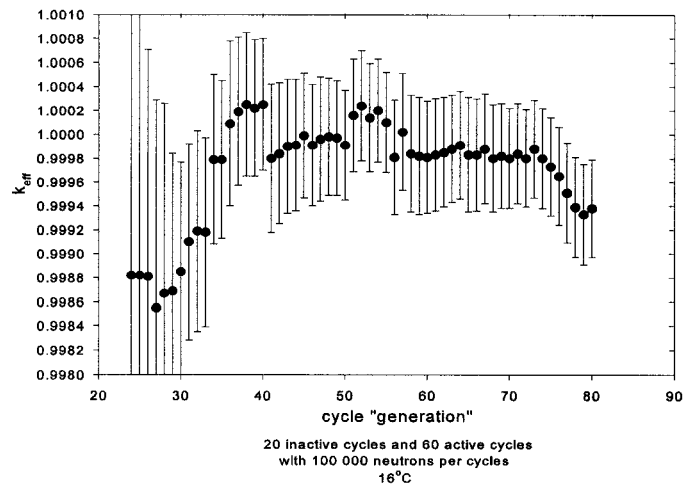


Figure D-10  $k_{\text{eff}}$  Combined estimator vs cycle  
control rod centred



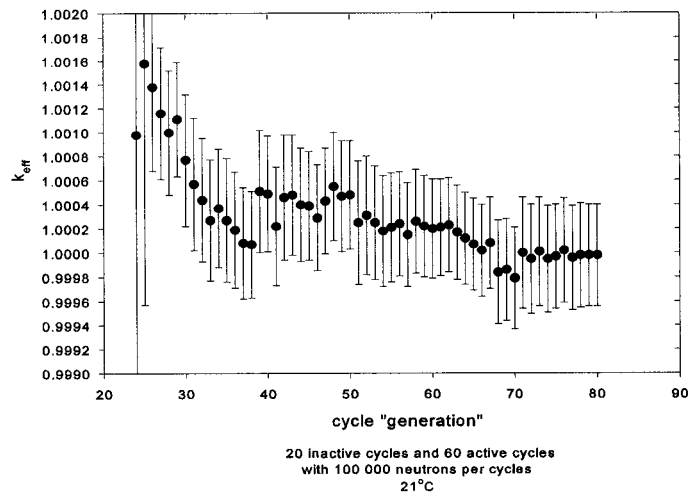


Figure D-13  $k_{\text{eff}}$  Combined estimator vs cycle  
control rod centred

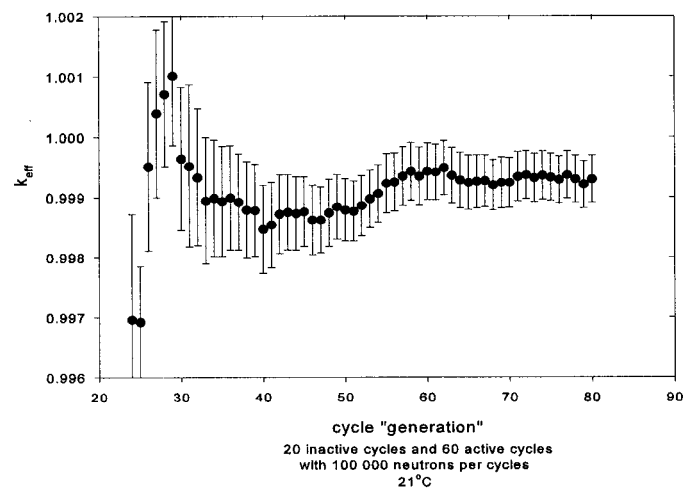
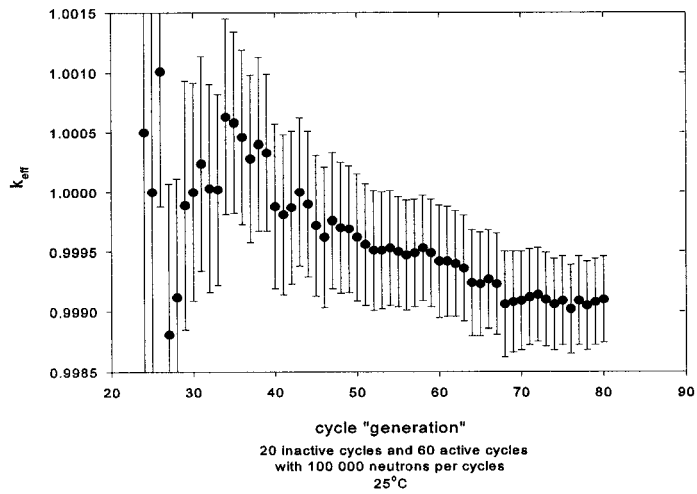
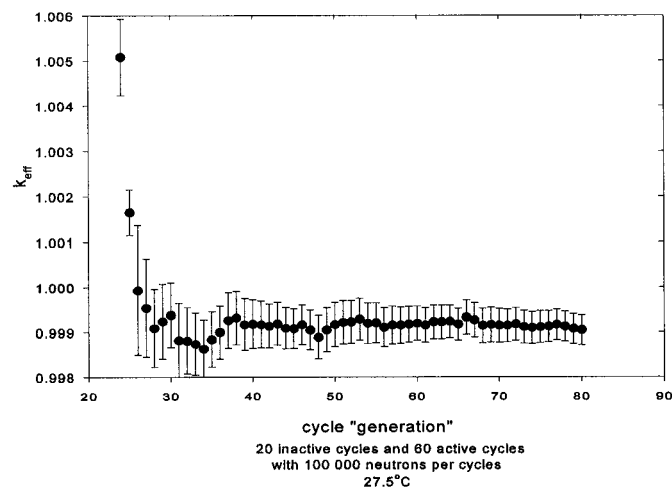


Figure D-14  $k_{\text{eff}}$  Combined estimator vs cycle  
control rod centred



**Figure D-15**  $k_{\text{eff}}$  Combined estimator vs cycle control rod centred



**Figure D-16**  $k_{\text{eff}}$  Combined estimator vs cycle control rod centred

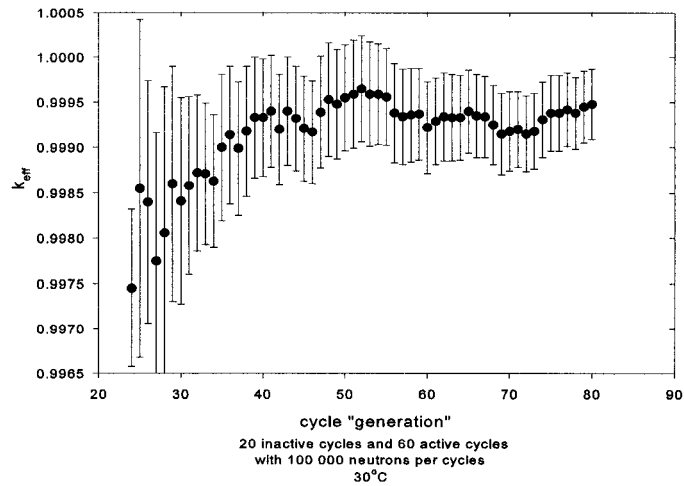


Figure D-17  $k_{\text{eff}}$  Combined estimator vs cycle  
control rod centred

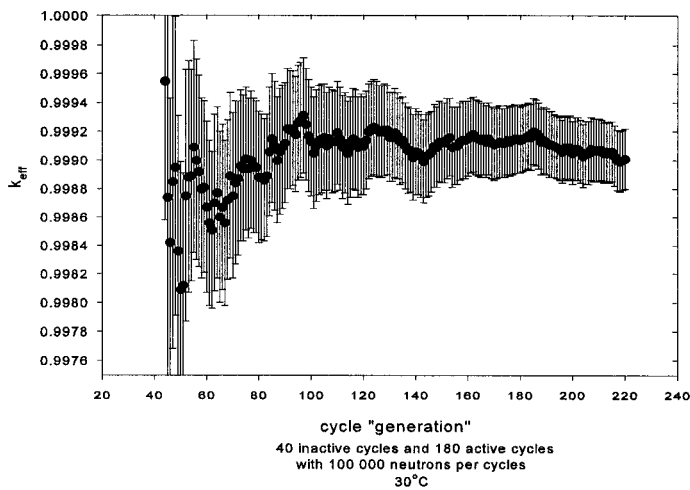


Figure D-18  $k_{\text{eff}}$  Combined estimator vs cycle  
control rod centred

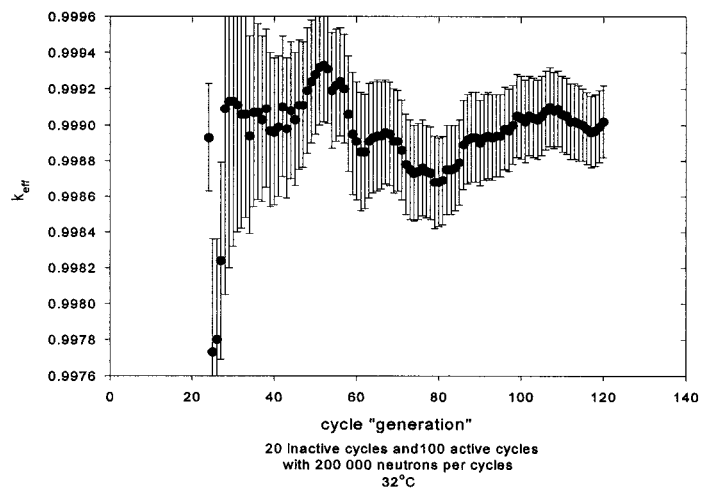


Figure D-19  $k_{\text{eff}}$  Combined estimator vs cycle  
control rod centred

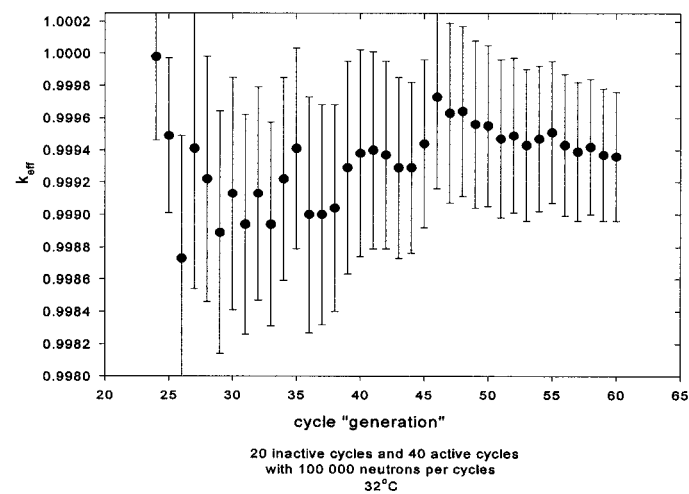


Figure D-20  $k_{\text{eff}}$  Combined estimator vs cycle  
control rod centred

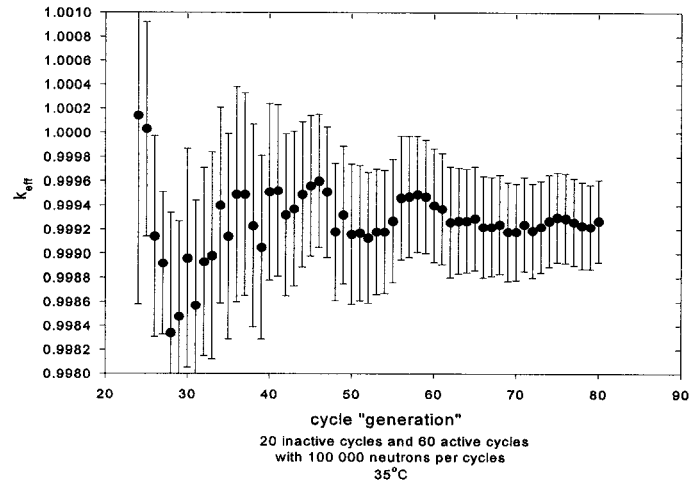


Figure D-21  $k_{\text{eff}}$  Combined estimator vs cycle  
control rod centred

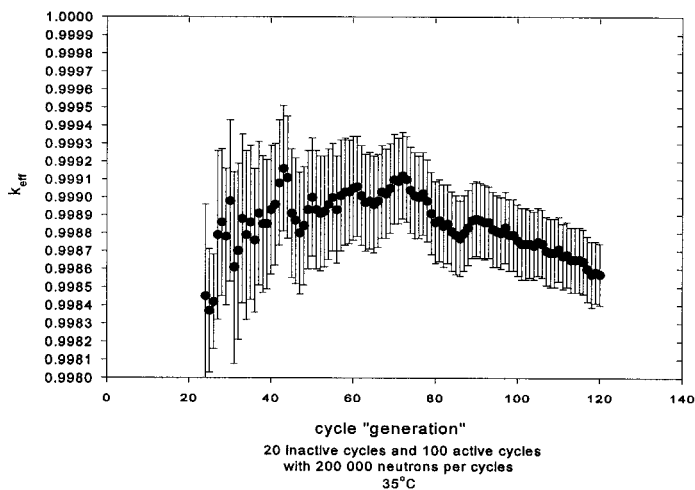


Figure D-22  $k_{\text{eff}}$  Combined estimator vs cycle  
control rod centred

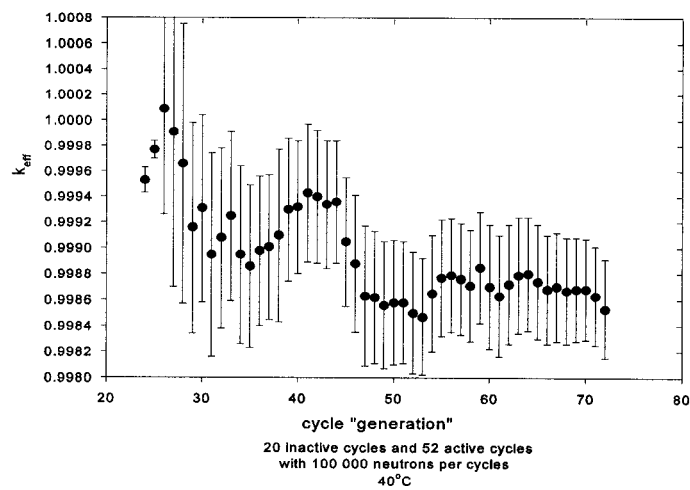


Figure D-23  $k_{\text{eff}}$  Combined estimator vs cycle control rod centred

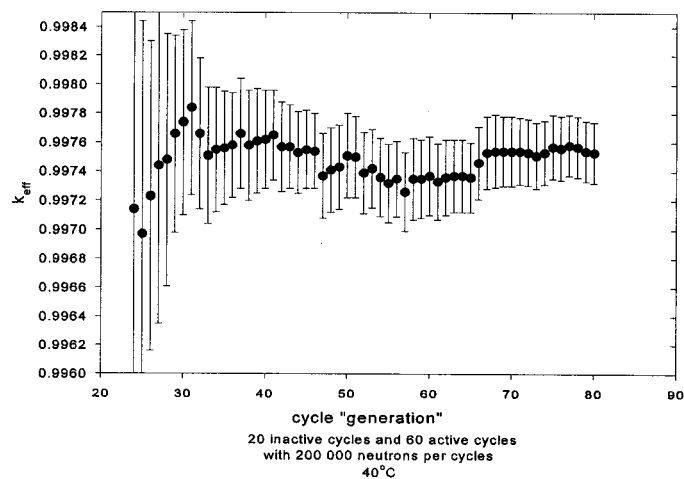
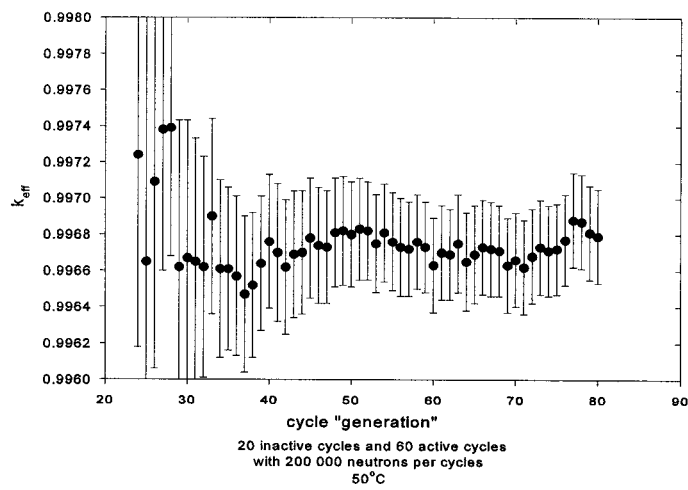
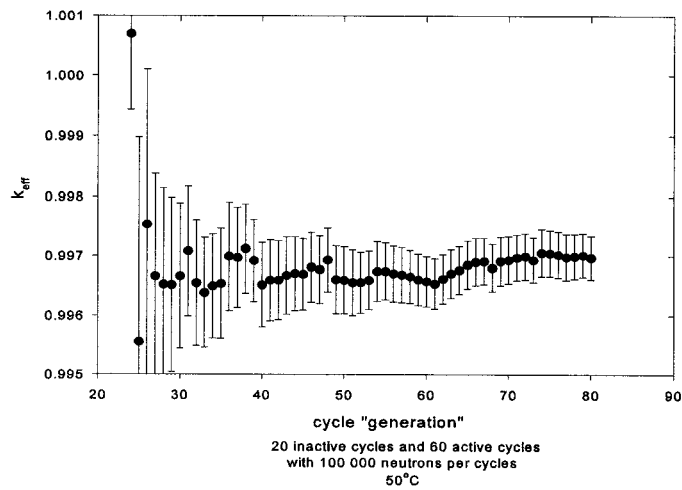
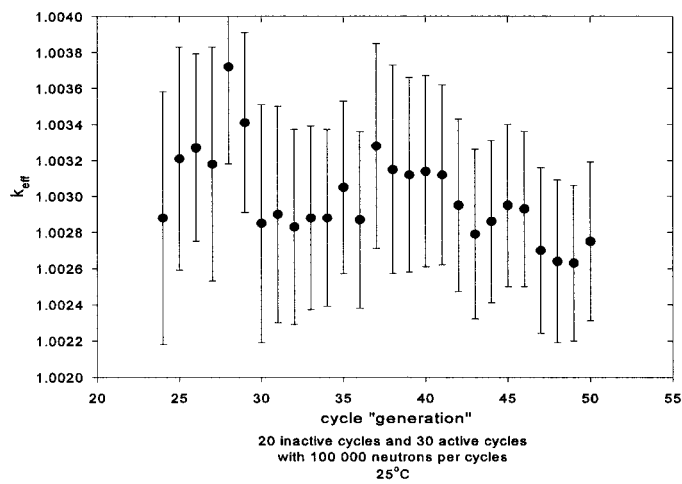
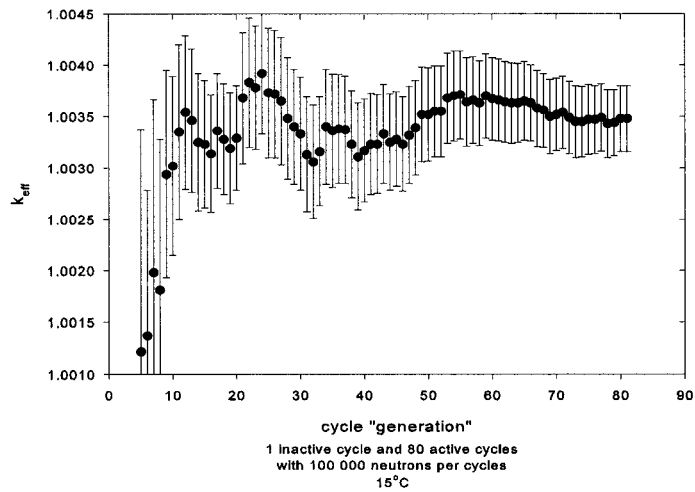
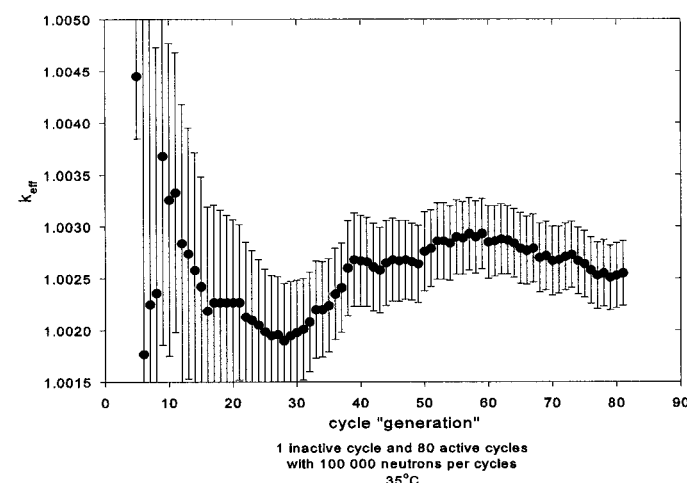
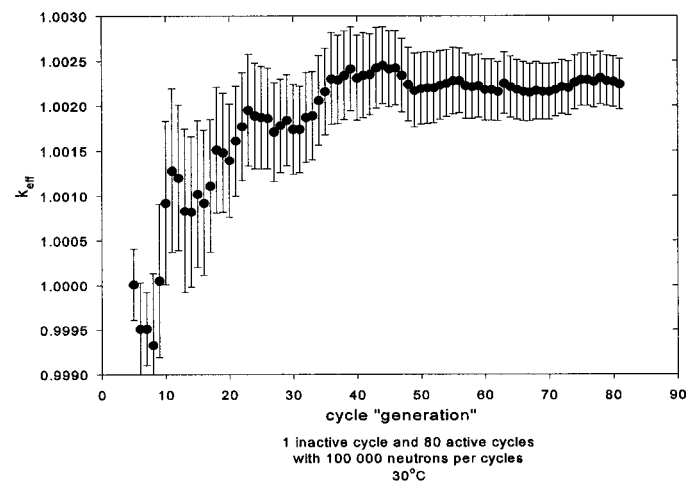


Figure D-24  $k_{\text{eff}}$  Combined estimator vs cycle control rod centred







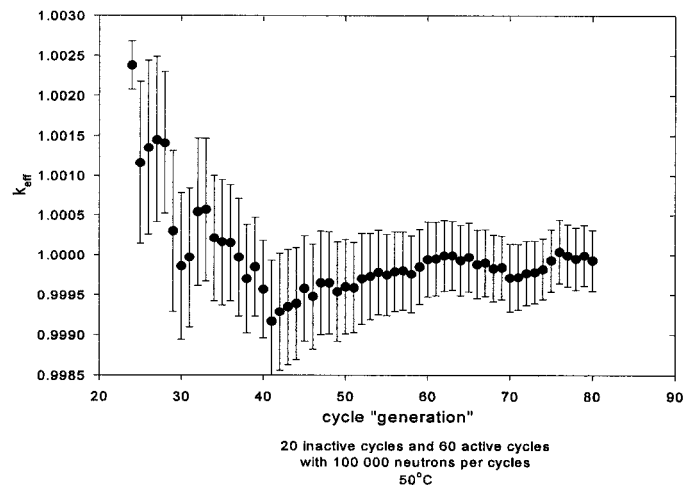


Figure D-31  $k_{\text{eff}}$  Combined estimator vs cycle  
control rod fully out

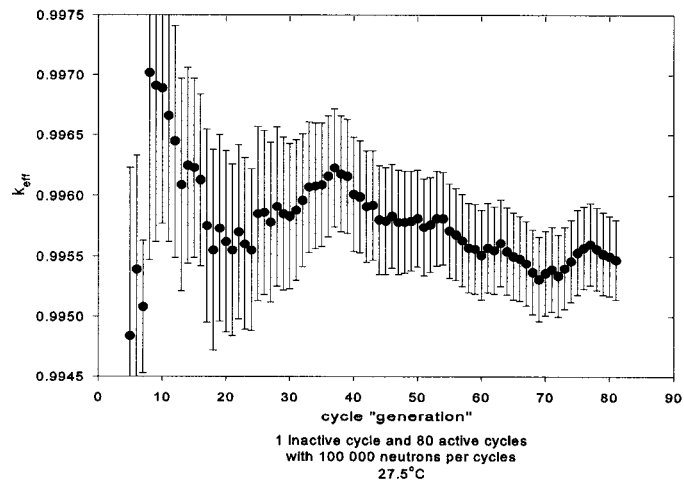


Figure D-32  $k_{\text{eff}}$  Combined estimator vs cycle  
control rod fully in  
(doubled linear coef. of expan.)

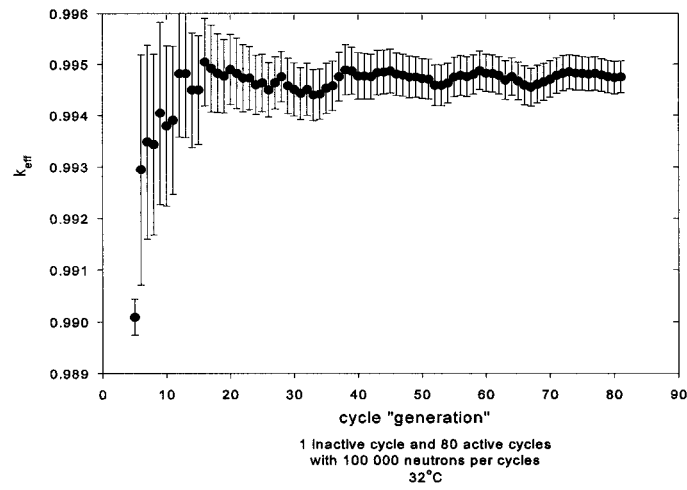


Figure D-33  $k_{\text{eff}}$  Combined estimator vs cycle  
control rod fully in  
(doubled linear coef. of expan.)

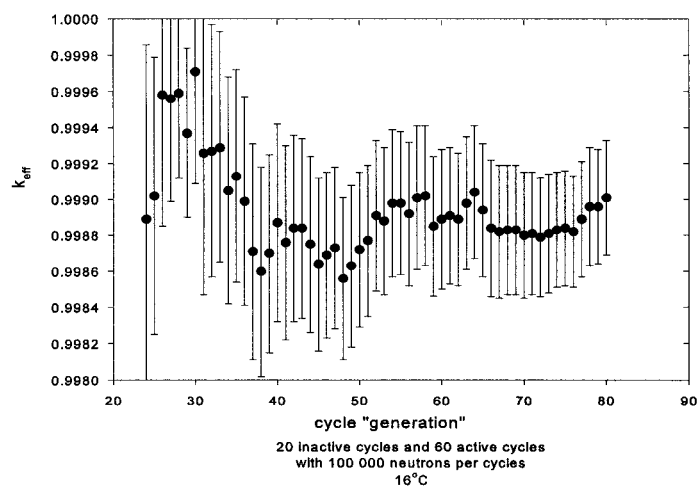


Figure D-34  $k_{\text{eff}}$  Combined estimator vs cycle  
control rod centred  
(doubled linear coef. of expan.)

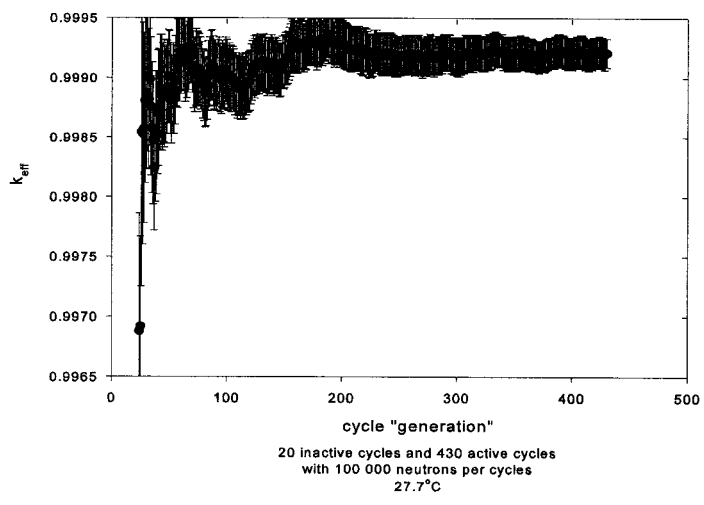


Figure D-35  $k_{\text{eff}}$  Combined estimator vs cycle  
 control rod centred  
 (doubled linear coef. of expan.)

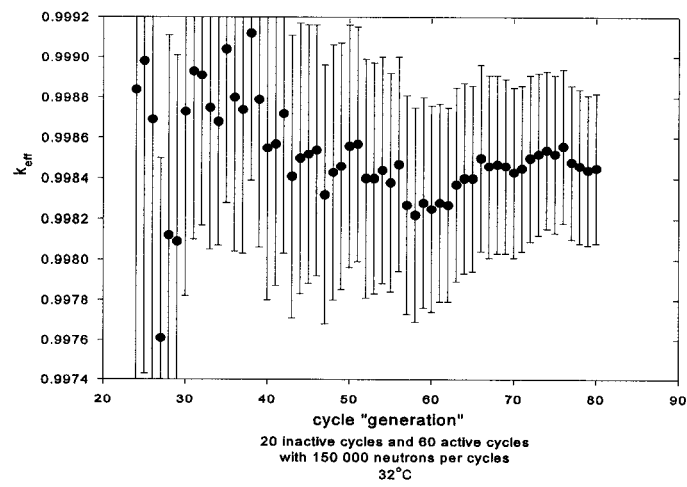
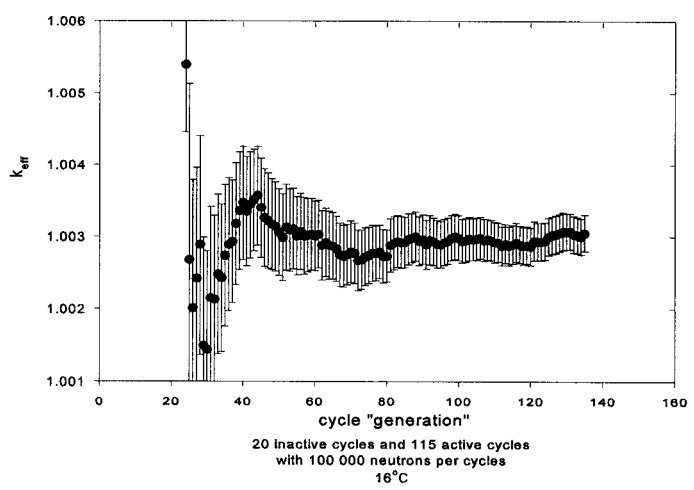
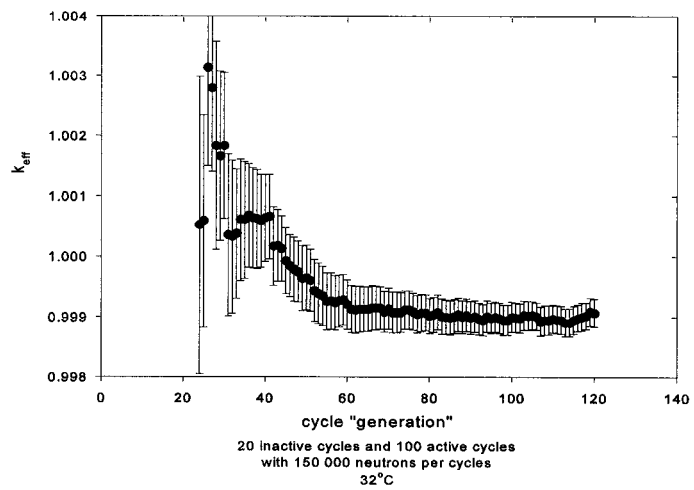
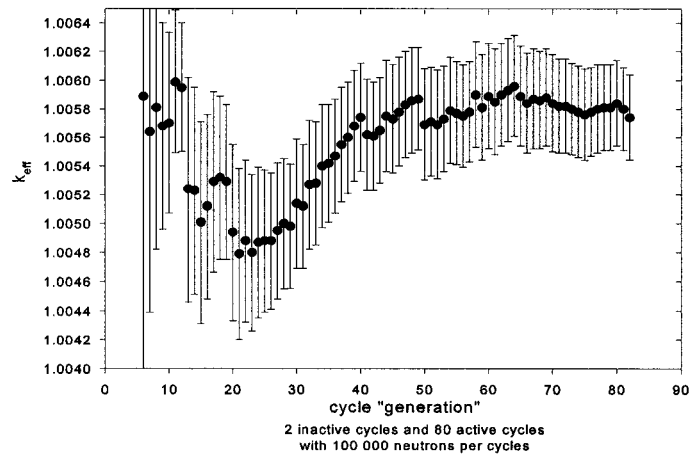
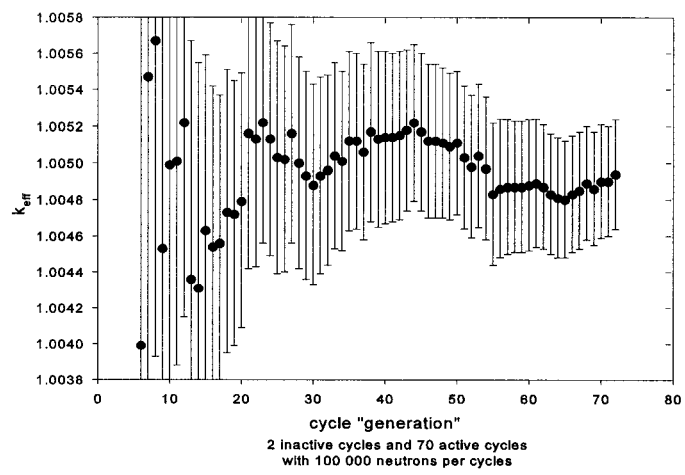


Figure D-36  $k_{\text{eff}}$  Combined estimator vs cycle  
 control rod centred  
 (doubled linear coef. of expan.)





**Figure D-39  $k_{\text{eff}}$  Combined estimator vs cycle  
600 K libraries no tmp command**



**Figure D-40  $k_{\text{eff}}$  Combined estimator vs cycle  
600 K libraries with tmp command**

## **APPENDIX E : OUTPUT DECK**

The listing of the output for the simulation of the excess reactivity with the control rod in the fully out position is contained in the next pages.













51	Px	10.693	\$ lower grid plate and cap	
52	Px	10.828	\$ lower air gap	
54	Px	32.914	\$ upper grid plate	
55	Px	33.193	\$ upper grid plate	
57	Px	33.9385	\$ upper grid plate	
58	Px	34.0735	\$ upper air gap	
327-	c	7	\$ upper cap	
328-		Px 35.932	\$ top shim	
329-		Px 36.09075	\$ top shim	
330-	c		\$ annulus holes	
331-		9	\$ annulus holes	
332-	c	10	\$ lower plate	
333-		CX 16.113125	\$ lower plate	
334-	c	11	CX 11.049	\$ annulus
335-		12	CX 21.2344	\$ annulus
336-				
337-	c			
338-		70	P 0.0 -0.72652847 1.0 0.0	\$ annulus hole out D
339-		71	P 0.0 -0.72658447 1.0 0.0	\$ annulus hole out D
340-		72	P 0.0 -3.07768 1.0 0.0	\$ annulus hole out D
341-		73	Pz 0.0	\$ annulus hole out D
342-		74	P 0.0 3.07768 1.0 0.0	\$ annulus hole out D
343-	c			
344-		13	C/x 14.56182 0.0 1.56718	\$ annulus hole out D
345-		14	C/x 4.49985 13.84911 1.56718	\$ annulus hole out D
346-		15	C/x -11.78076 8.55972 1.56718	\$ annulus hole out D
347-		16	C/x -11.78076 -8.55972 1.56718	\$ annulus hole out D
348-		17	C/x 4.49985 -13.84911 1.56718	\$ annulus hole out D
349-	c			
350-		131	C/x 14.56182 0.0 1.40208	\$ annulus hole ins D
351-		141	C/x 4.49985 13.84911 1.40208	\$ annulus hole ins D
352-		151	C/x -11.78076 8.55972 1.40208	\$ annulus hole ins D
353-		161	C/x -11.78076 -8.55972 1.40208	\$ annulus hole ins D
354-		171	C/x 4.49985 -13.84911 1.40208	\$ annulus hole ins D
355-	c			
356-	c			
357-	c			
358-		132	C/x -7.416 -22.825 1.905	\$ large site out R
359-		142	C/x 19.416 -14.107 1.56718	\$ small site out R
360-		152	C/x 19.416 14.107 1.61798	\$ cadmium lined out R
361-		162	C/x -7.416 22.285 1.56718	\$ flooded site out R
362-	c			
363-		153	C/x 19.416 14.107 1.56718	\$ cadmium lined bet R
364-	c			
365-		133	C/x -7.416 -22.825 1.600	\$ large site ins R
366-		143	C/x 19.416 -14.107 1.40208	\$ small site ins R
367-		154	C/x 19.416 14.107 1.40208	\$ cadmium lined ins R
368-		163	C/x -7.416 22.285 1.40208	\$ flooded site ins R
369-	c			
370-		19	CX 12.065	\$ top shim
371-		20	CX 1.3890625	\$ top shim
372-		21	Py 0.11190625	\$ top shim
373-	c			\$ water in reactor shell
374-		100	CX 30	

375-	101	cx 31	\$ reactor shell
376-	102	c/x 30 30 133	\$ outside world
377-	c		
378-	110	px -.8	\$ bottom of shell
379-	111	px -.9	\$ bottom of shell
380-	112	px -.31	\$ pool bottom
381-	113	px .533	\$ pool top
382-	c		
383-	200	p 0.0 -1.7321045	\$ lattice
384-	201	p 0.0 -1.7321045	\$ lattice
385-	202	pz 0.477902	\$ lattice
386-	203	pz -0.477902	\$ lattice
387-	c		
388-	500	cx 0.2064	\$ fuel rod
389-	501	cx 0.212	\$ fuel rod
390-	502	cx 0.262	\$ fuel rod
391-	c		
392-	550	c/x 0.551815 0.318516	.262 \$ grid plate hole
393-	551	c/x 0.551815 -0.318516	.262 \$ grid plate hole
394-	552	c/x -0.551815 0.318516	.262 \$ grid plate hole
395-	553	c/x -0.551815 -0.318516	.262 \$ grid plate hole
396-	554	c/x 0.0 0.637286	.262 \$ grid plate hole
397-	555	c/x 0.0 -0.637286	.262 \$ grid plate hole
398-	556	c/x 0.15	.19 \$ grid plate hole
399-	c		
400-	560	c/x 0.551815 0.318516	.19 \$ grid plate hole
401-	561	c/x 0.551815 -0.318516	.19 \$ grid plate hole
402-	562	c/x -0.551815 0.318516	.19 \$ grid plate hole
403-	563	c/x -0.551815 -0.318516	.19 \$ grid plate hole
404-	564	c/x 0.0 0.637286	.19 \$ grid plate hole
405-	565	c/x 0.0 -0.637286	.19 \$ grid plate hole
406-	c		
407-	600	cx 0.09652	\$ control rod
408-	601	cx 0.14732	\$ control rod
409-	602	cx 0.62357	\$ control rod cladding
410-	603	cx 1.229	\$ control rod hole
411-	604	cx 1.331	\$ control rod hole
412-	605	px 30.82	\$ bottom control rod cladding
413-	606	px 33.32	\$ bottom control rod
414-	607	px 58.08	\$ top control rod
415-	608	px 71.46	\$ top control rod cladding
416-	c		
417-	999	sx 21 1000	
418-	c		
419-	1000	p 0.0 1.0 2.43	1.082 \$ D2O side 1
420-	1001	p 0.0 1.0 2.43	0.0 \$ D2O side 1
421-	c		
422-	1002	py 0.0	
423-	c		
424-	1003	p 0.0 1.0 -2.43	1.082 \$ D2O side 2
425-	1004	p 0.0 1.0 -2.43	0.0 \$ D2O side 2
426-	c		
427-	1005	cx 22.2344	\$ D2O inner arch
428-	1006	cx 29	\$ D2O outer arch

```

429-          C      1007 px 32.6445      $ Top
430-          1008 px 11.947      $ Bottom
431-
432-
433-          C      materiel definition
434-          m1    4009.50c - .9953863 8016.50c - 9.701130e-6 13027.50c -1.010534e-3
435-          6000.50c - 1.515802e-3 26000.50c -1.21695e-3 14000.50c
436-          -6.063207e-4 5011.50c -1.616855e-6 25055.50c -1.515802e-4
437-          48000.50c -7.376901e-7 3006.50c -1.313695e-7 3007.55c
438-          -1.92001e-6 62149.50c -6.497736e-7 64155.50c -3.53687e-8
439-          64157.50c -3.132657e-8 63151.50c -2.425283e-7 63153.50c
440-          -2.667389e-7 5010.50c -4.345298e-7 $ Be plus impurities
441-          m2    1001.50c 2 8016.50c 1      $ H2O
442-          m3    92235.50c -1753 92238.50c -.7059 8016.50c -1.1188 $ UO2
443-          m4    8016.50c 0.21174 7014.50c 0.788826 $ Air
444-          m5    40000.50c 1      $ Zr
445-          m6    13027.50c -9792 14000.50c -0.006 29000.50c -0.0028 12000.50c
446-          m7    48000.50c 1      $ Cd
447-          m8    1002.50c 2 8016.50c 1      $ Al 6061 T6
448-          mt2   1wtr.01t
449-          mt8   hwtr.01t
450-          451- kcode 100000 1. 20 200
452-          c      single particle source at centre of the core
453-          c      ksrc 21 0 0
454-          c      ksrc 32 52 -12.83 2.709
455-          c      ksrc 21 2.25 0.0
456-          phys:n 20 .000001e-6
457-          c      lost 1 1
458-          c      dbcn j j 1 5
459-          prdmp 2j 1 1
total fission nubar data are being used.

warning. 2 of the materials had unnormalized fractions.

warning. 3 cells appear to consist of more than one piece.
1cells

          cell mat      atom      gram      density      volume      mass      pieces      neutron
          cell mat      atom      gram      density      volume      mass      pieces      importance
          1   999   0      0.0000E+00  .00000E+00  .00000E+00  .00000E+00  0      0.000E+00
          2   1     1.23285E-01 1.85000E+00 8.28711E+03 1.53312E+04 1      1.000E+00
          3   2     5.08070E-05 1.21700E-03 3.18260E+03 3.87323E+00 1      1.000E+00
          4   3     5.08070E-05 1.21700E-03 3.18260E+03 3.87323E+00 1      1.000E+00
          5   4     5.08070E-05 1.21700E-03 3.18260E+03 3.87323E+00 1      1.000E+00
          6   5     5.08070E-05 1.21700E-03 3.18260E+03 3.87323E+00 1      1.000E+00
          7   6     5.08070E-05 1.21700E-03 3.18260E+03 3.87323E+00 1      1.000E+00
          8   221   6.01587E-02 2.70000E+00 7.93656E+02 2.14287E+03 1      1.000E+00
          9   331   6.01587E-02 2.70000E+00 7.93656E+02 2.14287E+03 1      1.000E+00
          10  441   6.01587E-02 2.70000E+00 7.93656E+02 2.14287E+03 1      1.000E+00
          11  551   6.01587E-02 2.70000E+00 7.93656E+02 2.14287E+03 1      1.000E+00
          12  661   6.01587E-02 2.70000E+00 7.93656E+02 2.14287E+03 1      1.000E+00
          13  70    1.23285E-01 1.85000E+00 7.23112E+03 1.33776E+04 1      1.000E+00

```

14	71	1.23285E-01	1.85000E+00	.000000E+00	.000000E+00	0 1.0000E+00
15	72	1.23285E-01	1.85000E+00	.000000E+00	.000000E+00	0 1.0000E+00
16	73	1.23285E-01	1.85000E+00	.000000E+00	.000000E+00	0 1.0000E+00
17	74	1.23285E-01	1.85000E+00	.000000E+00	.000000E+00	0 1.0000E+00
18	75	1.23285E-01	1.85000E+00	.000000E+00	.000000E+00	0 1.0000E+00
19	222	4.08070E-05	1.21700E-03	4.20084E+03	5.11242E+00	1 1.0000E+00
20	332	4.08070E-05	1.21700E-03	3.22583E+03	3.92584E+00	1 1.0000E+00
21	442	4.08070E-05	1.21700E-03	3.22583E+03	3.92584E+00	1 1.0000E+00
22	552	4.08070E-05	1.21700E-03	3.22583E+03	3.92584E+00	1 1.0000E+00
23	223	6.01587E-02	2.70000E+00	1.75422E+03	4.73640E+00	1 1.0000E+00
24	333	6.01587E-02	2.70000E+00	8.04437E+02	2.17198E+03	1 1.0000E+00
25	443	6.01587E-02	2.70000E+00	8.04437E+02	2.17198E+03	1 1.0000E+00
26	553	6.01587E-02	2.70000E+00	8.04437E+02	2.17198E+03	1 1.0000E+00
27	444	7.463393E-02	8.65000E+00	1.15635E+01	1.000024E+02	1 1.0000E+00
28	8	1.23285E-01	1.85000E+00	.000000E+00	.000000E+00	0 1.0000E+00
29	10	2s	1.00108E-01	9.98000E-01	8.47333E+03	8.45638E+03
30	11	2s	1.00108E-01	9.98000E-01	.000000E+00	.000000E+00
31	12	3	7.11012E-02	1.06000E+01	.000000E+00	.000000E+00
32	14	4	5.08070E-05	1.21700E-03	.000000E+00	.000000E+00
33	15	5	4.28431E-02	6.49000E+00	.000000E+00	.000000E+00
34	16	2s	1.00108E-01	9.98000E-01	.000000E+00	.000000E+00
35	17	0	.00000E+00	.00000E+00	.000000E+00	.000000E+00
36	18	4	5.08070E-05	1.21700E-03	7.24661E-01	8.81912E-04
37	19	7	4.63393E-02	8.65000E+00	9.63539E-01	8.33461E+00
38	20	6	6.01587E-02	2.70000E+00	4.79566E+00	1.29483E+02
39	21	2s	1.00108E-01	9.98000E-01	1.08294E+02	1.08078E+02
40	22	5	4.28431E-02	6.49000E+00	1.90567E+01	1.23678E+02
41	230	2s	1.00108E-01	9.98000E-01	9.74158E+01	9.72210E+01
42	231	2s	1.00108E-01	9.98000E-01	5.24772E+02	5.23723E+02
43	2321	2s	1.00108E-01	9.98000E-01	7.16732E+02	7.15299E+02
44	232	2s	1.00108E-01	9.98000E-01	.000000E+00	.000000E+00
45	233	2s	1.00108E-01	9.98000E-01	2.04396E+04	2.03987E+04
46	234	2s	1.00108E-01	9.98000E-01	2.26195E+04	2.25742E+04
47	235	2s	1.00108E-01	9.98000E-01	.000000E+00	.000000E+00
48	236	2s	1.00108E-01	9.98000E-01	.000000E+00	.000000E+00
49	237	2s	1.00108E-01	9.98000E-01	.000000E+00	.000000E+00
50	238	2s	1.00108E-01	9.98000E-01	.000000E+00	.000000E+00
51	239	2s	1.00108E-01	9.98000E-01	.000000E+00	.000000E+00
52	240	2s	1.00108E-01	9.98000E-01	.000000E+00	.000000E+00
53	241	2s	1.00108E-01	9.98000E-01	.000000E+00	.000000E+00
54	242	2s	1.00108E-01	9.98000E-01	.000000E+00	.000000E+00
55	300	6	6.01587E-02	2.70000E+00	1.03676E+05	2.79924E+05
56	301	6	6.01587E-02	2.70000E+00	3.01907E+03	8.15149E+03
57	24	2s	1.00108E-01	9.98000E-01	1.02050E+02	1.01845E+02
58	25	2s	1.00108E-01	9.98000E-01	.000000E+00	.000000E+00
59	26	5	4.28431E-02	6.49000E+00	.000000E+00	.000000E+00
60	27	2s	1.00108E-01	9.98000E-01	.000000E+00	.000000E+00
61	28	2s	1.00108E-01	9.98000E-01	3.51923E-01	3.51219E-01
62	30	2s	1.00108E-01	9.98000E-01	1.56098E-02	1.55786E+02
63	31	2s	1.00108E-01	9.98000E-01	.000000E+00	.000000E+00
64	32	4	5.08070E-05	1.21700E-03	.000000E+00	.000000E+00
65	33	5	4.28431E-02	6.49000E+00	.000000E+00	.000000E+00
66	34	2s	1.00108E-01	9.98000E-01	.000000E+00	.000000E+00
67	35	5	4.28431E-02	6.49000E+00	1.05451E+02	6.84378E+02

68	36	5	4.28431E-02	6.49000E+00	.000000E+00	.000000E+00	0 1.0000E+00
69	37	5	4.28431E-02	6.49000E+00	.000000E+00	.000000E+00	0 1.0000E+00
70	38	2s	1.00108E-01	9.98000E-01	.000000E+00	.000000E+00	0 1.0000E+00
71	39	2s	1.00108E-01	9.98000E-01	.000000E+00	.000000E+00	0 1.0000E+00
72	40	2s	1.00108E-01	9.98000E-01	.000000E+00	.000000E+00	0 1.0000E+00
73	41	2s	1.00108E-01	9.98000E-01	.000000E+00	.000000E+00	0 1.0000E+00
74	42	2s	1.00108E-01	9.98000E-01	.000000E+00	.000000E+00	0 1.0000E+00
75	43	2s	1.00108E-01	9.98000E-01	.000000E+00	.000000E+00	0 1.0000E+00
76	44	5	4.28431E-02	6.49000E+00	.000000E+00	.000000E+00	0 1.0000E+00
77	45	2s	1.00108E-01	9.98000E-01	.000000E+00	.000000E+00	0 1.0000E+00
78	46	2s	1.00108E-01	9.98000E-01	.000000E+00	.000000E+00	0 1.0000E+00
79	47	2s	1.00108E-01	9.98000E-01	.000000E+00	.000000E+00	0 1.0000E+00
80	48	2s	1.00108E-01	9.98000E-01	.000000E+00	.000000E+00	0 1.0000E+00
81	49	2s	1.00108E-01	9.98000E-01	.000000E+00	.000000E+00	0 1.0000E+00
82	50	2s	1.00108E-01	9.98000E-01	.000000E+00	.000000E+00	0 1.0000E+00
83	51	2s	1.00108E-01	9.98000E-01	.000000E+00	.000000E+00	0 1.0000E+00
84	52	5	4.28431E-02	6.49000E+00	1.05451E+02	6.84378E-02	1 1.0000E+00
85	53	5	4.28431E-02	6.49000E+00	.000000E+00	.000000E+00	0 1.0000E+00
86	54	5	4.28431E-02	6.49000E+00	.000000E+00	.000000E+00	0 1.0000E+00
87	55	2s	1.00108E-01	9.98000E-01	.000000E+00	.000000E+00	0 1.0000E+00
88	56	2s	1.00108E-01	9.98000E-01	.000000E+00	.000000E+00	0 1.0000E+00
89	57	2s	1.00108E-01	9.98000E-01	.000000E+00	.000000E+00	0 1.0000E+00
90	58	2s	1.00108E-01	9.98000E-01	.000000E+00	.000000E+00	0 1.0000E+00
91	59	2s	1.00108E-01	9.98000E-01	.000000E+00	.000000E+00	0 1.0000E+00
92	60	2s	1.00108E-01	9.98000E-01	.000000E+00	.000000E+00	0 1.0000E+00
93	61	5	4.28431E-02	6.49000E+00	.000000E+00	.000000E+00	0 1.0000E+00
94	62	2s	1.00108E-01	9.98000E-01	.000000E+00	.000000E+00	0 1.0000E+00
95	63	2s	1.00108E-01	9.98000E-01	.000000E+00	.000000E+00	0 1.0000E+00
96	64	2s	1.00108E-01	9.98000E-01	.000000E+00	.000000E+00	0 1.0000E+00
97	65	2s	1.00108E-01	9.98000E-01	.000000E+00	.000000E+00	0 1.0000E+00
98	66	2s	1.00108E-01	9.98000E-01	.000000E+00	.000000E+00	0 1.0000E+00
99	67	2s	1.00108E-01	9.98000E-01	.000000E+00	.000000E+00	0 1.0000E+00
100	68	3	7.11012E-02	1.06000E+01	.000000E+00	.000000E+00	0 1.0000E+00
101	69	4	5.08070E-05	1.21700E-03	.000000E+00	.000000E+00	0 1.0000E+00
102	1000	6	6.01587E-02	2.70000E+00	.000000E+00	.000000E+00	0 1.0000E+00
103	1001	6	6.01587E-02	2.70000E+00	.000000E+00	.000000E+00	0 1.0000E+00
104	1002	6	6.01587E-02	2.70000E+00	.000000E+00	.000000E+00	0 1.0000E+00
105	1003	6	6.01587E-02	2.70000E+00	.000000E+00	.000000E+00	0 1.0000E+00
106	1004	6	6.01587E-02	2.70000E+00	.000000E+00	.000000E+00	0 1.0000E+00
107	1005	6	6.01587E-02	2.70000E+00	.000000E+00	.000000E+00	0 1.0000E+00
108	1006	8s	9.97001E-02	1.10500E+00	.000000E+00	.000000E+00	0 1.0000E+00

total

2.13670E+05 3.93650E+05

2 warning messages so far.  
1 cross-section tables

table length

tables from file rmccs2

print table 100

1001.50c	1153	njoy
3006.50c	6551	njoy
3007.55c	11053	njoy

(	1301)	79/07/31.
(	1303)	79/08/01.
(	3007)	07/29/82

4009.50c	6717	njoy
5010.50c	9587	njoy
6000.50c	16126	njoy
7014.50c	22772	njoy
8016.50c	23669	njoy
13027.50c	22891	njoy
24000.50c	89104	njoy
29000.50c	22473	njoy
63151.50c	25839	njoy
63153.50c	22680	njoy
92235.50c	44188	njoy
92238.50c	66440	njoy

tables from file endf5p2

1002.50c	2447	njoy
5011.50c	3242	njoy
14000.50c	48275	njoy
26000.50c	70549	njoy
40000.50c	35842	njoy

tables from file tmccs2

12000.50c	39283	njoy
25055.50c	60097	njoy
48000.50c	13426	njoy
62149.50c	11116	njoy
64155.50c	31471	njoy
64157.50c	27438	njoy

tables from file tmccs2

hwtr.01t	10193	deuterium in heavy water at 300 degrees kelvin
lwtr.01t	10193	hydrogen in light water at 300 degrees kelvin

total 754815

any neutrons with energy greater than emax = 2.00000E+01 from the source or from a collision will be resampled.

neutron cross sections outside the range from .0000E+00 to 2.0000E+01 mev are expunged.

warning. neutron energy cutoff is below some cross-section tables.

1 decimal words of dynamically allocated storage

general	1899894
tallies	0
bank	12403
cross sections	754815
total	2667112

\*\*\*\*\*  
dump no. 1 on file runtpc nps = 0 coll = 0 ctm = .00 nrn = 0

source distribution written to file srctp

cycle = 0

3 warning messages so far.

lestimated keff results by cycle

print table 175

cycle	k (collision)	1.015733	removal lifetime(abs)	1.6130E+04	source points generated	101399
*****	*****	*****	*****	*****	*****	*****
dump no.	2 on file runtpe	nps = 99994	coll = 19490288	ctm = 78.93	nrm =	177964498
cycle	2 k (collision)	1.003230	removal lifetime(abs)	1.6608E+04	source points generated	98729
*****	*****	*****	*****	*****	*****	*****
dump no.	3 on file runtpe	nps = 201393	coll = 39613914	ctm = 162.61	nrm =	361676360
cycle	3 k (collision)	1.003617	removal lifetime(abs)	1.6545E+04	source points generated	100053
*****	*****	*****	*****	*****	*****	*****
dump no.	4 on file runtpe	nps = 300122	coll = 59261525	ctm = 245.35	nrm =	540841813
cycle	4 k (collision)	1.001606	removal lifetime(abs)	1.6543E+04	source points generated	100305
*****	*****	*****	*****	*****	*****	*****
dump no.	5 on file runtpe	nps = 400175	coll = 79110018	ctm = 321.65	nrm =	721858789
cycle	5 k (collision)	1.005462	removal lifetime(abs)	1.63167E+04	source points generated	100277
*****	*****	*****	*****	*****	*****	*****
dump no.	6 on file runtpe	nps = 500480	coll = 98924356	ctm = 398.90	nrm =	902507650
cycle	6 k (collision)	1.005208	removal lifetime(abs)	1.6463E+04	source points generated	99964
*****	*****	*****	*****	*****	*****	*****
dump no.	7 on file runtpe	nps = 600757	coll = 118776532	ctm = 476.18	nrm =	1083566396
cycle	7 k (collision)	1.006254	removal lifetime(abs)	1.6404E+04	source points generated	100060
*****	*****	*****	*****	*****	*****	*****
dump no.	8 on file runtpe	nps = 700721	coll = 138532336	ctm = 557.28	nrm =	1263636574
cycle	8 k (collision)	1.006362	removal lifetime(abs)	1.6291E+04	source points generated	99915
*****	*****	*****	*****	*****	*****	*****
dump no.	9 on file runtpe	nps = 800781	coll = 158289556	ctm = 634.78	nrm =	1443650644
cycle	9 k (collision)	1.000489	removal lifetime(abs)	1.6570E+04	source points generated	99172

```

*****dump no. 10 on file runtpc nps = 900696 coll = 178200872 ctm = 712.00 nrn = 1625119671
*****cycle 10 k(ccollision) 1.002149 removal lifetime(abs) 1.6442E+04 source points generated 100249
*****dump no. 11 on file runtpc nps = 999868 coll = 197930816 ctm = 788.51 nrn = 1804581626
*****cycle 11 k(ccollision) 1.002997 removal lifetime(abs) 1.6505E+04 source points generated 99877
*****dump no. 12 on file runtpc nps = 1100117 coll = 217836092 ctm = 865.78 nrn = 1985940142
*****cycle 12 k(ccollision) 1.000645 removal lifetime(abs) 1.6545E+04 source points generated 99772
*****dump no. 13 on file runtpc nps = 1199994 coll = 237759510 ctm = 943.04 nrn = 2167272841
*****cycle 13 k(ccollision) 1.004707 removal lifetime(abs) 1.6427E+04 source points generated 100299
*****dump no. 14 on file runtpc nps = 1299766 coll = 257554567 ctm = 1019.88 nrn = 2347691357
*****cycle 14 k(ccollision) 1.007104 removal lifetime(abs) 1.6306E+04 source points generated 100268
*****dump no. 15 on file runtpc nps = 1400065 coll = 277378207 ctm = 1096.90 nrn = 2528269812
*****cycle 15 k(ccollision) 1.005690 removal lifetime(abs) 1.6322E+04 source points generated 100013
*****dump no. 16 on file runtpc nps = 1500333 coll = 297145327 ctm = 1173.78 nrn = 2708689050
*****cycle 16 k(ccollision) .999282 removal lifetime(abs) 1.6450E+04 source points generated 99434
*****dump no. 17 on file runtpc nps = 1600346 coll = 316959086 ctm = 1250.71 nrn = 2889291147
*****cycle 17 k(ccollision) 1.001190 removal lifetime(abs) 1.6537E+04 source points generated 100010
*****dump no. 18 on file runtpc nps = 1699780 coll = 336743001 ctm = 1327.55 nrn = 3069745270
*****cycle 18 k(ccollision) 1.003115 removal lifetime(abs) 1.6342E+04 source points generated 100277

```



```

source distribution written to file srctp
cycle = 198

***** dump no. 199 on file runtp *****
nps = 19803466   coll = 3930427138   ctm = 15382.72   nrm = 35830719644

estimator
k(collision)    cycle 199    ave of 179 cycles      combination      simple average      combined average      corr
k(collision)    1.006012    1.003253 .0002      k(col/abs)      1.003200 .0002      1.003172 .0002      .8257
k(absorption)   1.005762    1.003147 .0002      k(abs/tk ln)   1.003168 .0002      1.003158 .0002      .4133
k(trk length)   1.009090    1.003188 .0003      k(tk ln/coll)  1.003221 .0002      1.003235 .0002      .5571
rem life (col)  1.6431E+04   1.6506E+04 .0004      k(col/abs/tk ln) 1.003196 .0002      1.003157 .0002
rem life (abs)  1.6433E+04   1.6505E+04 .0004      life(col/abs)  1.6506E+04 .0004      1.6504E+04 .0004      .9915
source points generated 100707

source distribution written to file srctp
cycle = 199

***** dump no. 200 on file runtp *****
nps = 19902714   coll = 3950090900   ctm = 15459.24   nrm = 3610022142

estimator
k(collision)    cycle 200    ave of 180 cycles      combination      simple average      combined average      corr
k(collision)    1.002556    1.003249 .0002      k(col/abs)      1.003206 .0002      1.003183 .0002      .8224
k(absorption)   1.005877    1.003162 .0002      k(abs/tk ln)   1.003179 .0002      1.003171 .0002      .4140
k(trk length)   1.004559    1.003196 .0003      k(tk ln/coll)  1.003223 .0002      1.003235 .0002      .5564
rem life (col)  1.6404E+04   1.6506E+04 .0004      k(col/abs/tk ln) 1.003203 .0002      1.003172 .0002
rem life (abs)  1.6392E+04   1.6505E+04 .0004      life(col/abs)  1.6505E+04 .0004      1.6503E+04 .0004      .9915
source points generated 99553

source distribution written to file srctp
problem summary
run terminated when 200 kcode cycles were done.
+ slowpoke simulation control rod in
) neutron creation tracks weight energy
) (per source particle)
source          20003421  9.9983E-01  2.0305E+00
weight window    0       0.           0.
cell importance  0       0.           0.
weight cutoff   0       1.1505E-01  1.5261E-07
energy importance 0       0.           0.
dxtran          0       0.           0.
forced collisions 0       0.           0.
exp. transform  0       0.           0.
downscattering  0       6.3042E-07  0.
capture         0       0.           1.

probid = 02/13/96 17:54:58
probid = 02/02/96 10:06:22
weight        tracks weight energy
) (per source particle)
) escape energy cutoff
) time cutoff
) weight window
) cell importance
) weight cutoff
) energy importance
) dxtran
) forced collisions
) exp. transform
) downscattering
) capture

```

(n,xn)	1600878	7.3783E-02	8.0667E-02		loss to (n,xn)	800429	3.6891E-02	1.6664E-01
fission	0	0.	0.		loss to fission	0	4.1081E-01	1.7959E-02
total	21604299	1.1887E+00	2.1112E+00		total	21604299	1.1887E+00	2.1112E+00

number of neutrons banked	800449				average lifetime, escape	1.0364E+05	cutoffs	1.0000E+34
neutron tracks per source particle	1.0800E+00				capture	1.5898E+04	tco	1.0000E+00
neutron collisions per source particle	1.9844E+02				capture or escape	1.5911E+04	eco	.0000E+00
total neutron collisions	3969996021				any termination	1.8618E+04	wc1	-5.0000E-01
net multiplication	1.0369E+00	.0000					wc2	-2.5000E-01

computer time so far in this run 15537.06 minutes  
 computer time in mcrun 15536.56 minutes  
 source particles per minute 1.2875E+03  
 random numbers generated 36191484535

warning. random number stride 152917 exceeded 1 times.  
 range of sampled source weights = 9.8350E-01 to 1.0129E+00

4 neutrons from inelastic collisions had energies greater than emx.  
 1neutron activity in each cell

cell	tracks entering	population	collisions	collisions (per history)	number weighted energy	flux weighted energy	average track weight (relative)	average track mfp (cm)
2	1	15618730	4152362	155811935	5.5073E+00	5.4185E-05	1.9263E-01	1.5287E+00
3	2	1546176	710685	1800	6.0771E-05	8.8371E-05	2.8048E-01	3.6084E+03
4	3	1544195	710884	1771	5.9711E-05	8.8069E-05	2.7966E-01	3.6047E+03
5	4	1520487	704710	1820	6.3281E-05	9.0382E-05	2.8316E-01	3.6255E+03
6	5	1515970	703263	1790	6.1595E-05	9.1460E-05	2.8537E-01	3.6348E+03
7	6	1548563	7101047	1840	6.3281E-05	8.1293E-05	2.7700E-01	3.5848E+03
8	221	3177411	752373	128538	5.0302E-03	8.7766E-05	2.7662E-01	3.3410E-01
9	331	3175156	752599	129086	5.0532E-03	8.7224E-05	2.7547E-01	3.3427E-01
10	441	3126482	746495	127500	4.9958E-03	8.9412E-05	2.7798E-01	3.3640E-01
11	551	3116212	745031	126814	4.9883E-03	9.0636E-05	2.8067E-01	3.3762E-01
12	661	31184216	752960	129031	5.0363E-03	8.1218E-05	2.7146E-01	3.3138E-01
13	70	2252677	66689205	138907	5.0889E+00	7.6388E-05	2.4034E-01	1.5851E+00
14	71	9731214	2908347	58206398	2.1733E+00	8.7554E-05	2.6229E-01	7.6656E-01
15	72	9736306	2899038	58268919	2.1745E+00	8.6655E-05	2.6108E-01	7.6616E-01
16	73	9496419	2921354	56558550	2.1265E+00	9.1511E-05	2.6516E-01	7.7175E-01
17	74	9893522	2897340	59226213	2.1914E+00	8.4328E-05	2.5674E-01	7.5997E-01
18	75	9535092	2917061	56808399	2.0032E+00	9.0095E-05	2.6308E-01	7.5556E-01
19	222	842505	277371	1292	3.4053E-05	1.9422E-05	1.0700E-01	5.4861E-01
20	332	736214	240326	1036	2.6588E-05	1.8063E-05	1.0162E-01	5.4364E-01
21	442	169598	99859	220	6.9621E-06	1.3961E-04	3.5623E-01	6.9025E-01
22	552	806293	267821	1095	2.9594E-05	1.8809E-05	1.0272E-01	5.5554E-01
23	223	1809665	294259	111703	3.1645E-03	1.8887E-05	1.0467E-01	5.4757E-01
24	333	1529752	51414	14503	1.4503E-03	1.7591E-05	9.9020E-02	5.4268E-01
25	443	352706	107224	13924	5.1122E-04	1.3727E-04	3.5198E-01	6.8729E-01
26	553	1674425	277649	56333	1.6229E-03	1.8988E-05	1.0043E-01	5.5431E-01
27	444	337509	228056	185928	5.4772E-03	8.9314E-04	4.7979E-01	9.0072E-01
28	8	3613763	1043780	804746	2.5854E-02	5.5850E-05	2.6550E-01	6.6402E-01
29	10	0	0	0	0.0000E+00	0.0000E+00	0.0000E+00	0.0000E+00

print table 126

30	11	219304116	19711880	312064335	1.2794E+01	2.8931E-04	6.1118E-01	8.9552E-01	1.5052E+00
31	12	8455449	20343062	24430539	1.020E+00	9.1590E-04	9.4599E-01	9.2836E-01	2.3878E+00
32	14	137490974	20227299	434	1.8864E-05	6.4175E-04	8.5066E-01	9.1917E-01	6.0190E+03
33	15	155035182	20250630	3992605	1.8458E-01	5.6353E-04	8.0418E-01	9.1577E-01	4.2636E+00
34	16	316579875	20301861	260988556	1.0822E+01	3.8897E-04	6.8960E-01	1.6371E+01	1.0000E+00
35	17	4380	4380	0	0.000E+00	6.8113E-04	1.8235E+00	7.1275E-01	.0000E+00
36	18	11165	10883	1	4.2677E-08	3.3960E-03	8.0378E-01	9.7258E-01	5.9677E+03
37	19	76896	64237	50563	1.4109E-03	1.1907E-03	7.5983E-01	9.2728E-01	3.2616E+00
38	20	414087	238503	52088	2.0237E-03	1.1571E-04	4.2239E-01	7.2485E-01	9.4249E+00
39	21	2935564	1801313	12569440	5.0050E-01	2.0339E-04	5.4113E-01	8.7151E+00	1.3715E+00
40	22	5577924	1895548	286761	1.2814E-02	2.3895E-04	5.8583E-01	8.8198E-01	4.2985E+00
41	230	8508590	3039328	8491855	3.1962E-01	1.5155E-04	4.0644E-01	8.3548E-01	1.1776E+00
42	231	12871531	33016247	5302854	1.0485E-00	4.6731E-05	1.8400E-01	6.9936E-01	7.5824E-01
43	232	5180322	1298240	15238643	3.7379E-01	1.4664E-05	8.6014E-02	5.2052E-01	5.1419E-01
44	232	22033376	5137080	693436924	1.7702E+01	1.6795E-05	9.4105E-02	5.4438E-01	5.3620E-01
45	233	12985973	12985973	422521273	1.0511E+01	1.6513E-05	9.5669E-02	5.2971E-01	5.3356E-01
46	234	6558411	1705731	260095968	6.2414E+00	1.4002E-05	8.4851E-02	5.0750E-01	5.0668E-01
47	235	14127509	3220600	5052869	1.4234E+00	3.4965E-05	1.7050E-01	6.1738E-01	6.9430E-01
48	236	1966244	4555693	193822065	5.4915E+00	4.6132E-05	2.2792E-01	6.2894E-01	7.8611E-01
49	237	97389	61538	64741	2.0190E-03	7.2834E-05	3.1494E-01	7.0254E-01	9.4871E-01
50	238	5096301	1095416	47322274	1.2222E-01	5.5232E-05	4.3364E-01	6.2101E-01	6.2101E-01
51	239	9055958	1931956	1705731	2.2122E-01	3.5919E-05	1.9219E-01	5.9779E-01	7.1289E-01
52	240	12610022	35010370	666010243	1.6330103+01	2.8132E-05	1.7212E-01	5.3241E-01	6.5365E-01
53	241	39130	10996	1736519	3.9009E-02	4.3636E-05	3.2521E-01	4.9344E-01	8.3004E-01
54	242	6995989	2386103	371805997	8.15999E+00	2.1172E-05	1.5130E-01	4.6820E-01	5.9069E-01
55	300	1088413	2112565	2136244	5.3179E-02	1.7999E-05	1.1312E-01	4.8116E-01	1.0180E+01
56	301	1790838	356319	348999	8.2494E-03	1.8838E-05	1.2299E-01	4.5476E-01	1.0128E+01
57	24	0	0	0	.0000E+00	.0000E+00	.0000E+00	.0000E+00	.0000E+00
58	25	8718655	3882422	3759738	1.3588E-01	1.4922E-04	4.4177E-01	8.1324E-01	1.2152E+00
59	26	2419869	1840255	106415	4.45559E-03	1.8423E-04	5.0417E-01	8.2206E-01	4.2992E+00
60	27	9190960	4057216	3403533	1.2322E-01	1.6444E-04	4.7179E-01	8.1695E-01	1.2609E+00
61	28	79265	57074	28770	1.0088E-03	1.4545E-04	4.8033E-01	7.9542E-01	1.2446E+00
62	30	0	0	0	.0000E+00	.0000E+00	.0000E+00	.0000E+00	.0000E+00
63	31	9543477	4103851	5380319	1.92227E-01	1.5512E-04	4.7171E-01	8.0831E-01	1.2499E+00
64	32	2011184	1623956	144	5.40022E-06	2.2838E-04	5.9914E-01	8.2420E-01	4.8859E+03
65	33	2655995	1751138	52627	2.2001E-03	2.0763E-04	5.6290E-01	8.2017E-01	4.3091E+00
66	34	10407149	4342243	4803539	1.7203E-01	1.7811E-04	5.1264E-01	8.1406E-01	1.3197E+00
67	35	0	0	0	.0000E+00	.0000E+00	.0000E+00	.0000E+00	.0000E+00
68	36	671854	478117	439985	1.8240E-03	1.3334E-04	3.7278E-01	8.1421E-01	4.2804E+00
69	37	5170904	2252946	365032	1.5649E-02	1.7496E-04	4.4878E-01	8.4292E-01	4.2750E+00
70	38	645837	533282	137473	5.2063E-03	1.6895E-04	4.4258E-01	8.4127E-01	1.2339E+00
71	39	1517038	1063748	710786	2.6936E-02	1.65678E-04	4.3736E-01	8.4144E-01	1.2257E+00
72	40	1514460	1063459	1175756	2.6964E-02	1.6552E-04	4.3781E-01	8.4127E-01	1.2256E+00
73	41	643951	533559	1382778	5.2446E-03	1.6815E-04	4.4104E-01	8.4188E-01	1.2320E+00
74	42	645176	533101	1375758	5.2189E-03	1.6995E-04	4.4306E-01	8.4208E-01	1.2358E+00
75	43	646775	533696	138864	5.2593E-03	1.6776E-04	4.3811E-01	8.4157E-01	1.2282E+00
76	44	4242471	1819534	252072	1.0807E-02	1.6201E-04	4.3062E-01	8.4261E-01	4.2768E+00
77	45	502380	419447	108915	4.1341E-03	1.5977E-04	4.2946E-01	8.4248E-01	1.2117E+00
78	46	1203390	862991	568971	2.1626E-02	1.6237E-04	4.3343E-01	8.4265E-01	1.2170E+00
79	47	1211047	868771	570774	2.1726E-02	1.6126E-04	4.2952E-01	8.4297E-01	1.2124E+00
80	48	5051162	421742	109654	4.1690E-03	1.6118E-04	4.3319E-01	8.4249E-01	1.2167E+00
81	49	50797	421479	109172	4.1527E-03	1.6002E-04	4.2880E-01	8.4257E-01	1.2101E+00
82	50	505619	421976	109313	4.1493E-03	1.6099E-04	4.3072E-01	8.4242E-01	1.2132E+00
83	51	643933	530547	2555550	9.6946E-03	1.5882E-04	4.2497E-01	8.4139E-01	1.2049E+00

84	52	0	376972	0	.0000E+00	.0000E+00	.0000E+00
85	53	507296	33078	1.3498E-03	1.7930E-04	5.0754E-01	7.9864E-01
86	54	3685218	272452	1.1607E-02	2.3318E-04	5.9322E-01	8.3670E-01
87	55	150738	11202	4.1041E-04	2.2747E-04	5.9042E-01	8.3461E-01
88	56	638189	260112	9.5761E-03	6.1473E-04	6.1473E-01	1.4464E+00
89	57	637210	260537	9.6042E-03	2.4425E-04	6.0908E-01	8.4014E-01
90	58	152280	140330	4.0324E-04	2.3324E-04	6.3996E-01	1.4794E+00
91	59	151819	140130	10949	4.0004E-04	2.3381E-04	6.0028E-01
92	60	151927	139975	10772	3.9507E-04	2.3466E-04	5.9873E-01
93	61	4824724	2185387	291241	3.2581E-02	3.2484E-04	7.0382E-01
94	62	193619	180112	12928	4.7569E-04	2.8909E-04	6.5835E-01
95	63	793971	644899	314042	1.1582E-02	2.6650E-04	6.3450E-01
96	64	795844	645321	313984	1.1555E-02	2.6880E-04	6.2805E-01
97	65	193218	179510	12996	4.7986E-04	2.8567E-04	6.5809E-01
98	66	193261	179631	13086	4.8105E-04	2.8804E-04	6.5763E-01
99	67	192737	179074	13071	4.8207E-04	2.8893E-04	6.5790E-01
100	68	1159524	986109	239408	8.9051E-03	7.5222E-03	8.8691E-01
101	69	1171849	823109	7	2.7618E-07	5.0413E-04	8.6715E-01
102	100	1062546	360754	86849	2.6628E-03	1.9744E-05	9.1344E-02
103	1001	1062278	359975	85953	2.6347E-03	1.9894E-05	9.2890E-02
104	1002	2933361	910486	585147	1.9999E-02	3.1225E-05	1.2924E-01
105	1003	2124003	584925	381427	1.0622E-01	1.1646E-05	5.1822E-01
106	1004	660081	243222	89783	2.6022E-03	1.4901E-05	7.4481E-02
107	1005	789118	293729	164232	4.7920E-03	1.6124E-05	7.1137E-02
108	1006	3468266	934665	13002037	3.82535E-01	1.9582E-05	8.22220E-02
					225375898	396996021	1.1615E+02
					total	128626833	
					1keff results For:	slowpoke simulation control rod in	

probid = 02/02/96 10:06:22  
 the results of the w test for normality applied to the individual collision, absorption, and track-length keff cycle values are:  
 1keff results For: slowpoke simulation control rod in

the initial fission neutron source distribution was read from the srctp file named srctp  
 the criticality problem was scheduled to skip 20 cycles and run a total of 200 cycles with nominally 100000 neutrons per cycle.  
 this problem has run 20 inactive cycles with 199976 neutron histories and 180 active cycles with 18003655 neutron histories.

this calculation has completed the requested number of keff cycles using a total of 20003421 fission neutron source histories.  
 all cells with fissionable material were sampled and had fission neutron source points.

the final estimated combined collision/absorption/track-length keff = 1.00317 with an estimated standard deviation of .00020  
 the estimated 68, 95, & 99 percent keff confidence intervals are 1.00297 to 1.00338, 1.00277 to 1.00358, and 1.00263 to 1.00371  
 the estimated collision/absorption neutron removal lifetime = 1.65E-04 seconds with an estimated standard deviation of 6.95E-08

the estimated average keffs, one standard deviations, and 68, 95, and 99 percent confidence intervals are:

keff estimator	keff	standard deviation	68% confidence	95% confidence	99% confidence	corr
collision	1.00325	.00024	1.00301 to 1.00349	1.00278 to 1.00372	1.00263 to 1.00387	
absorption	1.00316	.00021	1.00295 to 1.00338	1.00273 to 1.00359	1.00259 to 1.00373	
track length	1.00320	.00029	1.00291 to 1.00349	1.00262 to 1.00377	1.00243 to 1.00396	
col/absorp	1.00318	.00021	1.00297 to 1.00340	1.00276 to 1.00361	1.00262 to 1.00375	.8224
abs/trk len	1.00317	.00020	1.00297 to 1.00337	1.00277 to 1.00357	1.00264 to 1.00371	.4140
col/trk len	1.00323	.00023	1.00301 to 1.00346	1.00278 to 1.00368	1.00264 to 1.00383	.5564
col/abs/trk len	1.00317	.00020	1.00297 to 1.00338	1.00277 to 1.00358	1.00263 to 1.00371	

if the largest of each keff occurred on the next cycle, the keff results and 68, 95, and 99 percent confidence intervals would be:

keff estimator	keff	standard deviation	68% confidence	95% confidence	99% confidence
collision	1.00331	.00024	1.00307 to 1.00355	1.00283 to 1.00379	1.00267 to 1.00395
absorption	1.00320	.00022	1.00299 to 1.00342	1.00277 to 1.00364	1.00263 to 1.00378
track length	1.00326	.00029	1.00296 to 1.00355	1.00267 to 1.00384	1.00248 to 1.00404
col/abs/trk len	1.00321	.00021	1.00301 to 1.00342	1.00280 to 1.00363	1.00266 to 1.00376

the estimated collision/absorption neutron lifetimes, one standard deviations, and 68, 95, and 99 percent confidence intervals are:

type	lifetime (sec)	standard deviation	68% confidence	95% confidence	99% confidence
removal	1.6503E-04	6.9493E-08	1.6496E-04 to 1.6510E-04	1.6489E-04 to 1.6517E-04	1.6485E-04 to 1.6521E-04
capture	1.5903E-04	6.0654E-08	1.5897E-04 to 1.5919E-04	1.5915E-04 to 1.5941E-04	1.5887E-04 to 1.5919E-04
fission	7.3697E-05	3.6988E-08	7.3660E-05 to 7.3734E-05	7.3623E-05 to 7.3770E-05	7.3599E-05 to 7.3794E-05
escape	1.0707E-03	2.8150E-05	1.0425E-03 to 1.0589E-03	1.0146E-03 to 1.1268E-03	9.9634E-04 to 1.1451E-03

average individual and combined collision/absorption/track-length keff results for 15 different batch sizes

cycles per batch	number of k batches	average keff estimators and deviations	normality	average $k_{(c/a/t)}$	$k_{(c/a/t)}$ confidence intervals	95% confidence	99% confidence
1	180	1.0032 .0002 1.0032 .0002 1.0032 .0003   95/95/95   1.00317	.00020	1.00277-1.00358	1.00263-1.00371		
2	90	1.0032 .0002 1.0032 .0002 1.0032 .0003   95/95/95   1.00316	.00021	1.00274-1.00357	1.00261-1.00370		
3	60	1.0032 .0003 1.0032 .0002 1.0032 .0003   95/95/95   1.00315	.00022	1.00270-1.00360	1.00255-1.00375		
4	45	1.0032 .0002 1.0032 .0002 1.0032 .0003   95/95/95   1.00317	.00020	1.00276-1.00358	1.00262-1.00372		
5	36	1.0032 .0002 1.0032 .0002 1.0032 .0003   95/95/95   1.00315	.00019	1.00277-1.00353	1.00264-1.00366		
6	30	1.0032 .0002 1.0032 .0002 1.0032 .0003   95/95/95   1.00317	.00018	1.00280-1.00355	1.00267-1.00368		
9	20	1.0032 .0002 1.0032 .0002 1.0032 .0003   95/95/95   1.00315	.00020	1.00272-1.00358	1.00256-1.00374		
10	18	1.0032 .0002 1.0032 .0001 1.0032 .0002   95/95/99   1.00316	.00015	1.00284-1.00348	1.00272-1.00361		
12	15	1.0032 .0002 1.0032 .0002 1.0032 .0002   95/95/95   1.00316	.00014	1.00284-1.00347	1.00272-1.00359		
15	12	1.0032 .0002 1.0032 .0002 1.0032 .0003   95/95/95   1.00314	.00017	1.00275-1.00352	1.00258-1.00369		
18	10	1.0032 .0002 1.0032 .0002 1.0032 .0003   95/95/95   1.00313	.00015	1.00276-1.00349	1.00259-1.00366		
20	9	1.0032 .0003 1.0032 .0001 1.0032 .0002   95/95/95   1.00309	.00010	1.00283-1.00334	1.00270-1.00347		
30	6	1.0032 .0002 1.0032 .0001 1.0032 .0001   95/95/95   1.00314	.00014	1.00270-1.00358	1.00233-1.00395		
36	5	1.0032 .0002 1.0032 .0001 1.0032 .0002   95/95/95   1.00299	.00005	1.00279-1.00318	1.00253-1.00344		



45	99230	.99866	1.00163	1.00136	1.00279	.00064	1.00285	.00062	1.00275	.00071	1.00283	.00052	1914
46	99864	1.00107	1.00276	.99901	1.00272	.00061	1.00285	.00059	1.00260	.00070	1.00278	.00050	1972
47	100130	1.00224	1.00223	1.00266	1.00271	.00059	1.00283	.00057	1.00261	.00067	1.00277	.00048	2057
48	99836	1.00780	1.00658	1.00600	1.00289	.00060	1.00296	.00057	1.00233	.00066	1.00286	.00047	2058
49	100940	1.00230	1.00192	1.00606	1.00287	.00058	1.00293	.00055	1.00284	.00065	1.00291	.00046	2119
50	99749	1.00544	1.00508	1.00271	1.00295	.00056	1.00300	.00054	1.00284	.00062	1.00293	.00044	2197
51	100375	1.00461	1.00236	1.00037	1.00301	.00055	1.00298	.00052	1.00276	.00061	1.00284	.00044	2133
52	99956	1.00111	1.00200	1.00831	1.00295	.00053	1.00295	.00050	1.00293	.00061	1.00294	.00044	2137
53	99744	1.00562	1.00624	1.00303	1.00052	1.00303	.00049	1.00303	.00060	1.00303	.00043	2104	
54	100456	1.00208	1.00125	.99968	1.00300	.00051	1.00298	.00048	1.00293	.00059	1.00295	.00043	2088
55	99847	1.00492	1.00428	1.00114	1.00306	.00050	1.00301	.00047	1.00288	.00058	1.00294	.00042	2146
56	100261	1.00363	1.00460	1.00668	1.00307	.00048	1.00306	.00046	1.00299	.00057	1.00303	.00041	2137
57	99652	1.00099	1.00169	.99707	1.00302	.00047	1.00302	.00045	1.00283	.00058	1.00295	.00041	2102
58	99738	1.00009	1.00142	1.00080	1.00294	.00047	1.00298	.00044	1.00277	.00057	1.00291	.00040	2143
59	99864	1.00029	1.00128	1.00033	1.00287	.00046	1.00294	.00043	1.00271	.00056	1.00287	.00039	2172
60	100013	1.00264	1.00246	1.00348	1.00286	.00045	1.00292	.00042	1.00273	.00054	1.00286	.00038	2235
61	100083	1.00404	1.00302	1.00184	1.00289	.00044	1.00293	.00041	1.00271	.00053	1.00285	.00037	2289
62	100181	1.00292	1.00493	1.00110	1.00289	.00043	1.00297	.00040	1.00267	.00052	1.00287	.00036	2330
63	99732	1.00745	1.00923	1.00755	1.00300	.00043	1.00312	.00042	1.00278	.00052	1.00301	.00038	2051
64	100740	1.00379	1.00290	1.00419	1.00302	.00042	1.00311	.00041	1.00282	.00051	1.00282	.00037	2106
65	999603	1.00189	1.00077	1.00291	1.00299	.00041	1.00306	.00040	1.00282	.00050	1.00298	.00037	2143
66	99810	1.00770	1.00716	1.00479	1.00309	.00042	1.00315	.00040	1.00286	.00049	1.00304	.00037	2105
67	100447	1.00540	1.00447	1.00491	1.00314	.00041	1.00318	.00040	1.00290	.00048	1.00308	.00036	2137
68	99982	1.00253	1.00080	1.00027	1.00313	.00040	1.00313	.00039	1.00285	.00047	1.00302	.00036	2122
69	99837	1.00678	1.00232	1.00068	1.00308	.00040	1.00311	.00038	1.00281	.00046	1.00300	.00035	2159
70	99935	1.00509	1.00289	1.00013	1.00312	.00039	1.00312	.00038	1.00275	.00046	1.00298	.00035	2175
71	100260	1.00208	1.00150	1.00236	1.00310	.00038	1.00308	.00037	1.00274	.00045	1.00295	.00034	2210
72	99708	1.00384	1.00554	1.00319	1.00312	.00038	1.00313	.00036	1.00275	.00044	1.00299	.00033	2230
73	99854	1.00490	1.00305	1.00312	1.00315	.00037	1.00312	.00036	1.00276	.00043	1.00277	.00033	2266
74	100005	1.00945	1.00829	1.00351	1.00327	.00038	1.00322	.00036	1.00277	.00042	1.00303	.00033	2199
75	100558	1.00334	1.00423	1.00647	1.00327	.00038	1.00324	.00036	1.00284	.00042	1.00308	.00033	2226
76	99503	1.00037	.99840	1.00859	1.00322	.00037	1.00315	.00036	1.00294	.00043	1.00306	.00032	2293
77	99691	1.00497	1.00288	1.00557	1.00325	.00037	1.00315	.00036	1.00299	.00042	1.00307	.00031	2328
78	100434	1.00663	1.00308	1.00223	1.00330	.00036	1.00315	.00035	1.00298	.00041	1.00307	.00031	2345
79	100030	1.00435	1.00519	1.00324	1.00332	.00036	1.00318	.00035	1.00298	.00041	1.00309	.00030	2374
80	99725	1.00520	1.00393	1.00812	1.00336	.00036	1.00319	.00034	1.00307	.00041	1.00313	.00030	2371
81	100326	1.00092	.99962	1.01393	1.00332	.00035	1.00313	.00034	1.00324	.00044	1.00316	.00030	2407
82	99466	.99959	1.00097	.99903	1.00326	.00035	1.00310	.00034	1.00318	.00044	1.00311	.00030	2397
83	100131	1.00451	1.00360	1.00599	1.00328	.00035	1.00311	.00033	1.00322	.00043	1.00313	.00029	2423
84	100452	1.00810	1.00661	1.00522	1.00336	.00035	1.00316	.00033	1.00325	.00043	1.00317	.00029	2394
85	100384	1.00028	1.00086	1.00651	1.00331	.00035	1.00313	.00033	1.00330	.00042	1.00317	.00029	2442
86	99303	1.00636	1.00609	1.00878	1.00336	.00034	1.00317	.00032	1.00339	.00043	1.00323	.00029	2374
87	100583	1.00745	1.00783	.99980	1.00342	.00035	1.00324	.00033	1.00333	.00042	1.00325	.00028	2391
88	99931	1.00059	1.00307	1.00174	1.00338	.00034	1.00324	.00032	1.00331	.00042	1.00325	.00028	2442
89	99601	1.00201	1.00389	1.00171	1.00336	.00034	1.00325	.00032	1.00329	.00041	1.00325	.00028	2487
90	100055	1.00147	1.00035	1.00035	1.00333	.00033	1.00321	.00032	1.00324	.00041	1.00321	.00027	2455
91	99842	1.00291	1.00154	1.00492	1.00332	.00033	1.00318	.00031	1.00327	.00040	1.00320	.00027	2484
92	100099	1.00637	1.00358	1.00770	1.00337	.00033	1.00319	.00031	1.00333	.00040	1.00322	.00027	2490
93	100470	1.00405	1.00276	1.00163	1.00338	.00032	1.00318	.00030	1.00331	.00040	1.00320	.00027	2511

94	99795	1.00059	.99914	1.00374	1.00334	.00032	1.00313	.00030	1.00331	.00039	1.00317	.00026	2497
95	99563	1.00867	1.00760	1.00985	1.00341	.00032	1.00319	.00031	1.00340	.00040	1.00324	.00027	2358
96	100714	1.00438	1.00354	1.00029	1.00342	.00032	1.00319	.00030	1.00336	.00039	1.00323	.00027	2379
97	99710	1.00427	1.00631	1.00382	1.00343	.00032	1.00323	.00030	1.00336	.00039	1.00326	.00027	2390
98	100118	1.00308	1.00373	.99405	1.00343	.00031	1.00324	.00030	1.00324	.00040	1.00323	.00026	2370
99	99948	.99941	1.00182	.99723	1.00338	.00031	1.00322	.00029	1.00317	.00040	1.00319	.00026	2368
100	99682	1.00156	1.00255	.99592	1.00335	.00031	1.00321	.00029	1.00308	.00041	1.00316	.00026	2355
101	100221	1.00177	1.00327	.99685	1.00334	.00031	1.00321	.00029	1.00300	.00041	1.00314	.00026	2367
102	99816	1.00553	1.00508	1.00686	1.00336	.00030	1.00324	.00028	1.00305	.00041	1.00317	.00026	2365
103	99990	1.01370	1.00621	1.00797	1.00349	.00033	1.00333	.00029	1.00311	.00041	1.00321	.00027	2191
104	100744	1.00674	1.00429	1.01037	1.00352	.00032	1.00334	.00029	1.00319	.00041	1.00324	.00027	2185
105	99502	1.00167	1.00482	1.00108	1.00350	.00032	1.00335	.00029	1.00317	.00041	1.00326	.00026	2220
106	99828	1.00092	1.00110	1.00038	1.00347	.00032	1.00333	.00029	1.00314	.00040	1.00323	.00026	2220
107	99926	1.00253	1.00243	1.00270	1.00346	.00031	1.00332	.00028	1.00313	.00040	1.00322	.00026	2244
108	100036	1.00554	1.00291	1.00809	1.00349	.00031	1.00331	.00028	1.00319	.00040	1.00323	.00026	2262
109	100256	1.00256	1.00421	1.00540	1.00348	.00031	1.00332	.00028	1.00321	.00040	1.00325	.00025	2286
110	99821	1.00256	1.00239	1.00700	1.00347	.00031	1.00331	.00027	1.00325	.00039	1.00326	.00025	2317
111	100146	1.00332	1.00256	1.00263	1.00346	.00030	1.00330	.00027	1.00325	.00039	1.00325	.00025	2337
112	99888	1.00083	1.00205	.99803	1.00343	.00030	1.00329	.00027	1.00319	.00039	1.00323	.00025	2341
113	99616	1.00626	1.00566	1.00163	1.00347	.00030	1.00333	.00027	1.00317	.00039	1.00324	.00024	2347
114	100677	1.00221	1.00154	1.00440	1.00345	.00030	1.00331	.00027	1.00319	.00038	1.00323	.00024	2371
115	99545	.99947	1.00363	1.00007	1.00341	.00030	1.00331	.00026	1.00315	.00038	1.00324	.00024	2411
116	99777	1.00448	1.00388	1.00700	1.00342	.00029	1.00332	.00026	1.00319	.00038	1.00325	.00024	2428
117	100539	1.00642	1.00278	1.00782	1.00345	.00029	1.00331	.00026	1.00324	.00038	1.00326	.00023	2446
118	100194	1.00377	1.00333	1.00409	1.00346	.00029	1.00331	.00025	1.00325	.00037	1.00326	.00023	2471
119	99736	1.00297	1.00510	1.00466	1.00345	.00029	1.00333	.00025	1.00327	.00037	1.00328	.00023	2483
120	99856	.99935	.99981	1.00169	1.00341	.00029	1.00329	.00025	1.00325	.00037	1.00325	.00023	2474
121	99628	1.00095	1.00222	1.00396	1.00338	.00028	1.00328	.00025	1.00326	.00036	1.00325	.00023	2505
122	100062	1.00466	1.00257	1.00377	1.00340	.00028	1.00328	.00025	1.00326	.00036	1.00325	.00022	2523
123	100397	1.00155	1.00222	1.00224	1.00338	.00028	1.00327	.00025	1.00325	.00035	1.00324	.00022	2546
124	99722	1.00757	1.00524	1.00427	1.00342	.00028	1.00328	.00024	1.00326	.00035	1.00325	.00022	2558
125	100631	1.01055	1.00868	1.01034	1.00348	.00028	1.00334	.00025	1.00333	.00035	1.00330	.00023	2429
126	100199	1.00100	.99794	1.00069	1.00346	.00028	1.00329	.00025	1.00330	.00035	1.00326	.00023	2330
127	99111	1.00041	.99857	1.00322	1.00343	.00028	1.00324	.00025	1.00330	.00035	1.00323	.00023	2299
128	100187	1.00039	1.00437	1.00522	1.00340	.00028	1.00325	.00025	1.00332	.00035	1.00325	.00023	2319
129	99971	1.00541	1.00573	1.00578	1.00342	.00028	1.00327	.00025	1.00334	.00034	1.00328	.00023	2316
130	100950	1.00233	1.00157	1.00579	1.00341	.00027	1.00326	.00025	1.00337	.00034	1.00327	.00022	2336
131	99386	1.00111	1.00172	1.00301	1.00339	.00027	1.00325	.00024	1.00326	.00034	1.00326	.00022	2356
132	99916	1.00910	1.01043	1.00824	1.00345	.00028	1.00331	.00025	1.00341	.00034	1.00332	.00023	2219
133	100844	1.00607	1.00666	1.00163	1.00347	.00028	1.00339	.00025	1.00340	.00034	1.00334	.00023	2229
134	99733	1.00248	1.00213	1.00395	1.00346	.00027	1.00333	.00025	1.00340	.00033	1.00333	.00022	2248
135	99788	1.00030	1.00049	.99822	1.00344	.00027	1.00330	.00025	1.00335	.00033	1.00330	.00023	2223
136	99940	1.00268	1.00217	1.00216	1.00343	.00027	1.00329	.00025	1.00334	.00033	1.00329	.00022	2237
137	100000	1.00542	1.00524	1.00499	1.00345	.00027	1.00331	.00024	1.00335	.00033	1.00331	.00022	2245
138	100349	1.00130	1.00219	1.00019	1.00343	.00027	1.00330	.00024	1.00333	.00033	1.00329	.00022	2257
139	99632	.99754	.99850	.99874	1.00338	.00027	1.00326	.00024	1.00329	.00033	1.00325	.00022	2210
140	99624	.99950	.99800	1.00090	1.00090	.00027	1.00322	.00025	1.00327	.00032	1.00322	.00022	2162
141	100110	.99734	1.00138	.99667	1.00330	.00027	1.00320	.00024	1.00321	.00033	1.00319	.00022	2164
142	99776	1.00002	1.00059	1.00113	1.00327	.00027	1.00318	.00024	1.00320	.00032	1.00317	.00022	2167

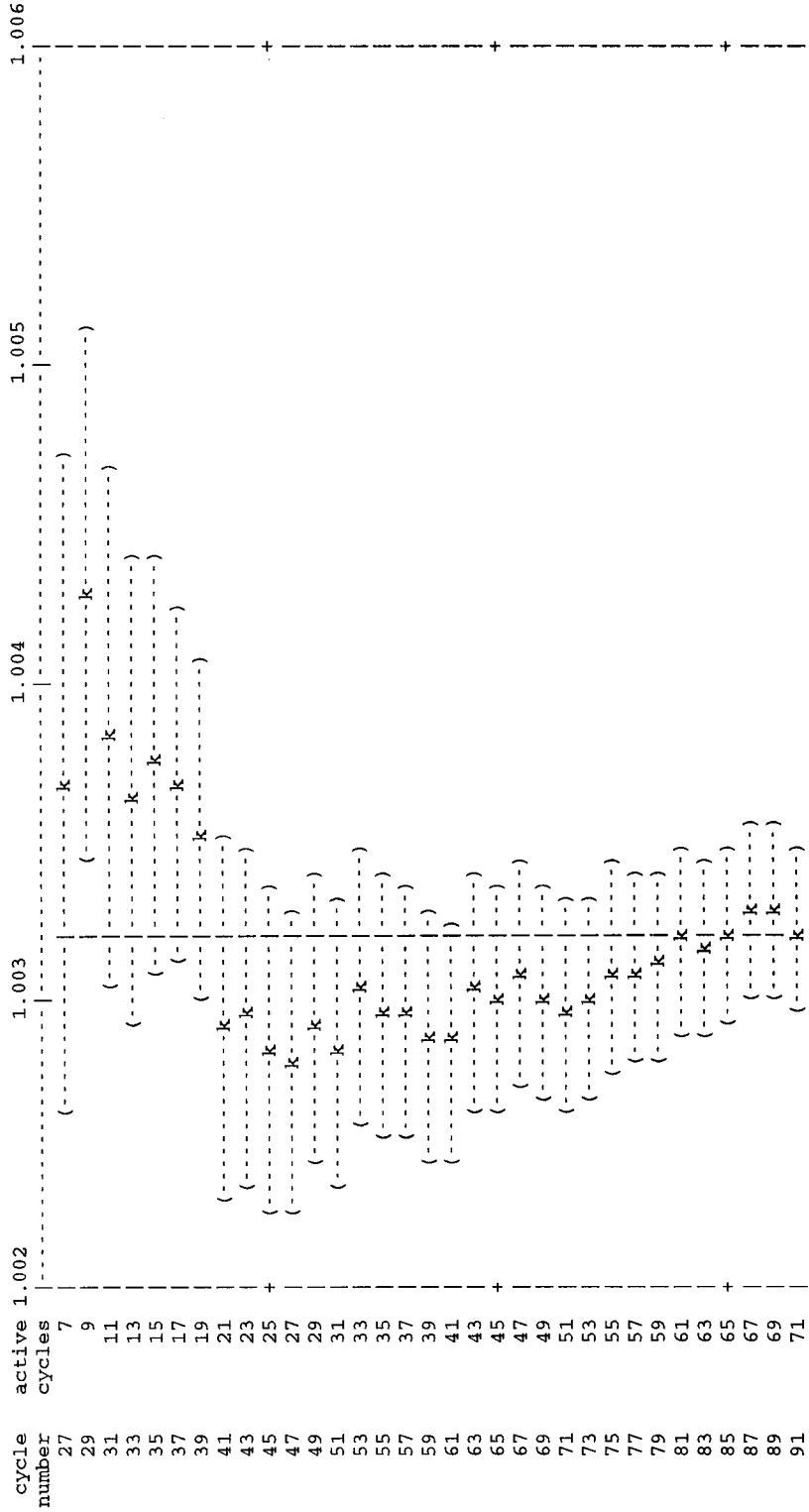
143	100310	.99927	.99999	.99458	1.00324	.00027	1.00315	.00024	1.00313	.00033	1.00313	.00022	2114
144	99721	1.00395	1.00547	1.00118	1.00324	.00027	1.00317	.00024	1.00311	.00033	1.00314	.00022	2128
145	100441	1.00516	1.01054	1.01178	1.00326	.00027	1.00323	.00025	1.00318	.00033	1.00322	.00023	1971
146	100142	1.00769	1.00574	1.00477	1.00329	.00027	1.00325	.00025	1.00319	.00033	1.00323	.00023	1973
147	100324	.99543	.99763	.99683	1.00323	.00027	1.00321	.00025	1.00314	.00033	1.00319	.00023	1913
148	98803	1.00186	1.00187	1.00452	1.00322	.00027	1.00320	.00025	1.00315	.00033	1.00318	.00023	1929
149	100567	1.00180	1.00143	.99946	1.00321	.00027	1.00318	.00024	1.00313	.00033	1.00317	.00023	1931
150	99896	1.01092	1.00971	1.01430	1.00327	.00027	1.00323	.00025	1.00321	.00033	1.00323	.00023	1818
151	100756	1.00054	1.00310	1.00649	1.00325	.00027	1.00322	.00025	1.00324	.00033	1.00323	.00023	1832
152	99401	1.00185	1.00167	.99171	1.00324	.00027	1.00322	.00024	1.00315	.00034	1.00320	.00023	1812
153	100253	1.00139	1.00675	.99941	1.00322	.00027	1.00325	.00024	1.00312	.00034	1.00322	.00023	1819
154	100018	.99968	.99757	1.00440	1.00320	.00027	1.00320	.00025	1.00313	.00034	1.00319	.00023	1804
155	99783	1.00643	1.00441	1.00307	1.00322	.00027	1.00321	.00024	1.00313	.00034	1.00319	.00023	1816
156	100400	.99276	.99110	.99847	1.00314	.00027	1.00315	.00025	1.00310	.00033	1.00313	.00024	1718
157	98833	1.00776	1.00536	1.00810	1.00318	.00027	1.00316	.00025	1.00313	.00033	1.00318	.00023	1717
158	101678	1.00880	1.00550	1.01027	1.00322	.00028	1.00318	.00025	1.00318	.00034	1.00318	.00023	1706
159	100028	1.00189	1.00057	.99534	1.00321	.00027	1.00316	.00025	1.00313	.00034	1.00315	.00024	1689
160	99529	1.00078	.99966	1.00745	1.00319	.00027	1.00314	.00025	1.00316	.00034	1.00314	.00023	1698
161	99794	1.00473	1.00480	1.00212	1.00320	.00027	1.00315	.00025	1.00315	.00033	1.00315	.00023	1709
162	100631	1.00607	1.00522	.99861	1.00322	.00027	1.00317	.00024	1.00312	.00033	1.00316	.00023	1720
163	100059	1.00178	1.00380	1.00547	1.00321	.00027	1.00317	.00024	1.00314	.00033	1.00316	.00023	1731
164	99642	1.00047	.99796	1.00217	1.00319	.00027	1.00313	.00024	1.00313	.00033	1.00313	.00023	1715
165	100014	.99986	1.00199	1.00169	1.00317	.00027	1.00313	.00024	1.00312	.00033	1.00312	.00023	1726
166	99756	1.00542	1.00449	1.00109	1.00319	.00026	1.00314	.00024	1.00311	.00033	1.00312	.00023	1737
167	100533	1.00378	1.00373	1.00547	1.00319	.00026	1.00314	.00024	1.00312	.00032	1.00314	.00022	1748
168	100074	1.00740	1.00323	1.00942	1.00322	.00026	1.00319	.00024	1.00316	.00032	1.00314	.00022	1754
169	100357	1.00463	1.00660	1.00691	1.00323	.00026	1.00316	.00024	1.00319	.00032	1.00317	.00022	1746
170	99757	1.00669	1.00833	1.01178	1.00325	.00026	1.00320	.00024	1.00325	.00033	1.00321	.00023	1701
171	100244	1.00538	1.00478	1.00209	1.00327	.00026	1.00321	.00024	1.00324	.00032	1.00322	.00022	1712
172	99989	1.00444	1.00269	1.00284	1.00327	.00026	1.00320	.00023	1.00324	.00032	1.00321	.00022	1722
173	99963	1.00110	1.00118	1.00345	1.00326	.00026	1.00319	.00023	1.00324	.00032	1.00320	.00022	1730
174	99877	1.00539	.99964	1.00175	1.00327	.00025	1.00317	.00023	1.00323	.00032	1.00319	.00022	1726
175	100412	1.00613	1.00587	1.00301	1.00329	.00025	1.00319	.00023	1.00323	.00032	1.00320	.00022	1731
176	100071	.99740	.99952	.99783	1.00325	.00025	1.00316	.00023	1.00319	.00032	1.00317	.00022	1715
177	99549	1.00827	1.00575	1.00602	1.00329	.00025	1.00318	.00023	1.00321	.00031	1.00319	.00022	1714
178	101309	1.00600	1.00409	1.00295	1.00330	.00025	1.00318	.00023	1.00321	.00031	1.00319	.00022	1722
179	99734	1.00606	1.00335	1.00485	1.00332	.00025	1.00318	.00023	1.00322	.00031	1.00319	.00022	1730
180	99876	1.00579	1.00541	1.00266	1.00334	.00025	1.00320	.00023	1.00321	.00031	1.00320	.00022	1737
181	99806	.99920	1.00015	.99860	1.00331	.00025	1.00318	.00023	1.00319	.00031	1.00318	.00022	1732
182	99382	.99929	1.00069	.99955	1.00328	.00025	1.00316	.00023	1.00316	.00031	1.00316	.00021	1733
183	99937	1.00296	1.00463	1.00118	1.00328	.00025	1.00317	.00022	1.00315	.00030	1.00316	.00021	1744
184	100431	.99904	1.00037	.99993	1.00326	.00025	1.00316	.00022	1.00313	.00030	1.00315	.00021	1743
185	99495	1.00026	1.00218	1.00448	1.00324	.00025	1.00315	.00022	1.00314	.00030	1.00314	.00021	1756
186	100194	1.00345	1.00371	1.00647	1.00324	.00025	1.00315	.00022	1.00316	.00030	1.00315	.00021	1765
187	100360	1.00486	1.00509	1.00380	1.00325	.00025	1.00316	.00022	1.00316	.00030	1.00316	.00021	1773
188	100286	1.00363	1.00487	1.00290	1.00320	.00024	1.00317	.00022	1.00316	.00030	1.00317	.00021	1782
189	99675	1.00067	1.00157	1.00295	1.00324	.00024	1.00317	.00022	1.00316	.00030	1.00316	.00021	1791
190	99485	1.00842	1.00760	1.01166	1.00327	.00024	1.00319	.00022	1.00321	.00030	1.00319	.00021	1759
191	100751	1.00237	1.00362	1.00212	1.00326	.00024	1.00319	.00022	1.00320	.00030	1.00319	.00021	1770

192	99089	1.00153	1.00171	1.00300	1.00325	1.00349	1.00320	1.00029	1.00319	1.00021	1.779
193	99787	1.00266	.99838	1.00574	1.00325	.00024	1.00316	.00022	1.00322	.00029	1.775
194	100019	1.00669	1.00418	1.00285	1.00327	.00024	1.00316	.00022	1.00322	.00029	1.783
195	100561	1.00217	1.00348	.99555	1.00326	.00024	1.00317	.00021	1.00317	.00029	1.789
196	99471	.99768	.99668	.99678	1.00323	.00024	1.00313	.00022	1.00314	.00029	1.740
197	99434	1.00771	1.00760	1.00357	1.00326	.00024	1.00315	.00022	1.00315	.00021	1.734
198	101178	1.00008	.99936	1.00608	1.00324	.00024	1.00313	.00022	1.00316	.00029	1.738
199	99248	1.00601	1.00576	1.00909	1.00325	.00024	1.00315	.00022	1.00319	.00029	1.732
200	100707	1.00256	1.00588	1.00460	1.00325	.00024	1.00316	.00021	1.00320	.00029	1.737

the largest active cycle keffs by estimator are:

collision 1.01370 on cycle 103  
 absorption 1.01061 on cycle 103  
 track length 1.01430 on cycle 150

plot of the estimated col/abs/track-length keff one standard deviation interval versus cycle number (| = final keff = 1.00317)



the smallest active cycle keffs by estimator are:

collision .99276 on cycle 156  
 absorption .99410 on cycle 156  
 track length .99171 on cycle 152

plot of the estimated col/abs/track-length keff one standard deviation interval versus cycle number (| = final keff = 1.00317)

93	73	( -   k   - )
95	75	( -   k   - )
97	77	( -   k   - )
99	79	( -   k   - )
101	81	( -   k   - )
103	83	( -   k   - )
105	85	( -   k   - )
107	87	( -   k   - )
109	89	( -   k   - )
111	91	( -   k   - )
113	93	( -   k   - )
115	95	( -   k   - )
117	97	( -   k   - )
119	99	( -   k   - )
121	101	( -   k   - )
123	103	( -   k   - )
125	105	( -   k   - )
127	107	( -   k   - )
129	109	( -   k   - )
131	111	( -   k   - )
133	113	( -   k   - )
135	115	( -   k   - )
137	117	( -   k   - )
139	119	( -   k   - )
141	121	( -   k   - )
143	123	( -   k   - )
145	125	( -   k   - )
147	127	( -   k   - )
149	129	( -   k   - )
151	131	( -   k   - )
153	133	( -   k   - )
155	135	( -   k   - )
157	137	( -   k   - )
159	139	( -   k   - )
161	141	( -   k   - )
163	143	( -   k   - )
165	145	( -   k   - )
167	147	( -   k   - )
169	149	( -   k   - )
171	151	( -   k   - )
173	153	( -   k   - )
175	155	( -   k   - )
177	157	( -   k   - )
179	159	( -   k   - )
181	161	( -   k   - )
183	163	( -   k   - )
185	165	( -   k   - )
187	167	( -   k   - )
189	169	( -   k   - )
191	171	( -   k   - )
193	173	( -   k   - )
195	175	( -   k   - )
197	177	( -   k   - )
199	179	( -   k   - )

lndividual and collision/absorption/track-length keffs for different numbers of inactive cycles skipped for fission source settling									
skip cycles	active cycles	average neutrons	k(col)	st dev	k(abs)	st dev	k(trk)	st dev	normality co/ab/t1
0	200	20003421	1.0033	.0002	1.0032	.0002	1.0033	.0003	95/95/95   1.00327
1	199	19503427	1.0032	.0002	1.0032	.0002	1.0033	.0003	95/95/95   1.00322
2	198	19502028	1.0032	.0002	1.0032	.0002	1.0033	.0003	95/95/95   1.00322
3	197	19703299	1.0032	.0002	1.0032	.0002	1.0032	.0003	95/95/95   1.00320
4	196	19503246	1.0032	.0002	1.0032	.0002	1.0033	.0003	95/95/95   1.00321
5	195	19502941	1.0032	.0002	1.0032	.0002	1.0032	.0003	95/95/95   1.00320
6	194	19402664	1.0032	.0002	1.0032	.0002	1.0032	.0003	95/95/95   1.00320
7	193	19502700	1.0032	.0002	1.0032	.0002	1.0032	.0003	95/95/95   1.00320
8	192	19502640	1.0032	.0002	1.0031	.0002	1.0032	.0003	95/95/95   1.00318
9	191	19102725	1.0032	.0002	1.0032	.0002	1.0033	.0003	95/95/95   1.00317
10	190	19503553	1.0032	.0002	1.0032	.0002	1.0032	.0003	95/95/95   1.00319
									.00020   1.00278   1.00356
									.00020   1.00280   1.00358
									.00020   1.00279   1.00357
11	189	18903304	1.0032	.0002	1.0032	.0002	1.0032	.0003	95/95/95   1.00318
12	188	18803427	1.0032	.0002	1.0032	.0002	1.0032	.0003	95/95/95   1.00320
13	187	18703655	1.0032	.0002	1.0032	.0002	1.0032	.0003	95/95/95   1.00318
14	186	18603356	1.0032	.0002	1.0032	.0002	1.0032	.0003	95/95/95   1.00318
15	185	18503088	1.0032	.0002	1.0032	.0002	1.0032	.0003	95/95/95   1.00317
16	184	18403075	1.0032	.0002	1.0032	.0002	1.0032	.0003	95/95/95   1.00318
17	183	18303641	1.0032	.0002	1.0032	.0002	1.0032	.0003	95/95/95   1.00318
18	182	18203631	1.0032	.0002	1.0031	.0002	1.0032	.0003	95/95/95   1.00316
19	181	18103354	1.0032	.0002	1.0032	.0002	1.0032	.0003	95/95/95   1.00317
20	180*	18003655	1.0032	.0002	1.0032	.0002	1.0032	.0003	95/95/95   1.00317
									.00020   1.00278   1.00358
									.00020   1.00277   1.00357
									.00020   1.00277   1.00358
22	178	17803731	1.0033	.0002	1.0031	.0002	1.0032	.0003	95/95/95   1.00317
24	176	17603289	1.0033	.0002	1.0032	.0002	1.0031	.0003	95/95/95   1.00316
26	174	17403496	1.0032	.0002	1.0032	.0002	1.0032	.0003	95/95/95   1.00316
28	172	17202917	1.0032	.0002	1.0031	.0002	1.0032	.0003	95/95/95   1.00312
30	170	17002868	1.0032	.0002	1.0031	.0002	1.0032	.0003	95/95/95   1.00313
32	168	16802898	1.0032	.0002	1.0031	.0002	1.0032	.0003	95/95/95   1.00312
34	166	16602954	1.0032	.0002	1.0031	.0002	1.0032	.0003	95/95/95   1.00312
36	164	16402587	1.0032	.0003	1.0031	.0002	1.0032	.0003	95/95/95   1.00311
38	162	16202733	1.0032	.0003	1.0031	.0002	1.0032	.0003	95/95/95   1.00312
40	160	16002728	1.0032	.0003	1.0032	.0002	1.0032	.0003	95/95/95   1.00316
									.00020   1.00276   1.00357
									.00020   1.00275   1.00358
									.00020   1.00275   1.00358
42	158	15802990	1.0033	.0003	1.0032	.0002	1.0032	.0003	95/95/95   1.00322
44	156	15602120	1.0033	.0003	1.0032	.0002	1.0033	.0003	95/95/95   1.00322
46	154	15403026	1.0033	.0003	1.0032	.0002	1.0033	.0003	95/95/95   1.00324
48	152	15203060	1.0033	.0003	1.0032	.0002	1.0033	.0003	95/95/95   1.00322
50	150	15002371	1.0033	.0003	1.0032	.0002	1.0033	.0003	95/95/95   1.00322
52	148	14802040	1.0033	.0003	1.0032	.0002	1.0033	.0003	95/95/95   1.00324
54	146	14601840	1.0033	.0003	1.0032	.0002	1.0033	.0003	95/95/95   1.00324
56	144	14401732	1.0033	.0003	1.0032	.0002	1.0032	.0003	95/95/95   1.00321
58	142	14202342	1.0033	.0003	1.0032	.0002	1.0033	.0003	95/95/95   1.00324
60	140	14002465	1.0034	.0003	1.0032	.0002	1.0033	.0003	95/95/95   1.00326
62	138	13802201	1.0034	.0003	1.0032	.0003	1.0034	.0003	95/95/95   1.00324

64	136	13601729	1.0033	-0.0003	1.0032	.0003	1.0033	.0003	95/95/95	1.0032	-0.0004	1.00273-1.00370	1.00257-1.00385
66	134	13402316	1.0033	-0.0003	1.0032	.0003	1.0033	.0003	95/95/95	1.0032	.0004	1.00272-1.00369	1.00256-1.00386
68	132	13201887	1.0033	-0.0003	1.0032	.0003	1.0033	.0003	95/95/95	1.0032	.0004	1.00272-1.00370	1.00256-1.00389
70	130	13002115	1.0033	-0.0003	1.0032	.0003	1.0033	.0003	95/95/95	1.0032	.0004	1.00273-1.00373	1.00256-1.00389
72	128	12802147	1.0033	-0.0003	1.0032	.0003	1.0033	.0003	95/95/95	1.0032	.0004	1.00265-1.00373	1.00255-1.00390
74	126	12602288	1.0032	-0.0003	1.0031	.0003	1.0032	.0003	95/95/95	1.0031	.0004	1.00268-1.00370	1.00252-1.00387
76	124	12402227	1.0033	-0.0003	1.0032	.0003	1.0033	.0003	95/95/95	1.0032	.0004	1.00268-1.00371	1.00251-1.00388
78	122	12202102	1.0032	-0.0003	1.0032	.0003	1.0033	.0004	95/95/95	1.0032	.0005	1.00267-1.00372	1.00250-1.00389
80	120	12002347	1.0032	-0.0003	1.0031	.0003	1.0033	.0004	95/95/95	1.0031	.0005	1.00264-1.00370	1.00247-1.00388
82	118	11802555	1.0032	-0.0003	1.0032	.0003	1.0032	.0004	95/95/95	1.0032	.0004	1.0026-1.00374	1.00249-1.00391
84	116	11601972	1.0032	-0.0003	1.0032	.0003	1.0032	.0004	95/95/95	1.0031	.0004	1.00262-1.00371	1.00244-1.00389
86	114	11402285	1.0032	-0.0003	1.0032	.0003	1.0031	.0004	95/95/95	1.0031	.0004	1.00259-1.00370	1.00244-1.00387
88	112	11201771	1.0032	-0.0003	1.0031	.0003	1.0031	.0004	95/95/95	1.0031	.0004	1.00256-1.00368	1.00238-1.00386
90	110	11002115	1.0032	-0.0003	1.0031	.0003	1.0032	.0004	95/95/95	1.0031	.0004	1.00258-1.00371	1.00233-1.00389
92	108	10802174	1.0032	-0.0003	1.0031	.0003	1.0031	.0004	95/95/95	1.0031	.0004	1.00256-1.00372	1.00233-1.00395
94	106	10601909	1.0032	-0.0003	1.0032	.0003	1.0031	.0004	95/95/95	1.0031	.0004	1.00259-1.00376	1.00244-1.00395
96	104	1041632	1.0031	-0.0003	1.0031	.0003	1.0031	.0004	95/95/95	1.0031	.0004	1.00254-1.00371	1.00235-1.00391
98	102	10201804	1.0031	-0.0003	1.0031	.0003	1.0032	.0004	95/95/95	1.0031	.0004	1.00252-1.00371	1.00232-1.00390
100	100	10002174	1.0032	-0.0003	1.0031	.0003	1.0033	.0004	95/95/95	1.0031	.0004	1.00255-1.00376	1.00236-1.00396
102	98	9802137	1.0032	-0.0004	1.0031	.0003	1.0033	.0004	95/95/95	1.0031	.0004	1.00253-1.00377	1.00233-1.00397
104	96	9601403	1.0030	-0.0003	1.0030	.0003	1.0032	.0004	95/95/95	1.0030	.0004	1.00244-1.00365	1.00224-1.00385
106	94	9402073	1.0030	-0.0003	1.0030	.0003	1.0033	.0004	95/95/95	1.0030	.0004	1.00244-1.00368	1.00224-1.00388
108	92	9202111	1.0030	-0.0004	1.0030	.0003	1.0032	.0004	95/95/95	1.0030	.0004	1.00242-1.00369	1.00222-1.00389
110	90	9001960	1.0030	-0.0004	1.0030	.0003	1.0031	.0004	95/95/95	1.0030	.0004	1.00240-1.00368	1.00220-1.00389
112	88	8801926	1.0031	-0.0004	1.0030	.0003	1.0032	.0004	95/95/95	1.0030	.0004	1.00241-1.00373	1.00220-1.00394
114	86	8601633	1.0030	-0.0004	1.0030	.0003	1.0032	.0004	95/95/95	1.0030	.0004	1.00238-1.00372	1.00216-1.00394
116	84	8402311	1.0031	-0.0004	1.0030	.0003	1.0032	.0004	95/95/95	1.0030	.0004	1.00235-1.00372	1.00213-1.00395
118	82	8201578	1.0030	-0.0004	1.0030	.0004	1.0031	.0005	95/95/95	1.0030	.0004	1.00232-1.00372	1.00209-1.00395
120	80	8001986	1.0030	-0.0004	1.0030	.0004	1.0031	.0005	95/95/95	1.0030	.0004	1.00232-1.00375	1.00208-1.00398
122	78	7802296	1.0031	-0.0004	1.0030	.0004	1.0031	.0005	95/95/95	1.0030	.0004	1.00231-1.00377	1.00207-1.00401
124	76	7602177	1.0030	-0.0004	1.0030	.0004	1.0031	.0005	95/95/95	1.0030	.0004	1.00227-1.00377	1.00202-1.00401
126	74	7401347	1.0029	-0.0004	1.0030	.0004	1.0030	.0005	95/95/95	1.0029	.0004	1.00225-1.00373	1.00200-1.00398
128	72	7202049	1.0030	-0.0004	1.0030	.0004	1.0030	.0005	95/95/95	1.0030	.0004	1.00226-1.00378	1.00202-1.00403
130	70	7001128	1.0030	-0.0004	1.0030	.0004	1.0029	.0005	95/95/95	1.0029	.0004	1.00222-1.00377	1.00198-1.00403
132	68	6801826	1.0029	-0.0004	1.0029	.0004	1.0029	.0005	95/95/95	1.0029	.0004	1.00214-1.00368	1.00188-1.00393
134	66	6601249	1.0029	-0.0004	1.0029	.0004	1.0029	.0005	95/95/95	1.0028	.0004	1.00208-1.00366	1.00182-1.00392
136	64	6401521	1.0029	-0.0004	1.0029	.0004	1.0029	.0006	95/95/95	1.0029	.0004	1.00211-1.00374	1.00185-1.00400
138	62	6201172	1.0029	-0.0005	1.0029	.0004	1.0029	.0006	95/95/95	1.0029	.0004	1.00207-1.00374	1.00180-1.00402
140	60	6001916	1.0031	-0.0005	1.0031	.0004	1.0031	.0006	95/95/95	1.0030	.0004	1.00222-1.00389	1.00194-1.00417
142	58	5802030	1.0032	-0.0005	1.0031	.0004	1.0032	.0006	95/95/95	1.0031	.0004	1.00230-1.00401	1.00201-1.00429
144	56	5601999	1.0033	-0.0005	1.0031	.0004	1.0034	.0006	95/95/95	1.0032	.0004	1.00233-1.00408	1.00204-1.00437
146	54	5401416	1.0031	-0.0005	1.0030	.0004	1.0032	.0006	95/95/95	1.0030	.0004	1.00215-1.00387	1.00186-1.00416
148	52	5202289	1.0033	-0.0005	1.0031	.0004	1.0033	.0006	95/95/95	1.0031	.0004	1.00227-1.00402	1.00198-1.00431
150	50	5001826	1.0032	-0.0005	1.0030	.0004	1.0032	.0006	95/95/95	1.0030	.0004	1.00220-1.00389	1.00192-1.00417
152	48	4801669	1.0033	-0.0005	1.0030	.0004	1.0033	.0006	95/95/95	1.0031	.0004	1.00225-1.00389	1.00186-1.00417
154	46	4601398	1.0034	-0.0005	1.0030	.0004	1.0034	.0006	95/95/95	1.0031	.0004	1.00224-1.00403	1.00194-1.00433
156	44	4401215	1.0036	-0.0005	1.0032	.0004	1.0035	.0006	95/95/95	1.0032	.0004	1.00247-1.00417	1.00219-1.00445
158	42	4200704	1.0033	-0.0005	1.0031	.0004	1.0032	.0006	95/95/95	1.0031	.0004	1.00234-1.00403	1.00206-1.00432
160	40	4001147	1.0034	-0.0005	1.0032	.0004	1.0033	.0006	95/95/95	1.0033	.0004	1.00244-1.00417	1.00215-1.00446

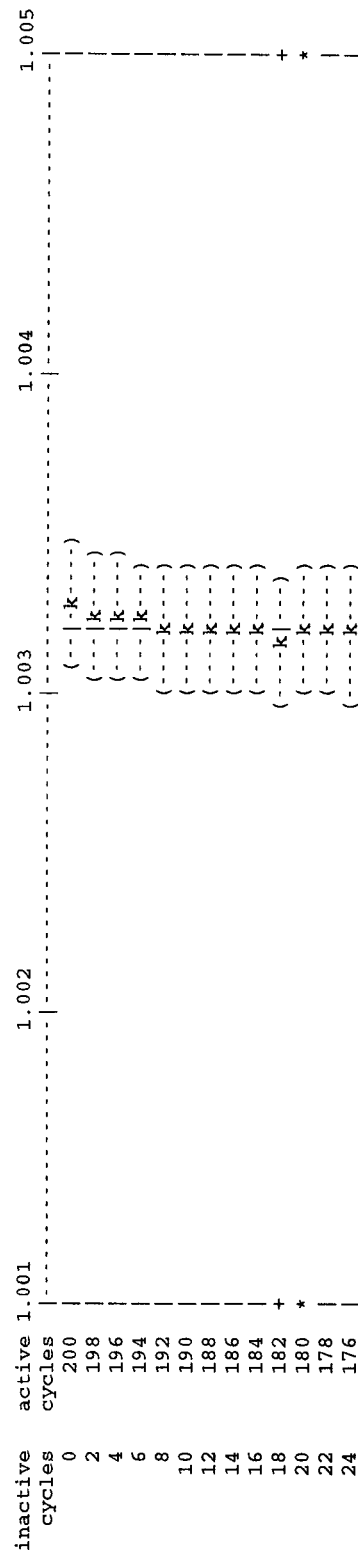
162	38	3800722	1.0033	.0005	1.0032	.0005	1.0035	.0006	95/95/95	1.00326	-0.0045	1.00235-1.00417
164	36	3601021	1.0035	.0005	1.0033	.0005	1.0035	.0006	95/95/95	1.00334	.00046	1.00241-1.00427
166	34	3401251	1.0035	.0005	1.0033	.0005	1.0036	.0006	95/95/95	1.00338	.00048	1.00239-1.00437
168	32	3200644	1.0034	.0005	1.0033	.0005	1.0033	.0006	95/95/95	1.00331	.00051	1.00227-1.00435
170	30	3000530	1.0032	.0006	1.0030	.0005	1.0029	.0006	95/95/95	1.00298	.00050	1.00196-1.00400
172	28	2800297	1.0031	.0006	1.0029	.0005	1.0030	.0007	95/95/95	1.00295	.00053	1.00186-1.00404
174	26	2600457	1.0031	.0006	1.0031	.0006	1.0030	.0007	95/95/95	1.00309	.00055	1.00195-1.00424
176	24	2399974	1.0032	.0006	1.0032	.0006	1.0032	.0007	95/95/95	1.00318	.00057	1.00200-1.00437
178	22	2199116	1.0029	.0006	1.0030	.0006	1.0031	.0008	95/95/95	1.00305	.00061	1.00174-1.00431
180	20	1999506	1.0026	.0007	1.0029	.0007	1.0030	.0009	95/95/95	1.00283	.00069	1.00138-1.00428
182	18	1800318	1.0029	.0007	1.0031	.0007	1.0035	.0009	95/95/95	1.00315	.00071	1.00164-1.00466
184	16	1599950	1.0032	.0007	1.0032	.0008	1.0039	.0010	95/95/95	1.00334	.00077	1.00169-1.00500
186	14	1400261	1.0034	.0008	1.0033	.0009	1.0036	.0011	95/95/95	1.00339	.00086	1.00148-1.00529
188	12	1199605	1.0032	.0010	1.0030	.0010	1.0037	.0013	95/95/95	1.00322	.00103	1.00089-1.00556
190	10	1000445	1.0029	.0010	1.0027	.0011	1.0029	.0013	95/95/95	1.00289	.00104	1.00042-1.00535
192	8	800605	1.0032	.0012	1.0027	.0014	1.0030	.0016	95/95/95	1.00307	.00140	9.9947-1.00666
194	6	600799	1.0027	.0015	1.0031	.0017	1.0026	.0022	95/95/95	1.00257	.00197	.99743-1.00870
196	4	400567	1.0041	.0017	1.0046	.0018	1.0058	.0012	95/95/95	1.00550	.00179	.98270-1.02830
197	3	301133	1.0029	.0017	1.0037	.0022	1.0066	.0013				.89129-1.11971
198	2	199955	1.0043	.0017	1.0058	.0001	1.0068	.0022				

the minimum estimated standard deviation for the col/abs/tl keff estimator occurs with 1 inactive cycles and 199 active cycles.

the first active half of the problem skips 20 cycles and uses 90 active cycles; the second half skips 110 and uses 90 cycles. the col/abs/trk-len keff, one standard deviation, and 68, 95, and 99 percent intervals for each active half of the problem are:

problem	keff	standard deviation	68% confidence	95% confidence	99% confidence
first half	1.00326	.00025	1.00301 to 1.00351	1.00276 to 1.00376	1.00260 to 1.00392
second half	1.00304	.00032	1.00272 to 1.00336	1.00240 to 1.00368	1.00219 to 1.00389
final result	1.00317	.00020	1.00297 to 1.00338	1.00277 to 1.00358	1.00263 to 1.00371

the first and second half values of k(collision/absorption/track length) appear to be the same at the 68 percent confidence level. plot of the estimated col/abs/track-length keff one standard deviation interval by active cycle number (| = final keff = 1.00317)



```

-----+-----+-----+-----+-----+-----+-----+-----+
66   -k-----| -)
64   -k-----| -)
62   -k-----| -)
+-----+-----+-----+-----+-----+-----+-----+-----+
138  -k-----| -)
136  -k-----| -)
60   -k-----| -)
+-----+-----+-----+-----+-----+-----+-----+-----+
140  -k-----| -)
142  -k-----| -)
58   -k-----| -)
+-----+-----+-----+-----+-----+-----+-----+-----+
144  -k-----| -)
146  -k-----| -)
56   -k-----| -)
+-----+-----+-----+-----+-----+-----+-----+-----+
148  -k-----| -)
146  -k-----| -)
52   -k-----| -)
+-----+-----+-----+-----+-----+-----+-----+-----+
150  -k-----| -)
152  -k-----| -)
50   -k-----| -)
+-----+-----+-----+-----+-----+-----+-----+-----+
152  -k-----| -)
154  -k-----| -)
48   -k-----| -)
+-----+-----+-----+-----+-----+-----+-----+-----+
154  -k-----| -)
156  -k-----| -)
46   -k-----| -)
+-----+-----+-----+-----+-----+-----+-----+-----+
156  -k-----| -)
158  -k-----| -)
42   -k-----| -)
+-----+-----+-----+-----+-----+-----+-----+-----+
160  -k-----| -)
162  -k-----| -)
40   -k-----| -)
+-----+-----+-----+-----+-----+-----+-----+-----+
162  -k-----| -)
164  -k-----| -)
38   -k-----| -)
+-----+-----+-----+-----+-----+-----+-----+-----+
164  -k-----| -)
166  -k-----| -)
36   -k-----| -)
+-----+-----+-----+-----+-----+-----+-----+-----+
166  -k-----| -)
168  -k-----| -)
34   -k-----| -)
+-----+-----+-----+-----+-----+-----+-----+-----+
168  -k-----| -)
170  -k-----| -)
32   -k-----| -)
+-----+-----+-----+-----+-----+-----+-----+-----+
170  -k-----| -)
172  -k-----| -)
30   -k-----| -)
+-----+-----+-----+-----+-----+-----+-----+-----+
172  -k-----| -)
174  -k-----| -)
28   -k-----| -)
+-----+-----+-----+-----+-----+-----+-----+-----+
174  -k-----| -)
176  -k-----| -)
26   -k-----| -)
+-----+-----+-----+-----+-----+-----+-----+-----+
176  -k-----| -)
178  -k-----| -)
24   -k-----| -)
+-----+-----+-----+-----+-----+-----+-----+-----+
178  -k-----| -)
180  -k-----| -)
22   -k-----| -)
+-----+-----+-----+-----+-----+-----+-----+-----+
180  -k-----| -)
182  -k-----| -)
20   -k-----| -)
+-----+-----+-----+-----+-----+-----+-----+-----+
182  -k-----| -)
184  -k-----| -)
18   -k-----| -)
+-----+-----+-----+-----+-----+-----+-----+-----+
184  -k-----| -)
186  -k-----| -)
14   -k-----| -)
+-----+-----+-----+-----+-----+-----+-----+-----+
186  -k-----| -)
188  -k-----| -)
12   -k-----| -)
+-----+-----+-----+-----+-----+-----+-----+-----+
188  -k-----| -)
190  -k-----| -)
10   -k-----| -)
+-----+-----+-----+-----+-----+-----+-----+-----+
1.001 1.002 1.003 1.004 1.005 1.005

```

\*\*\*\*\*  
 dump no. 201 on file runtpc nps = 20003421 coll = 3969996021 ctm =15536.56 nrm = 36191434535  
 \*\*\*\*

tally data written to file mctal

5 warning messages so far.

run terminated when 200 kcode cycles were done.

computer time=15537.20 minutes

mcmc version 4a 10/01/93

probid = 02/02/96 10:06:22

02/13/96 17:55:59

26	174	( $\cdots$   $\bar{k}$   $\cdots$ )
28	172	( $\cdots$   $k$   $\cdots$ )
30	170	( $\cdots$   $\bar{k}$   $\cdots$ )
32	168	( $\cdots$   $k$   $\cdots$ )
34	166	( $\cdots$   $\bar{k}$   $\cdots$ )
36	164	( $\cdots$   $k$   $\cdots$ )
38	162	( $\cdots$   $\bar{k}$   $\cdots$ )
40	160	( $\cdots$   $k$   $\cdots$ )
42	158	( $\cdots$   $\bar{k}$   $\cdots$ )
44	156	( $\cdots$   $k$   $\cdots$ )
46	154	( $\cdots$   $\bar{k}$   $\cdots$ )
48	152	( $\cdots$   $k$   $\cdots$ )
50	150	( $\cdots$   $\bar{k}$   $\cdots$ )
52	148	( $\cdots$   $k$   $\cdots$ )
54	146	( $\cdots$   $\bar{k}$   $\cdots$ )
56	144	( $\cdots$   $k$   $\cdots$ )
58	142	( $\cdots$   $\bar{k}$   $\cdots$ )
60	140	( $\cdots$   $k$   $\cdots$ )
62	138	( $\cdots$   $\bar{k}$   $\cdots$ )
64	136	( $\cdots$   $k$   $\cdots$ )
66	134	( $\cdots$   $\bar{k}$   $\cdots$ )
68	132	( $\cdots$   $k$   $\cdots$ )
70	130	( $\cdots$   $\bar{k}$   $\cdots$ )
72	128	( $\cdots$   $k$   $\cdots$ )
74	126	( $\cdots$   $\bar{k}$   $\cdots$ )
76	124	( $\cdots$   $k$   $\cdots$ )
78	122	( $\cdots$   $\bar{k}$   $\cdots$ )
80	120	( $\cdots$   $k$   $\cdots$ )
82	118	( $\cdots$   $\bar{k}$   $\cdots$ )
84	116	( $\cdots$   $k$   $\cdots$ )
86	114	( $\cdots$   $\bar{k}$   $\cdots$ )
88	112	( $\cdots$   $k$   $\cdots$ )
90	110	( $\cdots$   $\bar{k}$   $\cdots$ )
92	108	( $\cdots$   $k$   $\cdots$ )
94	106	( $\cdots$   $\bar{k}$   $\cdots$ )
96	104	( $\cdots$   $k$   $\cdots$ )
98	102	( $\cdots$   $\bar{k}$   $\cdots$ )
100	100	( $\cdots$   $k$   $\cdots$ )
102	98	( $\cdots$   $\bar{k}$   $\cdots$ )
104	96	( $\cdots$   $k$   $\cdots$ )
106	94	( $\cdots$   $\bar{k}$   $\cdots$ )
108	92	( $\cdots$   $k$   $\cdots$ )
110	90	( $\cdots$   $\bar{k}$   $\cdots$ )
112	88	( $\cdots$   $k$   $\cdots$ )
114	86	( $\cdots$   $\bar{k}$   $\cdots$ )
116	84	( $\cdots$   $k$   $\cdots$ )
118	82	( $\cdots$   $\bar{k}$   $\cdots$ )
120	80	( $\cdots$   $k$   $\cdots$ )
122	78	( $\cdots$   $\bar{k}$   $\cdots$ )
124	76	( $\cdots$   $k$   $\cdots$ )
126	74	( $\cdots$   $\bar{k}$   $\cdots$ )
128	72	( $\cdots$   $k$   $\cdots$ )
130	70	( $\cdots$   $\bar{k}$   $\cdots$ )
132	68	( $\cdots$   $k$   $\cdots$ )

## APPENDIX F :DEVELOPMENT OF THE THREE $k_{\text{eff}}$ ESTIMATORS

### **Estimation of $k_{\text{eff}}$ Collision**

Assume a point within a fissile isotope 'k' an a flux  $\phi$  then the rate of production of neutrons for a unit volume is:

$$N_k \overline{v}_k \sigma_{fk} \phi$$

If  $f_k$  is the atom fraction for isotope k then:

$$N_k = f_k N_{\text{total}}$$

therefore the rate of production becomes

$$f_k \overline{v}_k \sigma_{fk} \phi N_{\text{total}}$$

for all fissile isotopes we have

$$\sum_k f_k \overline{v}_k \sigma_{fk} \phi N_{\text{total}}$$

Similarly we can write the rate of collision of all types as

$$\sum_k f_k \sigma_{\text{total}} \phi N_{\text{total}}$$

The probability of neutron production when a neutron collides in a material containing fissile isotopes can be written as

$$\frac{\sum_k f_k \bar{v}_k \sigma_{fk} \phi N_{total}}{\sum_k f_k \sigma_{total k} \phi N_{total}}$$

simplifying

$$\frac{\sum_k f_k \bar{v}_k \sigma_{fk}}{\sum_k f_k \sigma_{total k}}$$

Since the weight of an incident particle is defined as the number of neutrons that it represents, the probability of neutron production, when a particle collides in a material containing fissile isotopes, can be written as:

$$W_i \frac{\sum_k f_k \bar{v}_k \sigma_{fk}}{\sum_k f_k \sigma_{total k}}$$

In a cycle we have N particle therefore

$$k_{eff}^{collision} = \frac{1}{N} \sum_i W_i \frac{\sum_k f_k \bar{v}_k \sigma_{fk}}{\sum_k f_k \sigma_{total k}}$$

$$(\rho W_i \bar{V} \sum_k f_k \bar{v}_k \sigma_{fk})(d/\bar{V}) = \rho W_i d \sum_k f_k \bar{v}_k \sigma_{fk}$$

For all collisions:

$$\sum_i \rho W_i d \sum_k f_k \bar{v}_k \sigma_{fk}$$

therefore:

$$k_{eff}^{track\ length} = \frac{1}{N} \sum_i \rho W_i d \sum_k f_k \bar{v}_k \sigma_{fk}$$

## Estimation of $k_{\text{eff}}$ Track Length

Assume a point within a fissile isotope 'k' an a flux  $\phi$  then the rate of production of neutrons for a unit volume is:

$$N_k \overline{v}_k \sigma_{fk} \phi$$

If  $f_k$  is the atom fraction for isotope k then:

$$N_k = f_k N_{\text{total}}$$

therefore the rate of production becomes

$$f_k \overline{v}_k \sigma_{fk} \phi N_{\text{total}}$$

for all fissile isotopes in the material

$$\phi N_{\text{total}} \sum_k f_k \overline{v}_k \sigma_{fk} = (n \bar{V}) N_{\text{total}} \sum_k f_k \overline{v}_k \sigma_{fk}$$

where  $n$  is the number of incident neutrons  
 $\bar{V}$  is their average velocity

Now lets define :       $n$       the number of incident neutrons  
 $W_i$       neutrons / particles  
 $\rho$       atom density of fissile material

Therefore the rate of production of neutrons is

$$\rho W_i \bar{V} \sum_k f_k \overline{v}_k \sigma_{fk}$$

If  $d$  is the track length from the last event, then  $d/\bar{V}$  is the time taken to travel distance  $d$ , during this time the number of neutrons produced will be the production rate x time therefore

Therefore the number of neutrons produced per neutrons collision with fissile isotope ‘k’ is

$$\left( \frac{v_k \sigma_{fk}}{(\sigma_{fk} + \sigma_{ak})} \right) \left( \frac{(\sigma_{fk} + \sigma_{ak})}{\sigma_{totalk}} \right)$$

Since the weight of an incident particle is defined as the number of neutrons that it represents the number of neutrons produced per particle collision with fissile isotope ‘k’ is :

$$W_i \left( \frac{v_k \sigma_{fk}}{(\sigma_{fk} + \sigma_{ak})} \right) \left( \frac{(\sigma_{fk} + \sigma_{ak})}{\sigma_{totalk}} \right)$$

And for all N neutrons of the source size and all collisions we have

$$k_{eff}^{absorbtion} = \frac{1}{N} \sum_i W_i \left( \frac{v_k \sigma_{fk}}{(\sigma_{fk} + \sigma_{ak})} \right) \left( \frac{(\sigma_{fk} + \sigma_{ak})}{\sigma_{totalk}} \right)$$

## Estimation of $k_{\text{eff}}$ Absorption

Assume a point within a fissile isotope 'k' at a flux  $\phi$  then the rate of production of neutrons for a unit volume is:

$$N_k \overline{v}_k \sigma_{fk} \phi$$

If  $f_k$  is the atom fraction for isotope k then:

$$N_k = f_k N_{\text{total}}$$

therefore the rate of production becomes

$$f_k \overline{v}_k \sigma_{fk} \phi N_{\text{total}}$$

The rate of absorption within the isotope 'k' is

$$f_k (\sigma_{fk} + \sigma_{ak}) \phi N_{\text{total}}$$

The number of neutrons produced per neutron absorbed is:

$$\frac{f_k \overline{v}_k \sigma_{fk} \phi N_{\text{total}}}{f_k (\sigma_{fk} + \sigma_{ak}) \phi N_{\text{total}}} = \frac{\overline{v}_k \sigma_{fk}}{(\sigma_{fk} + \sigma_{ak})}$$

The number of neutrons absorbed per collision is:

$$\frac{f_k (\sigma_{fk} + \sigma_{ak}) \phi N_{\text{total}}}{f_k \sigma_{\text{total}k} \phi N_{\text{total}}} = \frac{(\sigma_{fk} + \sigma_{ak})}{\sigma_{\text{total}k}}$$